

UNCLASSIFIED

ANTENNA (SELECTED ARTICLES), (U)
OCT 81 L A VENGROVICH, L D BAKHRAKH
FTD-ID(RS)T-0021-81

F/G 9/1

NL

1172
SUN 12

2004

2

FTD-ID(RS)T-0821-81

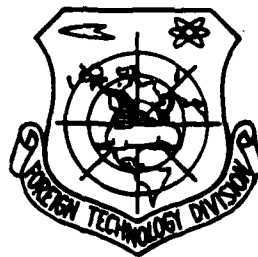
AD A106474

FOREIGN TECHNOLOGY DIVISION



ANTENNA
(Selected Articles)

DTIC
COLLECTED
NOV 3 1981
H



Approved for public release;
distribution unlimited.

DTIC FILE COPY

8 1 11 02 098

FTD- ID(RS)T-0821-81

UNEDITED MACHINE TRANSLATION

14 FTD-ID(RS)T-0821-81

11 15 October 1981

MICROFICHE NR: FTD-81-C-000953

6 ANTENNA (Selected Articles)

English pages: 160

Source: Antenny Nr. 5, 1969, pp. 20-34, 47-60/1
100-162 p-1-102 17-102 101.7

Country of origin: USSR

This document is a machine translation

Requester: FTD/TQFE

Approved for public release; distribution unlimited.

THIS TRANSLATION IS A RENDITION OF THE ORIGINAL FOREIGN TEXT WITHOUT ANY ANALYTICAL OR EDITORIAL COMMENT. STATEMENTS OR THEORIES ADVOCATED OR IMPLIED ARE THOSE OF THE SOURCE AND DO NOT NECESSARILY REFLECT THE POSITION OR OPINION OF THE FOREIGN TECHNOLOGY DIVISION.

PREPARED BY:

TRANSLATION DIVISION
FOREIGN TECHNOLOGY DIVISION
WP-AFB, OHIO.

FTD- ID(RS)T-0821-81

Date 15 Oct 1981

14 1600

TABLE OF CONTENTS

| | |
|---|-----|
| U. S. Board on Geographic Names Transliteration System..... | 11 |
| Some Properties of the Radiating Aperture Super-directionality, by L. A. Vengrovich..... | 1 |
| Solution of the Problem of the Synthesis of Antennas With the Aid of a Coherent Optical System, by L. D. Bakhrakh, Yu. A. Kolosov, A. P. Kurochkin, V. I. Troitskiy..... | 28 |
| Thin Magnetic Impedance Antennas, by E. A. Glushkovskiy, B. M. Levin, Ye. Ya. Rabinovich..... | 57 |
| Open Resonators, Formed by Confocal Mirrors With the Variable Reflection Coefficient and the Generalized Hyper-spheroidal Functions, by N. S. Kosmodamianskaya, V. F. Los'..... | 81 |
| Method of the Study of Complex Waveguide Junctions With One or Several Regions of Communication, by S. V. Butakova.... | 112 |
| Three-Stage Commutation Field of the System of the Repeated Use of Short-Wave Receiving Antennas, by V. D. Chelyshev..... | 143 |

| | |
|--------------------|--|
| Accession For | |
| NTIS GRA&I | <input checked="checked" type="checkbox"/> |
| DTIC TAB | <input type="checkbox"/> |
| Unannounced | <input type="checkbox"/> |
| Justification | |
| By | |
| Distribution/ | |
| Availability Codes | |
| Aval and/or | |
| Dist | Special |
| A | |

U. S. BOARD ON GEOGRAPHIC NAMES transliteration SYSTEM

| Block | Italic | Transliteration | Block | Italic | Transliteration |
|-------|------------|-----------------|-------|------------|-----------------|
| А а | <i>А а</i> | A, a | Р р | <i>Р р</i> | R, r |
| Б б | <i>Б б</i> | B, b | С с | <i>С с</i> | S, s |
| В в | <i>В в</i> | V, v | Т т | <i>Т т</i> | T, t |
| Г г | <i>Г г</i> | G, g | У у | <i>У у</i> | U, u |
| Д д | <i>Д д</i> | D, d | Ф ф | <i>Ф ф</i> | F, f |
| Е е | <i>Е е</i> | Ye, ye; E, e* | Х х | <i>Х х</i> | Kh, kh |
| Ж ж | <i>Ж ж</i> | Zh, zh | Ц ц | <i>Ц ц</i> | Ts, ts |
| З з | <i>З з</i> | Z, z | Ч ч | <i>Ч ч</i> | Ch, ch |
| И и | <i>И и</i> | I, i | Ш ш | <i>Ш ш</i> | Sh, sh |
| Й й | <i>Й й</i> | Y, y | Щ щ | <i>Щ щ</i> | Shch, shch |
| К к | <i>К к</i> | K, k | Ъ ъ | <i>Ъ ъ</i> | " |
| Л л | <i>Л л</i> | L, l | Ы ы | <i>Ы ы</i> | Y, y |
| М м | <i>М м</i> | M, m | Ь ь | <i>Ь ь</i> | ' |
| Н н | <i>Н н</i> | N, n | Э э | <i>Э э</i> | E, e |
| О о | <i>О о</i> | O, o | Ю ю | <i>Ю ю</i> | Yu, yu |
| П п | <i>П п</i> | P, p | Я я | <i>Я я</i> | Ya, ya |

*ye initially, after vowels, and after ъ, ь; e elsewhere.
When written as ё in Russian, transliterate as yě or ě.

RUSSIAN AND ENGLISH TRIGONOMETRIC FUNCTIONS

| Russian | English | Russian | English | Russian | English |
|---------|---------|---------|---------|----------|--------------------|
| sin | sin | sh | sinh | arc sh | sinh ⁻¹ |
| cos | cos | ch | cosh | arc ch | cosh ⁻¹ |
| tg | tan | th | tanh | arc th | tanh ⁻¹ |
| ctg | cot | cth | coth | arc cth | coth ⁻¹ |
| sec | sec | sch | sech | arc sch | sech ⁻¹ |
| cosec | csc | csch | csch | arc csch | csch ⁻¹ |
| | | | | | |
| | | Russian | English | | |
| | | rot | curl | | |
| | | lg | log | | |

Page 20.

Some properties of the radiating aperture superdirectionality.

L. A. Vengrovich ¹.

FOOTNOTE ¹. (L A Wengrowicz). Institute of the fundamental problems
the Polish Academy technique of Sciences, Warsaw. ENDFOOTNOTE.

In the work is derived the integral equation, which connects the
excitable in the aperture electric field with the transverse
component of magnetic field. Solution of integral equation and
introduction of equivalent outlines gives the possibility
subsequently to compute total power flux through the slot and the
energy, accumulated in its vicinity.

On this foundation is introduced the measure of
superdirectionality, which makes it possible to judge physical
limitations, to radiation/emission. The theory presented illustrate
the results of numerical calculations.

Introduction.

It is long ago already known that the equations of Maxwell admit the solutions which independent of the sizes/dimensions of the region, occupied by sources, they represent the arbitrarily concentrated radiation field.

These solutions, called superdirectional, were for the first time noticed by Oseen [1] and, for a while later, they were confirmed by Pradin [2]. Since then they attract attention as independent problem or in connection with the tasks of the synthesis of radiating systems.

Their characteristic feature is the presence of the highest types of fields, accompanied by the large accumulation of quadergy in the vicinity of sources.

To the initially superdirectional solutions was paid considerable attention. Still until recently there was an opinion about the advisability of using the superdirectional solutions for an increase in the efficiency in antenna radiation. There is a very vast literature, which concerns a question of superdirectionality; in the

accompanying bibliography is connected only its small part.

In the present work let us attempt to explain the physical limitations, inherent in electromagnetic radiation of the aperture in the form of slot in the infinite ideally conducting screen. As the fundamental mathematical apparatus is accepted the Fourier transform that it brings this work closer to those, in which is utilized the representation of field with the help of the spectrum of plane waves [8], [9] and [11]; however in contrast to them task is reduced here to the integral equation.

Page 21.

As a result expression for the power flux through the slot and other results they are obtained here directly, without resorting to concepts and methods, connected with the mentioned representation. These results are given to the form, which makes it possible to perform numerical calculations.

Fundamental prerequisites/premises.

Radiating system is shown in Fig. 1. It consists of ideally conducting flat/plane screen $y=0$, in which along x axis is symmetrically arranged/located the slot by width $2a$. By thickness of

screen negligible. Be examined there will be only fields of the type E, i.e., the electric field, parallel to the edges of slot. It is proposed also that the sources and, consequently, also fields do not depend on coordinate x. Dependence on the time is accepted in the form $e^{-i\omega t}$.

Taking into account the important role which in the theory of antennas play the sinusoidal distributions, let us suppose that the sources create in the slot the electric field of the form

$$E = \sum_n b_n \sin \left[n \left(\frac{\pi z_0}{2a} + \frac{\pi}{2} \right) \right]. \quad (1)$$

Each component/term/addend of sum we will subsequently call partial field E_n .

For computing the power, passing through the slot, is necessary to know transverse magnetic field in slot, H_z . Therefore let us begin from the determination of partial fields $H_{z,n}$ of those connected with E_n .

Determination of magnetic field.

a) Conclusion/output and the solution of integral equation. From the equations of Maxwell for the fields in question on plane $y=0$ we have

$$H_z = \frac{1}{ik} \left[\frac{\partial E}{\partial n} \right] \quad (2)$$

where n - external normal to region W_1 (Fig. 1). This dependence makes it possible to concentrate attention in factor $\frac{\partial E}{\partial n}$. For determination $\frac{\partial E}{\partial n}$ we will use the integral representation of Kirchhoff. By bounding surface let us select the plane of screen, then in region W_1

$$E(P) = -\frac{1}{4\pi} \int_{-\infty}^{\infty} \left(\frac{\partial E}{\partial n} \gamma - E \frac{\partial \gamma}{\partial n} \right) dz_0, \quad (3)$$

where $\gamma = i\pi H_0'(k\sqrt{y^2 + (z-z_0)^2})$ designates Green's function for the free space.

Page 22.

If we transfer observation point z to the plane of screen, then we obtain

$$E(z) = \frac{i}{4} \int_{-\infty}^{\infty} \frac{\partial E}{\partial n} H_0'(k|z-z_0|) dz_0. \quad (4)$$

The obtained result we will consider as integral equation relatively $\frac{\partial E}{\partial n}$. Special attention deserves the fact that the nucleus of equation is the function of a difference in the arguments. This makes it possible to assume that the solution of equation can be obtained, applying the apparatus of Fourier transform.

Let us assume that k has the small imaginary part, which ensures the band of analyticity in Fourier transform. However, when this does not play the significant role, we will as before count k by real number.

Let us note that

$$\int_{-\infty}^{\infty} H_0(k|z|) e^{i z t} dz = \frac{2}{k^2 - t^2}, \quad (5)$$

where for $|t| > k$ should be chosen the positive branch of root.

Fourier transform E_n takes the form

$$\begin{aligned} \frac{1}{2\pi} b_n \int_{-\infty}^{\infty} \sin \left[n \left(\frac{z}{2a} + \frac{\pi}{2} \right) \right] e^{i z t} dz = \\ = \begin{cases} na \int_{-\infty}^{\infty} \frac{\cos(at)}{\left(\frac{n\pi}{2} \right)^2 - (at)^2}; & n=2p+1, \\ -ina \int_{-\infty}^{\infty} \frac{\sin(at)}{\left(\frac{n\pi}{2} \right)^2 - (at)^2}; & n=2p+2. \end{cases} \end{aligned}$$

After the formal use/application of Fourier transform to equ. (4) and the solution of algebraic equation for transparency relatively $\frac{\partial E}{\partial n}$ inverse transformation gives

$$\frac{\partial E}{\partial n}(z) = t \cdot n \int_{-\infty}^{\infty} \frac{\cos(at)}{\left(\frac{n\pi}{2} \right)^2 - (at)^2} e^{-i z t} dt, \quad n=2p+1; \quad (7)$$

$$\frac{\partial E}{\partial n}(z) = -i b \cdot n \int_{-\infty}^{\infty} \frac{\sin(at)}{\left(\frac{n\pi}{2} \right)^2 - (at)^2} e^{-i z t} dt, \quad n=2p+2. \quad (8)$$

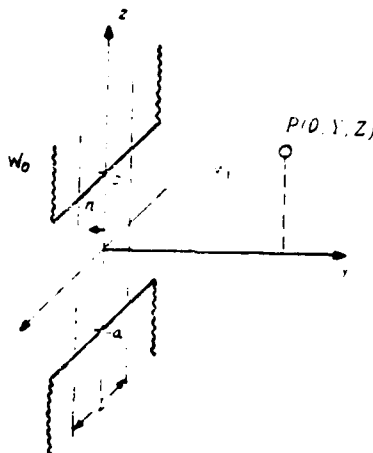


Fig. 1.

Page 23.

Integration is conducted here along the arbitrary straight/direct $\text{Im}t=c$, lying/horizontal at the band analyticity of integrands $|\text{Im}t| < |\text{Im}k|$.

Not difficult to show that the described procedure satisfies theorem conditions of Titchmarsh [12, theorem No 148], and consequently, (7) and (8) actually/really represent the unique in L^2 ($\rightarrow, -$) solutions of equ. (4).

b) The computation of integrals by complex integration.

Let us introduce parameter $q = \frac{2a}{\lambda^2}$ and let us lead integrand to the more convenient form:

$$\frac{\left[q \frac{\pi^2}{2} - (at)^2 \right]}{\left(\frac{n\pi}{2} \right)^2 - (at)^2} = F_1(t) + \left(\frac{\pi}{2} \right)^2 (q^2 - n^2) F_1(t) F_2(t), \quad (9)$$

where

$$F_1(t) = \left[q \frac{\pi^2}{2} - (at)^2 \right]^{-\frac{1}{2}}, \quad (10)$$

$$F_2(t) = \left[n \frac{\pi^2}{2} - (at)^2 \right]^{-\frac{1}{2}}. \quad (11)$$

If we moreover, express trigonometric functions in the exponential form and to introduce the following designations:

$$I_1 = \int_{i\epsilon-\infty}^{i\epsilon+\infty} F_1(t) e^{-i(z-a)t} dt, \quad (12)$$

$$I_2 = \int_{i\epsilon-\infty}^{i\epsilon+\infty} F_1(t) e^{-i(z+a)t} dt, \quad (13)$$

$$I_3 = \int_{i\epsilon-\infty}^{i\epsilon+\infty} F_1(t) F_2(t) e^{-i(z-a)t} dt, \quad (14)$$

$$I_4 = \int_{i\epsilon-\infty}^{i\epsilon+\infty} F_1(t) F_2(t) e^{-i(z+a)t} dt. \quad (15)$$

then for arbitrary z :

$$\frac{\partial E_n}{\partial n} = b_n \frac{n}{2} \left[I_1 - I_2 + \left(\frac{\pi}{2} \right)^2 (q^2 - n^2) (I_3 + I_4) \right], \quad n = 2p + 1, \quad (16)$$

$$\frac{\partial E_n}{\partial n} = -b_n \frac{n}{2} \left[I_1 - I_2 + \left(\frac{\pi}{2} \right)^2 (q^2 - n^2) (I_3 - I_4) \right], \quad n = 2p + 2, \quad (17)$$

Page 24.

Integrals I_1 and I_2 represent the transformations, reverse to formula (5), and they can be easily calculated. For computation I_1 and I_2 , let us continue analytically function F_1, F_2 to entire plane t , with exception of the sections/cuts, carried out from branch points $t = \pm q \frac{\pi}{2a}$ to infinity (Fig. 2). Let us introduce outlines l_1 and l_2 , and also outline l'_2 obtained from l_2 with the help of substitution $t = -t$. Since fields possess symmetry relative to the axis of slit, it suffices to examine only positive values of z .

Then the outlines of integration, which satisfy Jordan's lemma, will be the outlines the data about which are cited in Table 1.

In the integrals along l_2 let us carry out the appropriate replacement of variable/alternating and will record them as integrals lengthwise l'_2 . Determining deductions in poles $F_2(t)$ and taking into account equ. (2), we will obtain for $|z| < a$:

$$\begin{aligned}
 H_{z,n} = & -i b_n \sqrt{\frac{\varepsilon}{\mu}} \left\{ (-1)^{\frac{n-1}{2}} 2 \sqrt{1 - \frac{n^2}{q^2}} \cos \frac{n \pi z}{2a} + \right. \\
 & + \frac{n}{q} H_0^{(1)} \left(q \frac{\pi}{2} \left| 1 + \frac{z}{a} \right| \right) + \frac{n}{q} H_0^{(1)} \left(q \frac{\pi}{2} \left| 1 - \frac{z}{a} \right| \right) - \\
 & \left. - n q \frac{\pi}{4} \left(1 - \frac{n^2}{q^2} \right) a \int_U F_1(t) F_2(t) [e^{i(a+z)t} + e^{i(a-z)t}] dt \right\}, \quad n=2p+1; \quad (18)
 \end{aligned}$$

$$\begin{aligned}
 H_{z,n} = & -b_n \sqrt{\frac{\varepsilon}{\mu}} \left\{ (-1)^{\frac{n}{2}} 2 \sqrt{1 - \frac{n^2}{q^2}} \sin \frac{n \pi z}{2a} + \right. \\
 & + \frac{n}{q} H_0^{(1)} \left(q \frac{\pi}{2} \left| 1 + \frac{z}{a} \right| \right) - \frac{n}{q} H_0^{(1)} \left(q \frac{\pi}{2} \left| 1 - \frac{z}{a} \right| \right) - \\
 & \left. - n q \frac{\pi}{4} \left(1 - \frac{n^2}{q^2} \right) a \int_U F_1(t) F_2(t) [e^{i(a+z)t} - e^{i(a-z)t}] dt, \quad n=2p+2 \quad (19)
 \end{aligned}$$

where U designates integration along the sections/cuts.

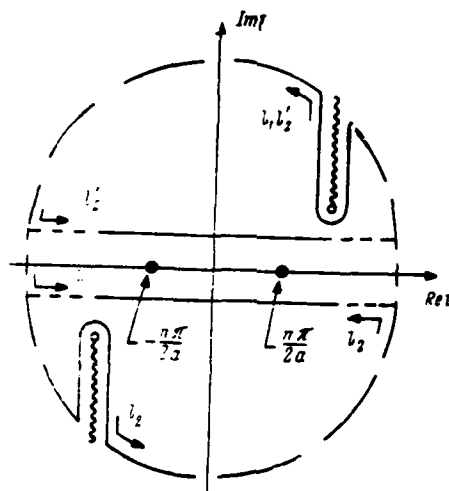


Fig. 2.

Table 1.

| z | l_1 | l_2 |
|---------|-------|-------|
| $z < a$ | l_1 | l_2 |
| $z > a$ | l_1 | l_2 |

Page 25.

For $|z| > a$

$$H_{z,n} = -[b_n] \left[\frac{n}{q} H_0^{(1)} \left(q \frac{\pi}{2} \left| \frac{z}{a} - 1 \right| \right) - \frac{n}{q} H_0^{(1)} \left(q \frac{\pi}{2} \left| \frac{z}{a} + 1 \right| \right) - \right. \\ \left. - nq \frac{\pi}{4} \left(1 - \frac{n^2}{q^2} \right) a \int_0^1 F_1(t) F_2(t) [e^{(z+a)t} - e^{(z-a)t}] dt \right], \quad n = 2p + 1, \quad (2.1)$$

$$H_{z,n} = -[b_n] \left[\frac{n}{q} H_0^{(1)} \left(q \frac{\pi}{2} \left| \frac{z}{a} - 1 \right| \right) - \frac{n}{q} H_0^{(1)} \left(q \frac{\pi}{2} \left| \frac{z}{a} + 1 \right| \right) - \right. \\ \left. - nq \frac{\pi}{4} \left(1 - \frac{n^2}{q^2} \right) a \int_0^1 F_1(t) F_2(t) [e^{(z+a)t} - e^{(z-a)t}] dt \right], \quad n = 2p + 2, \quad (2.2)$$

Integration along the sections/cuts in equ. (18)-(21) presents known difficulty. Therefore the obtained results can be effectively used only in the particular case when the terms, which contain integrals, disappear, i.e., when $n=q$.

c) The computation of integrals by integration along the real axis.

The difficulties which were met in the preceding/previous section, can be bridged. For this let us return to expressions (7) and (8). Integrating along the real axis, we will obtain:

$$\frac{\partial E_n}{\partial n}(z) = b_n \frac{n}{2} \left[I_1 - I_2 - \frac{\pi^2}{2} (q^2 - n^2) \int_{-\infty}^{\infty} F_1(t) F_2(t) \cos(at) e^{-izt} dt \right],$$

$$n = 2p + 1; \quad (22)$$

$$\frac{\partial E_n}{\partial n}(z) = -i b_n \frac{n}{2} \left[I_1 - I_2 - \frac{\pi^2}{2} (q^2 - n^2) \int_{-\infty}^{\infty} F_1(t) F_2(t) \sin(at) e^{-izt} dt \right],$$

$$n = 2p + 2. \quad (23)$$

Applying formula rolls to the integrals in the second terms of equ. (22) and (23), which let us designate as I_3 and I_4 , and taking

into account (5) and (6), we will obtain:

$$I_5 = (-1)^{\frac{n-1}{2}} \frac{1}{a^n n} \int_{-a}^a \cos \frac{n\pi t}{2a} H_0^{(1)}(k|z-t|) dt, \quad n = 2p+1; \quad (24)$$

$$I_6 = (-1)^{\frac{n}{2}} \frac{i}{a^n n} \int_{-a}^a \sin \frac{n\pi t}{2a} H_0^{(1)}(k|z-t|) dt, \quad n = 2p+2. \quad (25)$$

Page 26.

Subsequently we will use the theorem of the addition of Neumann, which we shall record in the more convenient for this purpose form:

$$H_0^{(1)}(k|z-t|) = \sum_{l=-\infty}^{\infty} [\operatorname{sgn}(z)]^l H_l^{(1)}(k|z|) J_l(kt); \quad |z| > a, \quad |t| \leq a; \quad (26)$$

$$H_0^{(1)}(k|z-t|) = \sum_{l=-\infty}^{\infty} [\operatorname{sgn}(t)]^l H_0^{(1)}(k|t|) J_l(kz); \quad |z| \leq a, \quad |t| > a. \quad (27)$$

Let us consider case $|z| < a$. In this case the expressions for I_5 and I_6 can be recorded as:

$$I_5 = (-1)^{\frac{n-1}{2}} \frac{1}{a^n n} \left\{ \int_{-a}^a H_0^{(1)}(k|z-t|) \cos \frac{n\pi t}{2a} dt - \int_a^{\infty} [H_0^{(1)}(k|z-t|) - H_0^{(1)}(k|z+t|)] \cos \frac{n\pi t}{2a} dt \right\}. \quad (28)$$

$$I_6 = (-1)^{\frac{n}{2}} \frac{i}{a^n n} \left\{ \int_{-a}^a H_0^{(1)}(k|z-t|) \sin \frac{n\pi t}{2a} dt - \int_a^{\infty} [H_0^{(1)}(k|z-t|) - H_0^{(1)}(k|z+t|)] \sin \frac{n\pi t}{2a} dt \right\}. \quad (29)$$

The first terms in equ. (28) and (29) can be easily calculated during use (5) by substituting $z-t=-u$. The second terms we convert, utilizing (26), then:

$$I_5 = \frac{4}{an\pi} \frac{1}{1-q^2-n^2} \cos \frac{n\pi z}{2a} - \frac{8}{an\pi} \sum_{l=0,2,4,\dots} \beta_{l,n} J_l \left(q \frac{\pi}{2} \frac{|z|}{a} \right), \quad n=2p-1; \quad (30)$$

$$I_6 = \frac{4}{an\pi} \frac{1}{1-q^2-n^2} \sin \frac{n\pi z}{2a} - \frac{8}{an\pi} \sum_{l=1,3,5,\dots} \beta_{l,n} J_l \left(q \frac{\pi}{2} \frac{|z|}{a} \right), \quad n=2p+2, \quad (31)$$

where

$$\beta_{l,n} = \int_{\pi/2}^{\pi} H_l^{(1)}(qt) \cos(nt) dt, \quad n=2p+1; \quad (32)$$

$$\beta_{l,n} = \int_{\pi/2}^{\pi} H_l^{(1)}(qt) \sin(nt) dt, \quad n=2p+2. \quad (33)$$

Page 27.

Let us consider case $|z| > a$. Applying (27) to the integrands, we will obtain:

$$I_5 = (-1)^{\frac{n-1}{2}} \frac{4}{an} \sum_{l=0,2,4,\dots} \gamma_{l,n} H_l^{(1)} \left(q \frac{\pi}{2} \frac{|z|}{a} \right), \quad n=2p+1; \quad (34)$$

$$I_6 = (-1)^{\frac{n}{2}} \frac{4i}{an} \sum_{l=1,3,5,\dots} \gamma_{l,n} H_l^{(1)} \left(q \frac{\pi}{2} \frac{|z|}{a} \right), \quad n=2p+2. \quad (35)$$

where

$$\gamma_{l,n} = \frac{2}{\pi} \int_0^{\pi/2} J_l(qt) \cos(nt) dt, \quad n=2p+1. \quad (36)$$

$$\gamma_{l,n} = \frac{2}{\pi} \int_0^{\pi/2} J_l(qt) \sin(nt) dt, \quad n=2p+2. \quad (37)$$

Finally placing, (30) and (31) in (22) and (23) and taking into account (2), we finally, substituting (obtain following field expressions $H_{z,n}$ in slot ($|z| < a$):

$$H_{z,n} = -i b_n \sqrt{\frac{\epsilon}{\mu}} \left\{ (-1)^{\frac{n-1}{2}} 2 \right\} \sqrt{1 - \frac{n^2}{q^2}} \cos \frac{n \pi z}{2a} - \frac{n}{q} H_0^{(1)} \left(q \frac{\pi}{2} \left| 1 + \frac{z}{a} \right| \right) + \frac{n}{q} H_0^{(1)} \left(q \frac{\pi}{2} \left| 1 - \frac{z}{a} \right| \right) - (-1)^{\frac{n-1}{2}} 4q \left(1 - \frac{n^2}{q^2} \right) \sum_{l=0,2,4,\dots} \beta_{l,n} J_l \left(q \frac{\pi z}{2a} \right), \quad n = 2p + 1; \quad (38)$$

$$H_{z,n} = -i b_n \sqrt{\frac{\epsilon}{\mu}} \left\{ (-1)^{\frac{n}{2}} 2 \right\} \sqrt{1 - \frac{n^2}{q^2}} \sin \frac{n \pi z}{2a} + \frac{n}{q} H_0^{(1)} \left(q \frac{\pi}{2} \left| 1 + \frac{z}{a} \right| \right) - \frac{n}{q} H_0^{(1)} \left(q \frac{\pi}{2} \left| 1 - \frac{z}{a} \right| \right) - (-1)^{\frac{n}{2}} 4q \left(1 - \frac{n^2}{q^2} \right) \sum_{l=1,3,5,\dots} \beta_{l,n} J_l \left(q \frac{\pi z}{2a} \right), \quad n = 2p + 2 \quad (39)$$

also, on screen ($|z| > a$):

$$H_{z,n} = -i b_n \sqrt{\frac{\epsilon}{\mu}} \left\{ \frac{n}{q} H_0^{(1)} \left(q \frac{\pi}{2} \left| \frac{z}{a} + 1 \right| \right) + \frac{n}{q} H_0^{(1)} \left(q \frac{\pi}{2} \left| \frac{z}{a} - 1 \right| \right) + (-1)^{\frac{n-1}{2}} 2 \pi q \left(1 - \frac{n^2}{q^2} \right) \sum_{l=0,2,4,\dots} \gamma_{l,n} H_l^{(1)} \left(q \frac{\pi}{2} \frac{|z|}{a} \right) \right\}, \quad n = 2p + 1; \quad (40)$$

$$H_{z,n} = -i b_n \sqrt{\frac{\epsilon}{\mu}} \left\{ \frac{n}{q} H_0^{(1)} \left(q \frac{\pi}{2} \left| \frac{z}{a} + 1 \right| \right) - \frac{n}{q} H_0^{(1)} \left(q \frac{\pi}{2} \left| \frac{z}{a} - 1 \right| \right) - (-1)^{\frac{n}{2}} 2 \pi q \left(1 - \frac{n^2}{q^2} \right) \operatorname{sgn}(z) \sum_{l=1,3,5,\dots} \gamma_{l,n} H_l^{(1)} \left(q \frac{\pi}{2} \frac{|z|}{a} \right) \right\}, \quad n = 2p + 2 \quad (41)$$

d) **The** discussion of the obtained results.

Expressions (38) and (39), that describe field in the slot,

consist even three members. The first, most important, represent the field of geometric optic/optics; it is possible to obtain directly from the equation of Maxwell, assuming/setting $E(y, z) = E(0, z)e^{-iky}$ in the vicinity of slot. Special attention should be paid to the dependence of this term on n . With $n > q$ the phase of magnetic field is shifted on $\pi/2$ with respect to the electric field. This can be traced in Fig. 3, where are given graphs/curves in relative unity $H_{z,n}(z)$ for $q=8$ ($2a=4\lambda$) and different n . Solid lines designate modulus/module $H_{z,n}(z)$, and broken - phase $H_{z,n}(z)$. Graphs/curves are constructed on the base of results numerical of calculations.

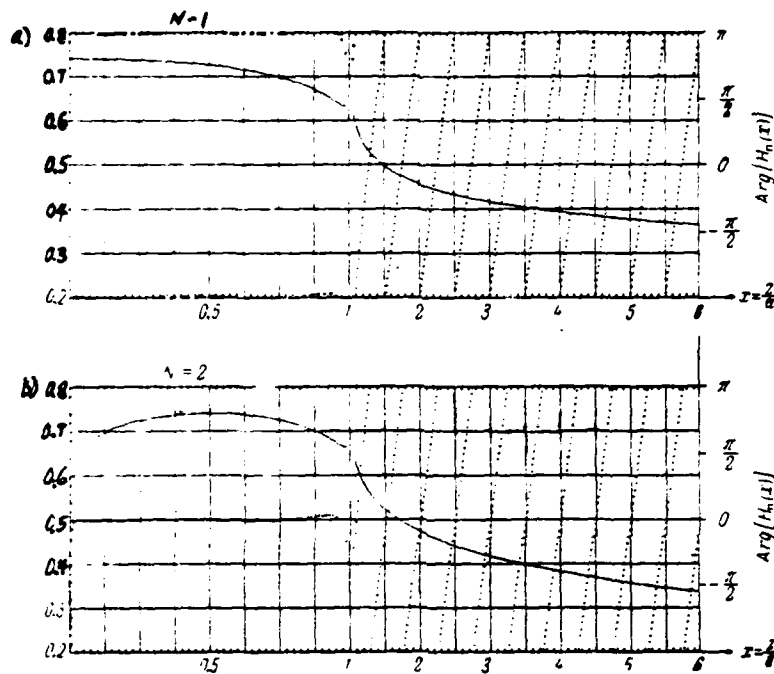


Fig. 3a, b.

Page 31.

Computation of Poynting's vector.

Now we can return to the initial problem and compute the power, transferred through the slot. Average/mean power coefficient, passing through the unit of area of slot,

$$P = \frac{1}{2a} \int_{-a}^a \sum_{n, m} E_n(z) H_{z, m}^*(z) dz. \quad (42)$$

Symbol "*" indicates the complexly conjugated/combined value.

The nonorthogcnality of the postulated partial fields which differ from the eigenfunctions of slot, imply the presence in (42) of "crossed" products. Formally these products are obliged to the second and third terms in expressions (38) and (39) for the transverse magnetic field.

Substituting (1) and (38) or (39) in (42) and carrying out simple transformations, we obtain with an accuracy to the unessential constant factor

$$P = -\frac{1}{2} \sum_n b_n b_n^* \left| \frac{i}{\mu} \right| \quad (43)$$

where

$$U_n = \frac{1}{2} \left(1 - \frac{n^2}{q^2} \right) \sum_m' \frac{b_m}{b_n} \left[\frac{m}{q} z_n^* - (-1)^{\frac{n-m}{2}} 2q \right. \\ \left. \times \left(1 - \frac{m^2}{q^2} \right) \sum_l'' \beta_{m,l} \gamma_{l,m} \right], \\ z_n = \frac{1}{\pi} \int_0^\pi H_0^{(1)}(qt) \sin(nt) dt.$$

For odd n the addition in the sum with the prime must be carried out through odd m , and in the sum with two primes - on even l , for even n - vice versa.

It is similar to expression for H_n , the obtained result consists of three members. Significant role in the transfer of power plays the first of them. With $n=q$ the connected with it flow disappears, with $n>q$ is contained only reactive power. The remaining terms which are obliged to the connection/communication between the partial fields, describe the flow of both active and reactive power. The form of these terms makes it possible to consider that the close couplings occur near $m=n$.

Thus, with $n>q$ the flow of active power through the slot is obliged to the presence of the second and third terms in the expression for $H_{L,n}$ and it is significantly connected with the accumulation of reactive power.

Page 32.

Determination of stored energy.

Although for us it was possible to find expression for the composite power flux however there are no data about the total energy of electrical and magnetic fields, accumulated in the vicinity slot.

This occurs because the imaginary part of Poynting's vector is proportional to a difference in the mentioned values.

For determining the total energy of field we will use the method of equivalent circuits. Let us replace the space into which emits the slot, by the set/dialing of the interconnected circuits. We will consider V_n as the input impedance (or admittance) of the n circuit. If $\frac{dU_n}{d\omega}$ exists, it is continuous and takes negative (positive) values, then we will deal concerning the consecutive (parallel) circuit concerning input impedance Z_n (admittance Y_n) as shown in Fig. 4 (series circuit) and 5 (parallel circuit). Therefore expression $\frac{1}{2} \int \overline{b_n b_n^*}$ can be treated as the square of current or voltage on the input of the n circuit.

DOC = 81082101

PAGE

23

Thus, to each partial field at the fixed/recorded frequency will correspond the specific current (or voltage) and impedance (or admittance).

For determining the total quadergy, which is contained in each circuit, let us use the method, proposed by Chew [4].

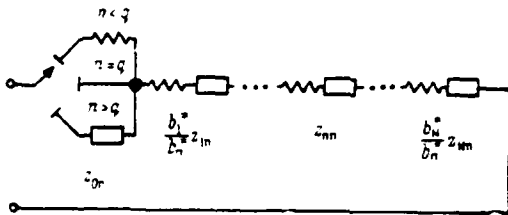


Fig. 4.

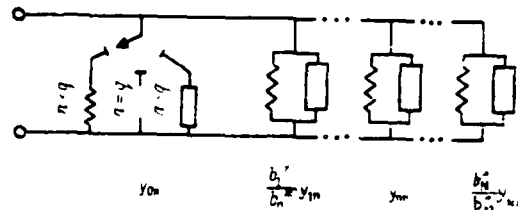


Fig. 5.

Page 33.

Let us replace each circuit with the simple RLC-outline, which possesses in the vicinity of the assigned operating frequency previous dependence on the frequency. Then, taking into account that $\omega \frac{d}{d\omega} = q \frac{d}{dq}$, the total reactive power, reserved in the system,

$$W_{as} = \frac{1}{2} \sum_n b_n b_n^* \sqrt{\frac{z}{\mu}} q \left| \frac{d}{dq} \right| (2 \operatorname{Im} U_n). \quad (46)$$

Measure of superdirectionality.

It is now already easy to introduce the following measure of superdirectionality:

$$Q_s = \frac{1}{2} \frac{\text{средняя суммарная реактивная энергия, запасенная в системе}}{\text{средняя активная энергия, теряемая в системе}} \quad \begin{matrix} (1) \\ (2) \end{matrix}$$

Key: (1). the average/mean total quadergy, stored up in the system.

(2). average/mean active energy, lost in system.

which in the case of the resonant slot coincides with the usual determination of the energy factor of resonant circuit.

The introduced value is the convenient measure for those physical limitations which are inherent in the electromagnetic radiation of slot. These limitations are obliged to the large accumulation of quadergy and low efficiency in the radiation/emission of the highest partial fields, excited in the slot.

In the general case

$$Q_z = \frac{\sum_n b_n b_n^* \left[q \left| \frac{d}{dq} 2 \operatorname{Im} U_n \right| \right]}{\sum_n b_n b_n^* [2 \operatorname{Re} U_n]} \quad (47)$$

In the particular case when only n partial field is excited in the slot, it is possible to speak about its measure of the superdirectionality:

$$Q_n = \frac{q \left| \frac{d}{dq} 2 \operatorname{Im} U_n \right|}{2 \operatorname{Re} U_n} \quad (48)$$

As an example Table 2 gives values Q_n for $q=8$, obtained as a result of numerical calculations. They are light to note that for $n > q$ Q_n accept the substantially high values.

Table 2.

| n | Q_n | n | Q_n |
|-----|------------------------|-----|------------------------|
| 1 | $0,3184 \cdot 10^{-1}$ | 2 | $0,4559 \cdot 10^{-1}$ |
| 3 | $0,3657 \cdot 10^{-1}$ | 4 | $0,7911 \cdot 10^{-1}$ |
| 5 | $0,4953 \cdot 10^{-1}$ | 6 | 0,2216 |
| 7 | $0,6096 \cdot 10^{-1}$ | — | — |
| 9 | $0,3575 \cdot 10^3$ | 10 | $0,3203 \cdot 10^3$ |
| 11 | $0,4767 \cdot 10^3$ | 12 | $0,4603 \cdot 10^3$ |
| 13 | $0,6390 \cdot 10^3$ | 14 | $0,6322 \cdot 10^3$ |
| 15 | $0,8487 \cdot 10^3$ | 16 | $0,8457 \cdot 10^3$ |
| 17 | $0,1109 \cdot 10^3$ | 18 | $0,1108 \cdot 10^3$ |
| 19 | $0,1425 \cdot 10^3$ | 20 | $0,1425 \cdot 10^3$ |
| 21 | $0,1805 \cdot 10^3$ | 22 | $0,1806 \cdot 10^3$ |
| 23 | $0,2254 \cdot 10^3$ | 24 | $0,2252 \cdot 10^3$ |

Page 34.

Conclusion/output.

In conclusion we come to the conclusion that for the high values of n , the n^{th} partial field emits less effectively and requires larger energy content, stored up in the vicinity of slot. Consequently, in practice it is considered advisable to consider only partial fields with $n < q$.

This conclusion will agree with the classical theory of the diffraction where it is disregarded by the effect of the highest types of fields in the aperture in the radiation field.

REFERENCES

1. Oseen C. W. Die Einsteinsche Nadelstichstrahlung und die Maxwell'schen Gleichungen. Ann. der Phys. IV, vol. 69, 1922, p. 202.
2. Фрадин А. З. К вопросу о точечном излучателе. «ЖТФ», vol. 19, 1939, p. 1161.
3. Bouwkamp C. J., N. G. de Bruin. The problem of optimum antenna current distribution. «Phillips Res. Repts», vol. 1, 1946, p. 135.
4. Chu L. Physical limitations of omni-directional antennas. «J. Appl. Phys.», vol. 19, 1948, p. 1163.
5. Solyman L. Maximum gain of the line-source antenna if the distribution function is a finite Fourier series. «IRE Trans.», vol. AP-6, 1958, p. 215.
6. Harrington R. F. Effect of antenna size on gain, bandwidth and efficiency. «J. Res. NBS», vol. 64D, 1960, p. 1.
7. Bouix M. Etude theorique des limitations de la directivite des dispositifs rayonnants. «Ann. Telecomm.», vol. 18, 1963, p. 247.
8. Collin R. E., Rothschild S. Reactive energy in aperture fields and aperture Q. Canadian «J. Phys.», vol. 41, 1963, p. 1967.
9. R. E. Collin, S. Rothschild, Evaluation of antenna Q. «IEEE Trans.», vol. AP-12, 1964, p. 23.
10. Borgiotti G. Evaluation of the Q of an aperture. «Alta Frequenza», vol. 34, 1965, p. 152.
11. Rhodes D. R. On the stored energy of planar apertures. «IEEE Trans.», vol. AP-14, 1966, p. 667.
12. Титчмарт Е. Введение в теорию интегралов Фурье. ОГИЗ, Гостехиздат, 1948.

Page 47.

SOLUTION OF THE PROBLEM OF THE SYNTHESIS OF ANTENNAS WITH THE AID OF
A COHERENT OPTICAL SYSTEM.

L. D. Bakhrakh, Yu. A. Kolosov, A. P. Kurochkin, V. I. Troitskiy.

In the article are given the results of the theoretical and experimental study of the task of the synthesis of flat/plane aperture with the use/application of a coherent optical system. Are analyzed the methods of the optical simulation of antennas in connection with the task of synthesis. Are examined the special features/peculiarities of the recording of the transparencies, which imitate the preset composite radiation patterns. Are given the diagram of optical installation for the synthesis of antennas with the flat/plane aperture and the results of the synthesis of some radiation patterns.

Introduction.

It is known that for the flat antennas with the large electrical

sizes/dimensions of aperture the task of synthesis can be sufficiently accurately solved by the rotation/access according to Fourier of the preset radiation pattern. In the majority of the cases the analytical expression of Fourier transform preset diagram is absent and it is necessary to resort to the numerical integration. In these cases the solution of problem is accompanied by bulky and prolonged computations even during the use/application of TSM [digital computer]. Besides entire other, a similar operation/process, as is known, it is mathematically incorrect.

On the other hand, it is known that the lens in the coherent optical system realizes a two-dimensional Fourier transform of one focal plane into another [1]. This fact makes it possible to utilize an optical system for the solution of the problem of the synthesis of antennas with the flat/plane aperture, i.e., the determination of field in the aperture by the preset radiation pattern [2].

Optical simulation reduces the problem indicated to the tasks of producing the transparency with the recording of the preset function and recording of the obtained distribution of light field. In connection with the simulation of radiation patterns these operations/processes are sufficiently developed. The solution of these problems in the case of the synthesis of antennas has a series/row of the special features/peculiarities which consist of the

following. First, the amplitude characteristic of radiation pattern has, as a rule, considerable drops/jumps in the levels.

Page 48.

Since photographic latitude and noises of photoemulsion are final, the recording of such distributions presents difficulties. In the second place, with the synthesis of antennas it is necessary to measure not only amplitude distribution, but also phase of light field. Finally, the intensity of the signal of substances the forming aperture is sufficiently weak, and therefore the significant role have the noises of optical system.

In the work are examined the fundamental and technical problems of the resolution of the task of the synthesis of antennas with the aid of the coherent optical system, are given the results of investigation on the synthesis of the simplest distributions.

Diagram of the solution of the problem of synthesis with the aid of the coherent optical system.

Radiation pattern in the general case is composite function, and for its reproduction in the optical system it is necessary simultaneously with the amplitude modulation to ensure phase

modulation of light wave. Most simply task it would be possible to solve via location in the field of the light wave of transparency with the variable/alternating transparency and by thickness.

Unfortunately, it is sufficient developed method of production with the optical accuracy of the films of variable/alternating thickness, which ensure direct three-dimensional/space phase modulation of light wave, there does not exist. Therefore for the creation of the amplitude-phase distribution, which coincides from the preset by radiation pattern, it is necessary to utilize different indirect methods which make it possible to form/shape the required distribution of light field with the aid of the transparencies, which have only variable/alternating transparency. For determining the amplitude distribution, which ensures as a result of conversion the preset phase, can be used the methods of the mixed synthesis of antennas [3, 4] or the method of recording on the carrier three-dimensional/space frequency. The present investigations were conducted during the recording of radiation patterns by the second of the methods indicated.

If $g(x, y)$ and $\phi(x, y)$ - respectively amplitude and phase radiation patterns, then in accordance with the method of recording at the carrier three-dimensional/space frequency is manufactured the transparency the coefficient of transmission of which is changed according to the law

$$p(x, y) = [a_0 + b_0 g(x, y)]^2 \cos [u_1 x + u_2 y + \varphi(x, y)]^2. \quad (1)$$

moreover

$$g(x, y) \leq 1, a_0 > b_0.$$

Here a_0 and b_0 - amplitude of constant component and radiation pattern; u_1, u_2 - components of the carrier three-dimensional/space frequency; x, y - coordinate in the plane of transparency.

Page 49.

Field in the focal plane of the lens, in front focus of which is placed the transparency with the recording of the distribution of form (1), it is possible to present in the form three components, one of which is the Fourier transform the preset radiation pattern and is arranged/located in the vicinity of the point:

$$\xi = \frac{u_1 f}{\kappa}; \quad \eta = \frac{u_2 f}{\kappa}.$$

where f - focal length of lens, $\kappa = \frac{2\pi}{\lambda}$, ξ, η - transverse (Cartesian) coordinates in the output plane. This distribution is the solution of the problem of synthesis.

Second component $F_2(\xi, \eta)$ is formed/shaped in the vicinity of point $\xi = -\frac{u_1 f}{\kappa}; \eta = -\frac{u_2 f}{\kappa}$ and it proves to be compositely conjugated/combined with the Fourier transform of the preset radiation pattern. Third component/term/addend - "constant component"

$-F_0(\xi, \eta)$ is the Fourier transform of even distribution with an amplitude of a_0 .

Photographic recording of distributions at the carrier three-dimensional/space frequency.

For the recording of radiation pattern at the carrier three-dimensional/space frequency it is necessary to prepare the transparency the coefficient of transmission of which is changed according to the law (1). Virtually lapping recording it is realized by a photographic method.

Let us examine some special features/peculiarities of this recording. The first special feature/peculiarity is connected with the limited photographic latitude and the amplitude noises of film. By photographic latitude of film here is understood the ratio of the maximum and minimum coefficients of transmission, which can be realized with the aid of the photographic film in the limits of the linear section of characteristic curve. For the majority of photoemulsions this relation has value on the order of 100. In the recording the maximum coefficient of transmission corresponds to the points, at which function (1) is maximum. Is obvious, $p_{\text{max}} = (a_0 + b_0)^2$. Respectively $p_{\text{min}} = (a_0 - b_0)^2$. From condition $\frac{p_{\text{max}}}{p_{\text{min}}} = 100$ we find that, $\frac{b_0}{a_0} = 0.8$. The amplitude noises of photographic film are connected with

grain structure of photoemulsion. The root-mean-square deviation of the amplitude factor of transmission, which corresponds to average/mean photographic density 1.5, for the utilized photographic material composes 0.02. Consequently, the values of function $g(x, y)$ are less than 0.02, prove to be at the level of noise and accurately they cannot be reproduced.

Page 50.

Relative, for example, to the recording of function $(\sin ax/ax)$ latter/last evaluation/estimate means that via recording at the carrier three-dimensional/space frequency it is possible to reproduce only on 10 lobes/lugs to each side from the principal maximum. However, as show experiments, this it is completely sufficient for the synthesis of uniform linear aperture.

The second special feature/peculiarity of recording is connected with the limited resolution of recording equipment, that it does not make it possible to accurately reproduce function (1). Most noticeably this special feature/peculiarity is developed during the recording of the radiation patterns, which have complicated phase response. An increment in the phase is evinced by a change in the period of carrier, and in order to correctly transmit this change, it is necessary in the limits of each period to have sufficiently large

number of elements/cells of recording. For this it is necessary to increase the overall size of recording, which leads to the decrease of sizes of the forming aperture and it is connected with the inconveniences of measurements. During the recording of the radiation patterns which are expressed by the real functions, which take positive and negative values, limitations in the resolution are manifested to a lesser degree. In this case it is possible not to reproduce precise values of function $p(x, y)$ within the limits of the period of carrier, but to write/record only its values in those currents where $\cos ux$ takes value of ± 1 . For example, in the case of one-dimensional film recording is reproduced the function

$$p(x_n) = a_0 + b_0(-1)^n g(n\Delta x)^2. \quad (2)$$

This recording is equivalent to the replacement by the sinusoidal carrying by square pulses length, equal to the half-period of sinusoid. For each period of carrier now fall only two elements/cells of recording, and it means, the density writing of the preset function $g(x, y)$ can be sufficiently high. It is obvious that the rectangular shape of pulses is not necessary. It is required only so that correctly would be transmitted the values of the written/recorded function in the maximums of carrier. Thus, as carrier can serve any periodic function. In the case of carrier, different from the sinusoid, appear the images of aperture at the three-dimensional/space frequencies of multiple ones to fundamental

frequency.

Actually/really, let the carrying signal $s(x)$ periodic and its Fourier series take the form

$$s(x) = \sum_{n=1}^{\infty} c_n \cos \frac{2\pi}{T} nx, \quad (3)$$

where $2\pi/T = u$ - fundamental frequency. Substituting $s(x)$ into formula (1), we will obtain

$$p(x, y) = [a_0 + b_0 c_1 g(x, y) \cos ux + b_0 c_2 g(x, y) \cos 2ux + \dots]^2. \quad (4)$$

Page 51.

The first two members in expression (4) coincide with the functions, entering in (1), and the third and those following cause the preset radiation pattern at the three-dimensional/space frequencies, multiple of basis. The presence of these components/terms/addends in the written/recorded distribution leads to the appearance of supplementary images of aperture in the appropriate places for focal plane. However, the intensity of these images proves to be small, since during the practical recording $s(x)$ it is such, that always $|c_n| \ll |c_1|$ for any $n > 1$.

Amplitude relationships/ratios with the synthesis of uniform linear and rectangular apertures.

The question about the amplitude relationships/ratios with the solution of the problem of synthesis with the aid of the optical system arises on the following reason. Of the aforesaid above it is clear that simultaneously with unknown field $F_1(\xi, \eta)$ is always present the field of constant component $F_0(\xi, \eta)$. Function $F_0(\xi, \eta)$ decreases with the increase/growth ξ and η and in the region of shaping of useful distribution has low values relative to its maximum. However, as it will be shown below, the intensity of field $F_1(\xi, \eta)$ is also small. Consequently, the presence even of weak extraneous field can lead to the undesirable distortions consisting in the parasitic oscillations of the intensity of field in the forming aperture. On the same reason the significant role play the noises of optical system. Fundamental energy of field at the output of transparency falls to the constant component; the noises of system are determined in essence by area and diaphragm shape, which limits light field at the output of transparency with recording (1). It is obvious, formation conditions for useful distribution depend on the form of diaphragm to a lesser degree when field $g(x, y)$ out of the aperture of diaphragm is sufficiently weak. Therefore, selecting by correspondingly form and size/dimension of the forming aperture, it is possible to bring together undesirable distortions to the minimum. Let us determine the relationship/ratio of useful and interfering signals based on the

example of the synthesis of linear and rectangular apertures with the uniform cophasal distribution.

The radiation pattern of linear aperture with the uniform cophasal distribution takes the form

$$g(x) = \frac{\sin \alpha x}{\alpha x}. \quad (5)$$

Function (5) is not composite; however, it takes both positive and negative values, that it does not make it possible to reproduce it directly with the aid of the transparency, which has only variable/alternating transparency.

Page 52.

Let us record the preset diagram on the carrier three-dimensional/space frequency, for which in accordance with (1) let us prepare transparency with the coefficient of transmission, which changes according to the law

$$p(x, y) = \begin{cases} \left(a_0 + b_0 \cos \alpha x \frac{\sin \alpha x}{\alpha x} \right)^2 & \text{при } |x| \leq \frac{l}{2}, |y| \leq \frac{h}{2}, \\ 0 & \text{при } |x| > \frac{l}{2}, |y| > \frac{h}{2}. \end{cases} \quad (6)$$

Key: (1). with.

During the recording the transparency always has finite dimensions, that also is reflected by the corresponding inequalities

in formula (6). From the point of view of useful signal the limited sizes/dimensions of transparency do not play the significant role, if in interval $|x| < \frac{l}{2}$ is arranged/located a large number of lobes/lugs of radiation pattern, which occurs with $\alpha l \gg 1$. Calculating for this by $g(x)$ function $F_1(\xi, \eta)$, $F_0(\xi, \eta)$, it is possible to find that the ratio of field level of useful signal to the constant value component in the region of shaping of the synthesized aperture

$$M = \pi \frac{b_0}{2a_0} \frac{l}{T}, \quad (7)$$

where T - period of the carrier three-dimensional/space frequency;
 $\alpha = \pi/a$ - extent along x axis of one lobe/lug of radiation pattern on the transparency.

In the case of rectangular aperture the coefficient of the transmission of transparency takes the form

$$p(x, y) = \begin{cases} \left[a_0 + b_0 \cos \alpha x \frac{\sin \alpha x}{\alpha x} \frac{\sin \beta y}{\beta y} \right]^2 & \text{при } |x| \leq \frac{l}{2}, |y| \leq \frac{h}{2} \\ 0 & \text{при } |x| > \frac{l}{2}, |y| > \frac{h}{2} \end{cases} \quad (8)$$

Key: (1). with.

The distribution of constant component depends on the orientation of the rectangular diaphragm, which limits the sizes/dimensions of transparency. Let us examine two cases. In the first - the pair of the sides of rectangle is perpendicular to x axis, i.e., it is parallel to the bands, which fill the lobes/lugs of

radiation pattern (see Fig. 3). The secondly - the sides of diaphragm are directed at angle toward the direction indicated.

Under the assumption $\alpha l \gg 1$ and $\beta h \gg 1$ it is possible to find for the case when the sides of limiting diaphragm are parallel to the bands, which fill the lobes/lugs of radiation pattern, that

$$M = \pi \frac{b_n}{2a_0} \frac{r}{T} \frac{q}{h} . \quad (9)$$

where r, q - respectively the sizes/dimensions of the lobe/lug of radiation pattern along x and y axes.

Page 53.

When square diaphragm with the side l is expanded/scanned at angle of 45° to the direction of bands, value M is maximum and is determined by the formula

$$M = \frac{b_0}{4a_0} \pi^2 \frac{r}{T} \frac{q}{T} . \quad (10)$$

Thus, the ratio of useful signal to that mixing in the cases examined is given by expressions (7), (9), (10). Value b_0/a_0 entering in them, characterizes the ratio of constant component to the maximum of the written/recorded signal and is selected, as a rule, the equal to 0.5-0.8 of the considerations of linearity recording (see above). It is obvious, the accuracy of the determination of distribution in the aperture will be the greater, the greater the value M . On the

basis of the obtained relationships/ratios we come to the conclusion that for this it is necessary to increase a number of periods of carrier in the limits of each lobe/lug of radiation pattern. In this case, however, operate the following limitations. An increase in the size/dimension of lobe/lug with the retention/preservation/maintaining of period leads to the decrease of size of the forming aperture, which creates difficulty in the measurement of distribution $F_1(\xi, \eta)$. Whereas the decrease of the period of recording is limited by the possibilities of recording equipment. usually the step/pitch of recording, realized in the available equipment, it is 0.02 mm. In this case for example, considering $r=q=0.1$ and as the $h=3$ mm, we find that M equally to with respect 4: 0.1 and 30.

A decrease in the level of the constant component in the region of shaping of aperture can be also achieved/reached by use during the recording of function $p(x, y)$ of supporting/reference component of form $a \cdot r(x, y)$ with values of $r(x, y)$, which abate to the edges of aperture [$r(x, y) \leq 1$] under condition $a_0 r(x, y) > b_0 g(x, y)$. For the selection of function $r(x, y)$ it is possible to use the known dependences between the side-lobe level of radiation pattern and the means of distribution in antenna aperture.

Experiments show that in the optical system the ratio of useful

signal to that mixing is sufficiently close to the value, obtained on the basis of formulas (7) and (9), and strongly it differs from the value, given by formula (10). The reason for disagreement consists of the following. All preceding/previous formulas are written under the assumption about the fact that the interference, superimposed on the useful image, are the remote lobes/lugs of the regular diffraction pattern of constant component $F_0(\xi, \eta)$. In the first two cases examined this assumption it proves to be valid. But in the case, when image is formed/shaped in the diagonal section of constant component, the level of the mixing field is determined by the noises of optical system, proportional to the maximum of constant component $F_0(\xi, \eta)$. It is easy to find that the ratio of useful signal to the interference is inversely proportional to the area of limiting diaphragm lh :

$$\frac{F_1(\xi, \eta)}{F_0(0, 0)} \sim \frac{1}{lh}.$$

Page 54.

Thus, to the sizes/dimensions of diaphragm are presented contradictory requirements. On one hand, of the condition of the most precise reproduction of field in the aperture it is desirable to have large-size how possible diaphragm. However, from the point of view of the smallest effect of the noises of optical system it is necessary to decrease the size/dimension of diaphragm.

Experimental results.

As it was noted above, one of the special features/peculiarities of the solution of the problem of the synthesis of antennas is the need of determining phase field distribution in the aperture.

In the present work for measuring the phase was utilized the method, which consists in recording of interference pattern, which is formed as a result of adding the measured field with the supporting/reference, by the field whose distribution is known. The special features/peculiarities of this method in connection with the measurement of phase distribution in the optical range are examined in work [5].

Experiments in the synthesis of antennas were moved on the installation whose schematic was depicted in Fig. 1. The lower part of the diagram (microaperture 3, microscope objective 2, collimator 4, converting lens 6) is analogous to the diagram, utilized during the optical simulation of radiation patterns. Semitransparent mirror 9 splits the beam of laser to two, moreover so that the power, which goes into the lower (fundamental) channel of system, considerably exceeds power in the supporting channel. As the collimator of supporting channel serves the converting lens of 6 fundamental channels.

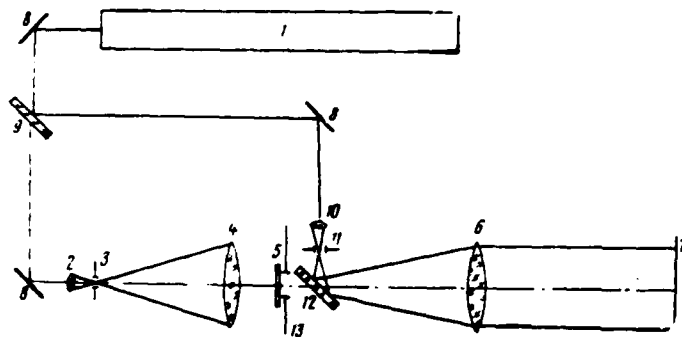


Fig. 1.

Page 55.

Plane-parallel plate 12 turns at necessary angle the front of supporting/reference beam with respect to output plane 7.

Transparency 5 with the recording of radiation pattern and limiting diaphragm 13 were placed in the front/leading focal plane of lens 6 taking into account the effect of plate 12. As collimator 4 and converting lens 6 were utilized the objectives in focal length 400 mm. As the light source served a laser generator of the type LG-35 in wavelength 6328 \AA , which works in the one-mode mode/conditions.

Investigations were conducted with the radiation patterns of the form

$$\frac{\sin \frac{\pi x}{2}}{\frac{\pi x}{2}} \cos \left(\frac{\pi}{2} + \psi \right). \quad (11)$$

which, as it is known [6], are created by linear aperture by length 2π with the uniform amplitude distribution and by phase distribution, which changes according to the law (Fig. 2):

$$\begin{aligned} \varphi(y) &= \psi, & 0 < y < \pi | \\ \varphi(y) &= -\psi, & -\pi < y < 0 | \end{aligned} \quad (12)$$

Furthermore, was conducted the synthesis of the square aperture, which has radiation pattern $\frac{\sin \alpha x}{\alpha x} \frac{\sin \alpha y}{\alpha y}$, which corresponds to cophasal equal-amplitude distribution.

Transparencies with the recording of radiation patterns at the carrier three-dimensional/space frequency were manufactured with photographic method on the photographic plates of the type "Mikrat". Recording was conducted at the different values of the period of the carrier three-dimensional/space frequency, the approximately equal to 0.02, 0.04, 0.08 mm⁻¹ and $a_0/b_0=2$. From the considerations of maximum density and simplicity of recording the carrying signal was assigned in the form of the sequence of square pulses with the width, equal to the half-period of carrier.

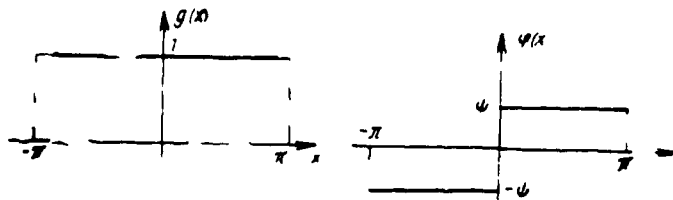


Fig. 2.

Page 56.

Due to scatter of light/world in the emulsion layer and blurred image of the edges of the recording slot the carrying signal was somewhat different from the sequence of square pulses. This property of recording in this case is useful, since it leads to the decrease of the value of signals at the three-dimensional/space frequencies, multiple to fundamental frequency.

Fig. 3 depicts photographs of the recording of the radiation patterns, which correspond to formula (11) with $2\psi=0$; $\pi/4$; $\pi/2$; π ; with the period of the carrier 0.08 mm^{-1} , while in Fig. 4 - the microphotogram of the recording of radiation pattern at the carrier frequency when $\psi=0$, i.e. diagram $\frac{\sin \pi x}{\pi x}$ (Fig. 3a). On the microphotogram are noticeable the noises of recording the caused by grain structure photoemulsions and leading to the divergences of results recordings from the preset function, by especially noticeable

in the region of weak side lobes. Statistical processing of microphotograms shows, however, that on the average the preset function is reproduced with the relative accuracy not worse than 100/o. For eliminating the effect of the phase noises of photographic material, caused by the inconstancy of the thickness of emulsion and support/base, the transparencies with the recording of radiation patterns were placed into the immersion (cedar or castor oil).

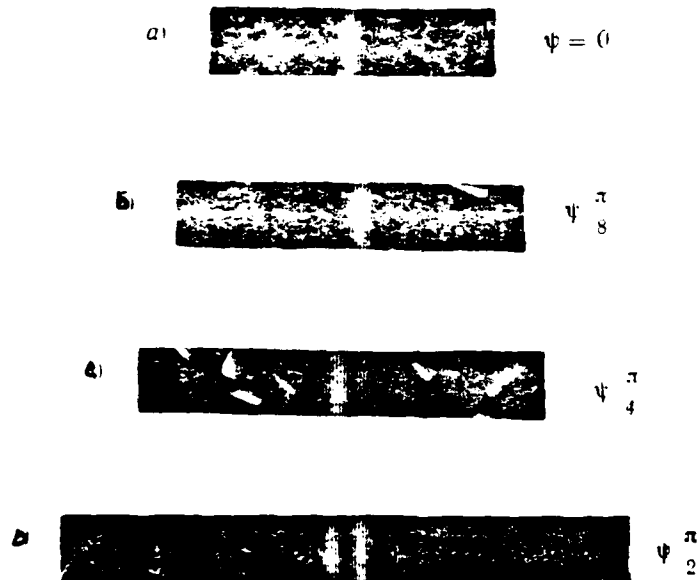


Fig. 3.

Page 57.

Fig. 5 depicts the photograph of field distribution in the output plane for the case of the synthesis of square aperture with $\alpha = \beta = 6w$; $u = 80w$ [see (8)].

The image of aperture (a) is formed/shaped at a distance of 10.5 mm from the maximum of constant component (b). The square diaphragm (see 13 in Fig. 1) by the size/dimension 3×3 of mm^2 , that limits the aperture of transparency with the recording of radiation pattern at

DOC = 81082102

PAGE ~~22~~
49

the carrier three-dimensional/space frequency, was oriented at angle of 45° to the direction of the bands, which correspond to the carrying signal.

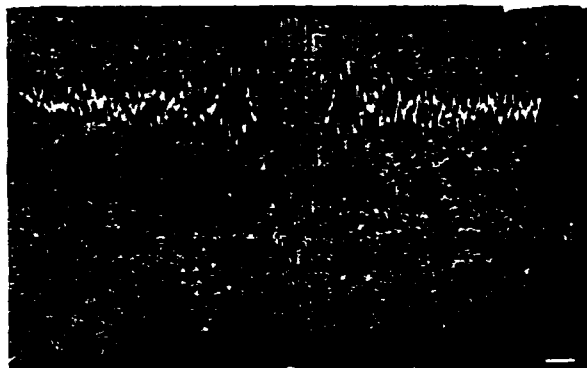


Fig. 4.

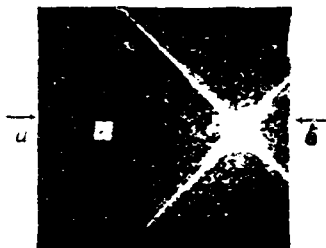


Fig. 5.

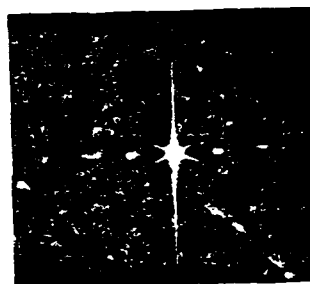


Fig. 6.

Page 58.

Fig. 6 depicts the photograph of distribution in the output plane in the case of the synthesis of linear aperture with $u=50\lambda$ and $\varphi=0$. In Fig. 6 are noticeable the images of aperture at the three-dimensional/space frequencies, multiple to fundamental frequency, which were discussed above. The intensity of these images is more than by an order lower than intensity of image at the

fundamental frequency. At other values ψ is observed the similar pattern. For decreasing the level of the constant component in the region of shaping of aperture the lateral sides of aperture 13, which limits field at the output of transparency, were arranged/located at small (20-30°) angle to each other. In this case was utilized the known property of flat/plane aperture in the form of trapezoid, which consists in the fact that in the flat/plane section of three-dimensional/space radiation pattern, parallel to the foundations of trapezoid, the level of lobes/lugs is considerably lower than the level of the lobes/lugs of rectangular aperture in the same section.

The distributions, depicted in Fig. 5 and 6, correspond to the case when reference signal is absent, and they make it possible to determine amplitude distribution in the aperture. The results of measurements show that it is close to the uniform; however, are observed the small divergences, caused by the background of constant component. With the synthesis of linear aperture they have regular character and can be easily measured or calculated independent of the forming distribution and are introduced into the final results as the correction. With the noise character of background the latter is considered by the corresponding statistical processing.

For measuring the phase distribution was input/embedded the

plane supporting/reference wave whose intensity was selected by the equal to the intensity of field in the aperture. Obtained in this case pictures are depicted in Fig. 7. When supporting/reference wave falls to the output plane at the angle, which differs from 90° , appears interference figure, width and orientation of which depend on angle of incidence. From Fig. 7a it is evident that the bands have on everything apertures equal width, moreover structure regularity is not disrupted during their arbitrary orientation. These facts testify about the constancy of phase in the synthesized aperture.

For measuring the phase the front of supporting/reference beam was established/installed at the zero angle to the measurement plane. Obtained in this case picture is depicted in Fig. 7b. The intensity of total field at any point of aperture comprises not more than 0.02 from the intensity of reference signal. Consequently, the divergences of phase from the constant value within the limits of aperture do not exceed 10° .

Fig. 8 as an example gives the pictures of field distribution of output plane with the synthesis of linear aperture for $\Psi=0$ and $\Psi=\frac{\pi}{2}$. Measurements of phase distribution in the aperture, which is formed into the result of the synthesis of the radiation patterns of form (11) when $\psi=0, \frac{\pi}{8}, \frac{\pi}{4}, \frac{\pi}{2}$, give the values of a phase difference on the faults of aperture, the respectively equal to 0° , to 45° , 90° , 180°

(with accuracy of $\pm 7^\circ$), close to the given ones. The coincidence of the preset phase distributions with those measured testifies, on one hand, about the high accuracy of shaping of distribution in the synthesized aperture and, therefore, about the sufficiently high accuracy of the recording of transparencies, on the other hand, about the possibility of measurement with the high accuracy of phase distribution.

Page 59.

Conclusion.

The results of theoretical and experimental studies make it possible to make a conclusion about the possibility of using the coherent optical systems for the solution of the problem of the synthesis of antennas. The problem of the recording of composite radiation patterns is solved with the aid of the method of recording at the carrier three-dimensional/space frequency. Appearing in this case interferences, connected with the background of constant component, can be suppressed by the adequate/approaching selection of size/dimension and diaphragm shape, value of the carrier frequency and form of reference signal. The problem of determining the phase distribution with a sufficient accuracy is solved by the measurement of interference pattern, which is formed as a result of adding the

DOC = 81082102

PAGE ~~27~~
54

forming field with the known reference signal.

Is considered by advisable further development of the synthesis of antennas by the method of optical simulation, in particular, development of the methods of the synthesis of antennas with the nonplanar aperture.

a)



b)

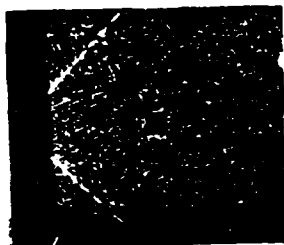


Fig. 7.

a)



b)

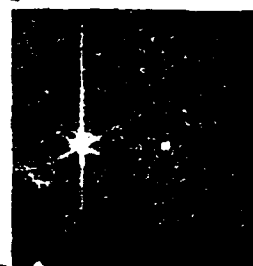


Fig. 8.

Page 60.

REFERENCES

1. Cuperone L. J., Leith E. N., Palermo C. J., Porcello L. J. «Optical data processing and filtering systems». «IRE Trans. on Information Theory», 1963, T-9, 366.
Имеется русский перевод — «Зарубежная радиоэлектроника», 1963, № 10, стр. 3.
2. Бахрах Л. Д., Курочкин А. П. Использование методов голографии для решения задачи синтеза диаграмм направленности антенн. Доклады XXIII всесоюзной научной сессии НТОРиЭ им. А. С. Попова о радиотехнических устройствах, 1967.
3. Бахрах Л. Д., Троицкий В. И. Смешанные задачи синтеза антенн. «Радиотехника и электроника», 1967, т. XII, № 3, 437.
4. Троицкий В. И. Смешанные задачи синтеза антенн. «Вопросы радиотехники» Серия Общетехническая 1968, № 2.
5. Курочкин А. П. Оптическое моделирование антенн СВЧ. «Радиотехника и электроника», 1968, т. XIII, №№ 7, 8.
6. Зелкин Е. Г. Построение излучающей системы по заданной диаграмме направленности. ГЭИ, 1963.

Page 108.

THIN MAGNETIC IMPEDANCE ANTENNAS.

E. A. Glushkovskiy, B. M. Levin, Ye. Ya. Rabinovich.

Are given the results of applying the impedance boundary conditions to the solution of the problem about the excitation of thin magnetic radiator/resonator/element. Specifically are examined the thin ferrite of the finite length, excited by the framework, and the narrow slot, gashed in the conducting cylinder.

In the preceding/previous work of the authors [1-3] were investigated thin electrical impedance antennas. Using the obtained there results, in the present work will be examined magnetic impedance radiators/resonators/elements, i.e., the antennas on surface of which it is possible to formulate boundary conditions of the type

$$\frac{E_y}{H_z} = -Z,$$

where E_y and H_z - components of the intensity/strength of

respectively electrical and magnetic fields; z_A^{and} - orthogonal coordinates on the surface of antenna; Z - surface impedance, in the general case composite.

In this case will be investigated the case, when impedance Z affects current distribution already in the zero according to χ the approximation/approach where $\chi = \left(2 \ln \frac{2l}{a}\right)^{-1}$ - low parameter. (Here l - the reach of radiator/resonator/element, a - a radius of radiator/resonator/element). Such antennas, as it will be shown below, are, in particular, the magnetic bar, excited by the framework, and the narrow slot, gashed in the conducting cylinder. These antennas were investigated by the method of eigenfunctions by A. A. Pistol'kors [4-6]. In the works indicated primary attention was given to the explanation of the structure of electromagnetic field and to the determination of the transmission modes, which appear during different excitation of these antennas.

In this work it will be shown that, using the concept of surface impedance, it is possible easily to obtain and to clearly interpret the series/row of the fundamental conclusion/output, done in [4-6], to do a series/row of new conclusion/output, and to also record expression for this virtually interesting characteristic as input antenna resistance.

Page 109.

Magnetic current distribution along the antenna. Input resistance.
Radiation pattern.

In work [7] was obtained the integrodifferential equation for the magnetic current J , which flows along the impedance radiator/resonator/element (along the axis z):

$$J'' + \left(k^2 - 2i k Z_0 \frac{\gamma}{QZ} \right) J = -4\pi i \omega \mu_0 \gamma [H_z^{sr}(z) - G(J, z)]. \quad (2)$$

where k - wave propagation constant in the free space, μ_0 and Z_0 - respectively magnetic permeability and wave impedance of free space.

It is obvious that for the expression

$$k_1 = \sqrt{k^2 - 2i \frac{k \gamma}{a} \frac{Z_0}{Z}} \quad (3)$$

it is necessary to ascribe the sense of the propagation constant of magnetic current along the radiator/resonator/element in question.

From expression (3) it is evident that with satisfaction of condition $\frac{Z}{Z_0} \sim \frac{\gamma}{ka}$ the impedance will affect the propagation of current already in the zero approximation, and also, that, if impedance Z purely reactive/jet and does not satisfy the inequality

$$k^2 - 2i \frac{k \gamma}{Q} \frac{Z_0}{Z} > 0. \quad (4)$$

then propagation constant k_1 will be imaginary, i.e., magnetic current will not be propagated along the antenna.

Using the results, obtained in [2] for the electrical impedance antennas, it is possible, without solving equ. (2), to write formulas for the current distribution and input admittance of the magnetic impedance radiator/resonator/element, excited by concentrated magnetomotive force ε_m of that applied to its middle. In the first on χ the approximation/approach we will obtain the sinusoidal distribution of the magnetic current

$$J = i \gamma \frac{k}{k_1} \frac{240\pi}{\cos k_1 l} \varepsilon_m \sin k_1 (l - |Z|) \quad (5)$$

and purely susceptance:

$$Y = i W_1 \operatorname{ctg} k_1 l; \quad W_1 = \frac{1}{(120\pi)^2} \frac{60}{\gamma} \frac{k_1}{k} \quad (6)$$

where W_1 - has the sense of wave impedance.

Page 110.

The account of the following approximation/approach gives expression for the magnetic current in the place of the feed

$$J(0) = i \frac{k 240\pi}{k_1 \cos k_1 l} \gamma \varepsilon_m \sin k_1 (l - |Z|) - \left(\frac{k}{k_1} \right)^2 \gamma^2 \frac{120\pi^2}{\cos^2 k_1 l} \varepsilon_m b(k_1, k, l) \quad (7)$$

and for input admittance

$$Y = \frac{I_m}{J(0)} = \frac{Z_0}{(120\pi)^2} \quad (8)$$

where Z_0 - input resistance of the electrical radiator/resonator/element, which has the same geometric parameters and the same value of propagation constant k_1 as magnetic radiator/resonator/element. Expression for Z_0 and for $\theta(k_1, k, l)$ is the sufficiently bulky combination of integral sines and cosines and is given in [1] and [2].

Utilizing the expression, obtained in [1] for the field in the remote zone, created by electrical impedance antennas, let us record formula for the radiation pattern of the magnetic impedance radiator/resonator/element:

$$F(\varphi, \theta) = \frac{\sin \theta}{\left(\frac{k_1^2}{k^2} - \cos^2 \theta \right)} [\cos(kl \cos \theta) - \cos k_1 l]. \quad (9)$$

Let us note that with $k_1 = k$ formula (5)-(9) they pass into the appropriate formulas for ideal radiators/resonators/elements ($Z=0$).

Let us determine the input resistance, introduced by magnetic radiator/resonator/element into its feeding framework with the

current:

$$Z_{nas} = \frac{U_{nas}}{J_p} \quad (10)$$

where U_{nas} - emf, induced by magnetic radiator/resonator/element at the framework, J_p - current, which flows along the framework.

Induced emf is equal to the magnetic current of radiator/resonator/element at the point of excitation $J(0)$, and the current of the framework is magnetomotive force \mathcal{E}_m applied also to the point of excitation. Then

$$Z_{nas} = \frac{J(0)}{\mathcal{E}_m} = \frac{1}{Y} = \frac{(120\pi)^2}{Z_0} \quad (11)$$

For the practical calculations of the input resistances of relatively short radiators/resonators/elements ($2l \leq \frac{\lambda}{2}$) it is possible to determine according to the sufficiently simple formula:

$$Z_s = R_s + iX_s = 80 \left(\frac{k}{k_1} \right)^2 \operatorname{tg}^2 \frac{k_1 l}{2} - i 120 \frac{k_1}{k} \left(\ln \frac{l}{a} - 1 \right) \operatorname{ctg} k_1 l. \quad (12)$$

From (11) and (12) it is evident that the coupled impedance will have resonance character and reach maximum at the points where $X_s = 0$.

This first resonance will be in region $k_1 l \approx \frac{\pi}{2}$.

Ferrite, excited by the framework.

In order to use the results of the first section, it is

necessary for each concrete/specific/actual antenna to know the value of surface impedance.

Page 111.

The surface impedance of ferrite core can be approximately found from the solution of diffractive problem for the round infinitely long uniform rod on surface of which is satisfied boundary condition (1).

Examining the excitation of this rod by convergent cylindrical wave, we will obtain the system of equations of Maxwell in the cylindrical coordinates:

$$\left. \begin{aligned} \frac{\partial H_z}{\partial \rho} &= -i\omega\epsilon E_\varphi \\ \frac{1}{\rho} \frac{\partial}{\partial \rho} (\rho E_z) &= -i\omega\mu H_z \end{aligned} \right\}, \quad (13)$$

where μ and ϵ - parameters of ferrite.

Utilizing a condition of the finiteness of electrical field component E_z with $\rho=0$, we find

$$Z = -\frac{E_z}{H_z} \Big|_{\rho=a} = i120\pi \sqrt{\frac{\mu_r}{\epsilon_r}} \frac{J_1(ma)}{J_0(ma)}, \quad (14)$$

where $m = k\sqrt{\mu_r\epsilon_r}$; μ_r, ϵ_r - with respect the relative magnetic and dielectric permeability of the ferrite: (in actuality one must take

into account the demagnetizing factor, i.e., by μ_r to understand effective permeability): $J_1(ma)$ and $J_0(ma)$ - the corresponding Bessel functions. By losses in the ferrite negligible. To take into account them is possible the introduction to composite permeability $\mu_r = \mu' - i\mu''$ as this done in [1].

Expression (14) for the surface impedance is approximate. It is correct for the case of stems ($ma \ll 1$).

In this case the surface impedance

$$Z = i60\pi\mu_r ka \quad (15)$$

After substituting (15) in (3), we will obtain expression for the propagation constant

$$k_1 = \sqrt{k^2 - \frac{2}{\mu_r a^2 \ln \frac{2l}{a}}} \quad (16)$$

From (16) it immediately follows that for the propagation of magnetic current along the rod it is necessary to satisfy the following condition:

$$\frac{k^2 a^2}{2} \ln \frac{2l}{a} > \frac{1}{\mu_r^2} \quad (17)$$

Approximately/exemplarily the same expression was obtained by A. A. Pistol'kors for the antenna being investigated in [4] as the

condition with fulfilling of which the antenna loses elementary directional characteristic, inherent in the framework. As it follows of the aforesaid above, this condition acquires now supplementary interpretation as the condition of the onset of magnetic current in the rod.

Page 112.

It is obvious that solution of the equation

$$\frac{(2\pi)^2}{\lambda^2} = \frac{2}{a^2 \mu_r \ln \frac{2l}{a}} \quad (18)$$

gives critical wavelength λ_{kp} in the assigned parameters of antenna. When $\lambda > \lambda_{kp}$ magnetic current attenuates, when $\lambda < \lambda_{kp}$ from zero to k . The first phase speed much more than the speed of light, then approaches it. With $k \rightarrow \infty$ or when $\mu_r \rightarrow \infty$ ferrite becomes ideal magnetic radiator/resonator/element.

Input resistance and directivity of the antennas in question can be calculated according to the appropriate formulas of the first section. As far as is known, at present industry does not release such ferrites that the prepared of them antenna of acceptable thickness would possess the parameters, which satisfy condition (17). Therefore the experimental check of the relationships/ratios,

obtained in this section, was not conducted.

At the high values of ma expression (14) becomes very approximate and for determining of k_1 is expedient to use the transcendental equation, which are obtained with the solution of its own problem about the propagation of symmetrical magnetic ground wave along the ferrite. However, even in this case use of an expression for the surface impedance gives the possibility very simply to obtain the series/row of the conclusion/output, obtained by other previously path in [4] and to give to them demonstrative interpretation.

Thus, for instance, during the analysis of field expression, created by the antenna in question in the remote zone, in [4] it was established that:

1. When value ma corresponds to the roots of function $J_0(ma)$, field is obtained the same as from the ideal magnetic-conducting rod.

2. When value ma corresponds to roots of function $J_1(ma)$, field is obtained the same as from ideally conducting rod, excited by framework.

3. Values ma , which satisfy equation

$$mJ_0(ma) + \nu_r J_1(ma) k^2 a \ln 0.89ka = 0, \quad (19)$$

are also singular points.

After substituting (14) in (3), we will obtain expression for the propagation constant

$$k_1^2 = k^2 - \frac{mJ_0(ma)}{a\mu_r J_1(ma)} \frac{1}{\ln \frac{2l}{a}}, \quad (20)$$

from which the enumerated three conclusion/output follow immediately.

1. If $J_0(ma)=0$, then $k_1=k$ and ferrite is converted into ideal magnetic radiator/resonator/element, analogous in duality principle to ideal electrical radiator/resonator/element.

Page 113.

2. If $J_1(ma)=0$, then from (14) it follows that $Z=0$ and boundary condition (1) passes under condition $E_z=0$, that implementing on metallic surface.

3. Let us record condition with fulfilling of which $k_1=0$:

$$k^2 a \mu_r J_1(ma) \ln \frac{2l}{a} - mJ_0(ma) = 0. \quad (21)$$

Equation (21) coincides with equ. (19) during replacement of $\ln \frac{2l}{a}$ on $\ln(0.89 ka)$, which corresponds to the selection of another

value

$$\gamma = - \frac{1}{2 \ln 0.89ka}$$

Thus, all these conclusions obtain demonstrative interpretation.

Narrow slot, gashed in the conducting cylinder.

From inequality (4) it follows that the propagation constant of magnetic current along the antenna will be real, if the surface impedance Z has capacitive character.

Capacitive surface impedance can be created in a following manner. Fig. 1 depicts metallic cylinder 1, in which is gashed narrow slot 2. Along the slot is distributed certain capacity/capacitance. It can be created with several capacitors/condensers 3. Antenna is excited by the framework with the current. For the generality we will consider that the cylinder capacity is filled with ferrite with effective magnetic permeability μ_r . Let us consider the in practice interesting case when a radius of cylinder r_0 is small in comparison with the wavelength in the ferrite. The surface impedance, to which is loaded the slot, will be composed of the inductance of cylinder and distributed capacitance.

The inductance of cylinder L let us find, utilizing expression (15) for Z :

$$Z_{\text{ant}} = i \omega L = \frac{Z 2\pi r_0}{l} = i \frac{60\pi^2 \mu_r k r_0^2}{l} \quad (22)$$

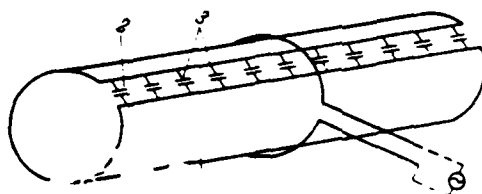


Fig. 1.

Page 114.

Impedance taking into account the distributed capacitance

$$Z_{\text{полн}} = i \frac{\omega L}{\left(1 - \frac{\omega^2}{\omega_0^2}\right)}, \quad (23)$$

where: $\omega_0 = \frac{1}{\sqrt{LC}}$ the frequency of antiresonance; C - the available capacity, distributed on the slot.

Considering that the slot with width $2a$ is loaded to resistor/resistance $Z_{\text{полн}}$, we will obtain formula for the surface impedance

$$Z = \frac{l}{a} Z_{\text{полн}}. \quad (24)$$

Let us note that from (22) it follows that the linear conductivity of cylinder $\gamma = -\frac{i}{60\pi^2 r_0^2 k}$. This formula completely coincides

with the expression, obtained by A. A. Pistol'kors in [5] for the linear conductivity of metallic groove.

In [5] and [6] the problem about the excitation of the infinitely long conducting groove was solved by the method of eigenfunctions (Mathieu functions). As has already been indicated, primary attention in these works was given to the explanation of the structure of electromagnetic field and to the determination of the transmission modes, which appear during different excitation of groove.

The series/row of the conclusion/output, done in [6], will be obtained below from the examination by the propagation constant of magnetic current.

Expression for the propagation constant of magnetic current along the narrow slit we will obtain from the equation, analogous to equ. (2) for cylindrical antenna [7]:

$$J''(z) + k^2 J(z) = -2\pi i \omega \epsilon_0 / \left[H_z^{(0)}(z) + G(J, z) - \frac{J}{2a} \frac{1}{z} \right], \quad (25)$$

hence, it is analogous (with 3), it is obtained

$$k_1^2 = k^2 - \pi i \frac{k}{a} \frac{Z_0}{Z}. \quad (26)$$

After substituting in (26) expression (24) taking into account

(22) and (23), let us find

$$k_1^2 = \left(\frac{2\pi}{c}\right)^2 f^2 + \frac{2\epsilon_0 \left(\frac{f}{f_0} - 1\right)}{f_0^2 \mu_r}, \quad (27)$$

where c - speed of light, f - frequency.

From (27) it follows that there is a critical frequency, determined by the equation

$$\left(\frac{2\pi}{c}\right)^2 f_{kp}^2 + \frac{2\epsilon_0}{f_0^2 \mu_r} \left(\frac{f_{kp}^2}{f_0^2} - 1\right) = 0. \quad (28)$$

The existence of critical frequency was obtained also in [6] for flat/plane component of plane-cylindrical waves, which are propagated along the slot.

If $f < f_{kp}$, then magnetic current is not propagated.

Page 115.

With $f=f_0$, propagation constant $k_1=k$, i.e., the slot in question behaves as ideal magnetic radiator/resonator/element. If $f>f_0$, then with an increase in the frequency sharply grows/rises the value of propagation constant k_1 . This leads to the fact that along the antenna begins to be placed a large number of half-waves of current whose radiation/emission mutually extinguishes each other, which

strongly decreases the actually radiating length of antenna.

Let us note that frequencies f_{np} and f_0 lie/rest very closely to each other, so that virtually $f_{np} \approx f_0$. Thus, the antenna in question will be effective only in the very small frequency band.

We will obtain expression for the input resistance, introduced into the framework of antenna, it is possible to count according to formula (11):

$$R_{ax} = \frac{(120\pi)^2 R_s}{R_s^2 + X_s^2}; \quad X_{ax} = -\frac{(120\pi)^2 X_s}{R_s^2 + X_s^2}; \quad (29)$$

$R_s + iX_s = Z_s$ and it is determined from (12).

Since for the antennas $R_s \ll |X_s|$, in question the coupled impedance will be noticeable only in the region of frequencies where $X_s \approx 0$.

The points of resonance will be frequencies, with which $k_1 l \approx \frac{\pi}{2} n$, where n - the whole number. With increase in n the value of resonance resistor/resistance decreases.

Let us consider first resonance $|k_1 l \approx \frac{\pi}{2}|$. We will obtain at the point of the resonance

$$R_{res} = \frac{(120\pi)^2}{80 \left(\frac{2kl}{\pi} \right)^2}. \quad (30)$$

The frequency of resonance will differ from $f_0 = \frac{1}{2\pi\sqrt{LC}}$ by the insignificant value:

$$f_{\text{res}} - f_0 = f_0 \frac{\pi^2 r_0^2}{16 l^2} \left(1 - 16 \frac{l^2}{\lambda_0^2} \right). \quad (31)$$

It is evident that the nearer the reach of antenna 1 to quarter wavelength λ_0 , the nearer f_{res} to f_0 .

Let us determine the bandwidth on level 0.707, i.e.

$$\left| \frac{Z_{\text{res}}}{Z_{\text{in}}} \right|^2 = 2. \quad (32)$$

In this frequency band it is possible to consider that

$$R_s \approx 80 \left(\frac{k}{k_1} \right)^2; X_s = \pm \frac{60}{l} \frac{k_1}{k} \Delta k_1 l, \quad (33)$$

where Δk_1 - change of the propagation constant of current in the unknown band.

Page 116.

After substituting (33) in (32), let us find

$$\Delta k_1 = \frac{4}{3} \frac{1}{l} \left(\frac{k}{k_1} \right)^2. \quad (34)$$

From (34), utilizing (26), we will obtain with an accuracy to the

factor, very close to unity,

$$\frac{2\Delta f}{f} = \frac{32}{3} \frac{V}{\lambda_{pe3}^3} \nu_r, \quad (35)$$

where $V = \pi r_0^2 l$ - cylinder capacity.

Losses in the ferrite and the loss AN skin effect in the metallic cylinder can be taken into account, considering the surface impedance Z composite.

If

$$Z = Z_0 e^{i\alpha}, \quad (36)$$

where Z_0 - impedance without taking into account losses, and loss angle $\alpha \ll 1$, then, after making the appropriate linings/calculations, we will obtain

$$\frac{2\Delta f}{f} = \frac{32}{3} \frac{V}{\lambda_{pe3}^3} \nu_r \frac{R_s + R_n}{R_s}, \quad (37)$$

where

$$R_n = \frac{60}{\lambda} \frac{\pi^2}{4kl} \frac{a}{2}.$$

The antennas in question found use, in particular, as the receiving VHF antennas range [8]. Considering these antennas frame, in the work were obtained the expressions for their parameters which can be rewritten as follows:

$$R_{\text{res}} = \frac{(120\pi)^2}{80 (kl)^2} \quad (38)$$

$$\frac{2\Delta f}{f} = \frac{8}{3} \pi^2 y_r \frac{V}{\lambda_{\text{res}}^3} \quad (39)$$

The resistor/resistance, computed from (38), can be considered as the resistor/resistance, introduced into the framework by magnetic Hertz doublet, since for this dipole $R_0 = 80 (kl)^2$.

The effective height of dipole - $2l$. The effective height of radiator/resonator/element with the sinusoidal current distribution with $k_1 l = \pi/2$ is equal to $\frac{4l}{\pi}$. The square of the relation of these effective height, equal to $\left(\frac{2}{\pi}\right)^2$, gives factor to which and they differ from (30), (38) and (35), (39) respectively. Thus, approach to the antenna being investigated as to the frame, can be considered as the first approximation, which does not consider magnetic current distribution along the slot.

Page 117.

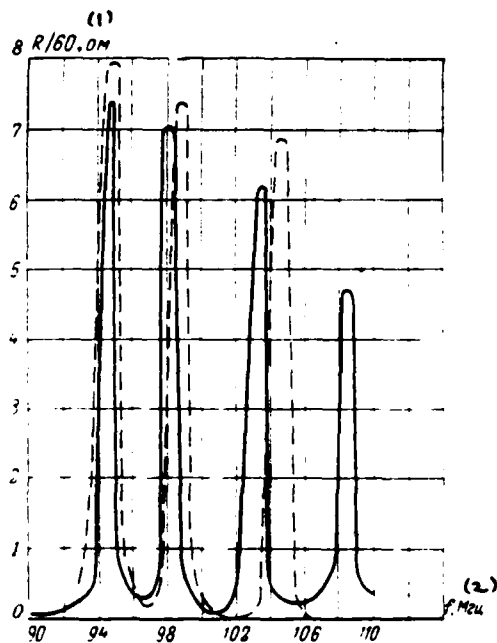


Fig. 2.

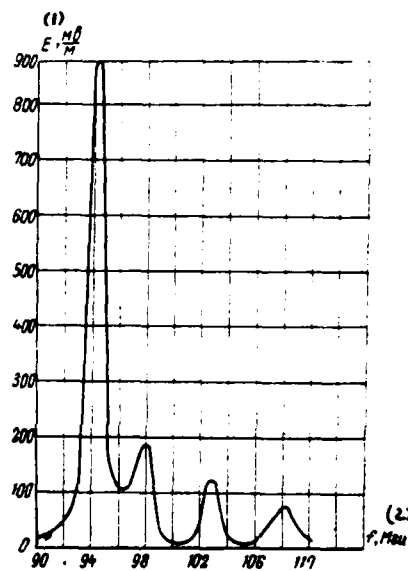


Fig. 3.

Fig. 2.

Key: (1). ohm. (2). f, MHz.

Fig. 3.

Key: (1). E, mV/m. (2). f, MHz.

Page 118.

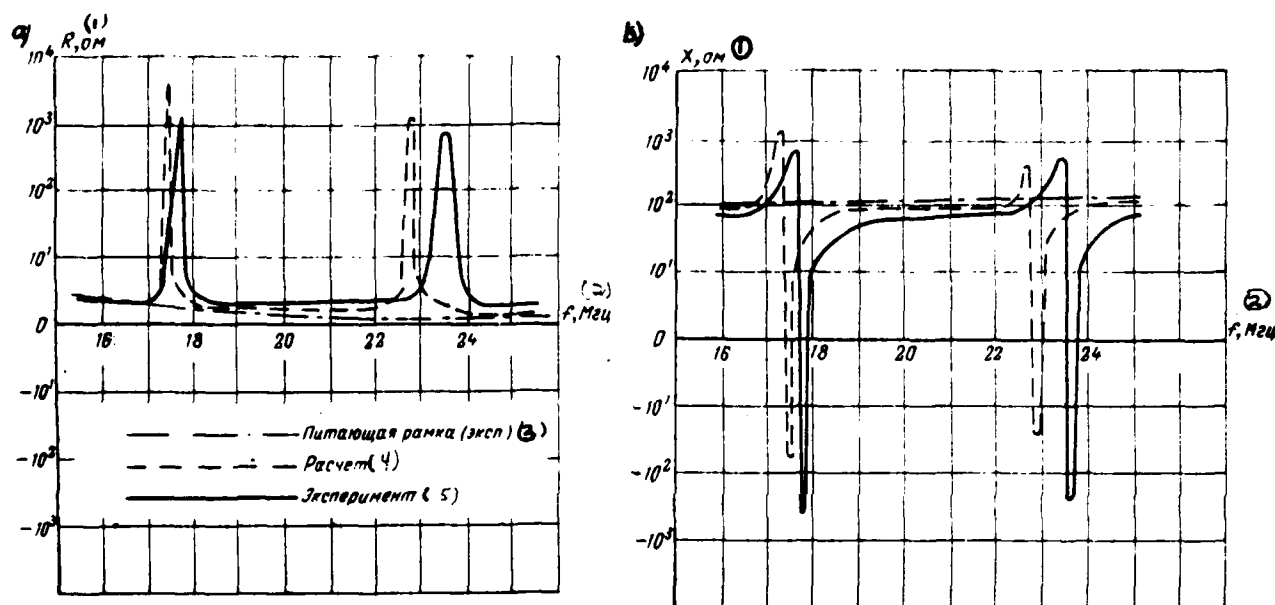


Fig. 4a, b.

Key: (1). ohm. (2). MHz. (3). Feeding framework (exp.). (4). Calculation. (5). Experiment.

Page 119.

Furthermore, this approach does not give the subsequent resonances (with $n=2, 3$, etc.) and cannot explain the dependence of the frequency of the first resonance on the length of antenna, which follows from (31).

The antennas in question were investigated also experimentally. Fig. 2 gives input antenna resistance, the length of $2l=60$ cm, $r_0=2.1$ cm, $2a=1$ cm. Capacity/capacitance was created by capacitors/condensers on 25 and 20 pF, soldered on through one at a distance of 1.2 cm from each other. Dotted curve plotted/applied computed values R , calculated according to (11) taking into account the resistor/resistance of the mast feeding framework. Fig. 3 gives obtained for the same antenna dependence of field in remote zone ($\theta=\pi/2$) on the frequency with the direct current within the feeding framework.

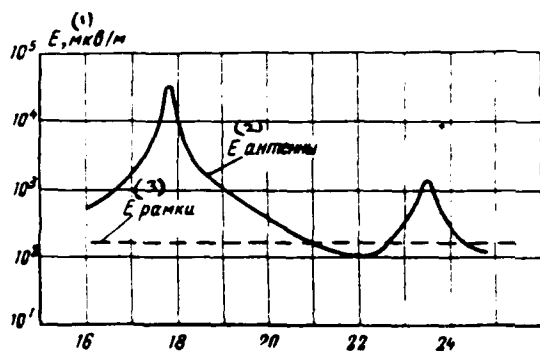


Fig. 5.

Fig. 5.

Key: (1). $\mu\text{V}/\text{m}$. (2). antenna. (3). framework. (4). MHz.

Fig. 6.

Key: (1). mV/m . (2). MHz.

Page 120.

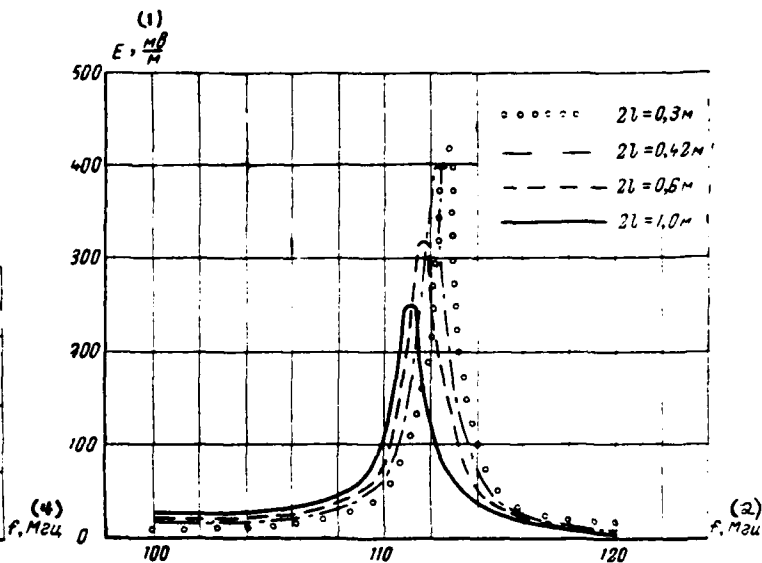


Fig. 6.

Fig. 4 gives the input resistance of another antenna with a length of $2l=2$ m, $r_0=11$ cm, $2a=3$ cm. Capacity/capacitance was created by capacitors/condensers on by 51 pF, soldered on through 2.5 cm. Dotted line designated computed values. The losses AN skin effect during calculations were not considered. Fig. 5 depicts the dependence of field in the reactive zone on the frequency for this antenna.

Fig. 6 gives the experimental dependence of the frequency of the first resonance on the length of antenna ($2a=1$ cm, $r_0=2.1$ cm, capacity/capacitance it was created by capacitors/condensers on 25 pF, soldered on through 2 cm, the lengths of antennas were indicated in the figure).

It is evident that the experimental data confirm well theoretical conclusions.

REFERENCES

1. Гуршковский Э. А., Израйлит А. Б., Левин Б. М., Рабинович Е. Я. «Радиотехника», 1968, т. 23, № 1, стр. 40.
2. Гуршковский Э. А., Левин Б. М., Рабинович Е. Я. «Радиотехника», 1967, т. 22, № 12, стр. 18.
3. Гуршковский Э. А., Израйлит А. Б., Левин Б. М., Рабинович Е. Я. Сборник «Антенны». Вып. 2. Издво «Связь», 1967, стр. 154.
4. Пестельков А. А. Труды НИИИС СВ, 5(40), 1947, стр. 3.
5. Пестельков А. А. «ЖТФ», 1946, т. 16, № 10, стр. 1061.
6. Пестельков А. А. «ЖТФ», 1946, т. 16, № 10, стр. 1087.
7. Миллер М. А. «ЖТФ», 1954, т. 24, № 8, стр. 1483.
8. Schuster G. Archiv. der elektrischen. «Ubertaguny», 1963, v. 17, № 6, p. 289.

Page 121.

Open resonators, formed by confocal mirrors with the variable reflection coefficient and the generalized hyper-spheroidal functions.

N. S. Kosmodamianskaya, V. F. Los'.

Are examined the characteristics of confocal resonator with the rectangular and circular mirrors whose transparency is changed according to the specific law. It is shown that, as for the mirrors with the ideal reflection, in this case problem is reduced to the examination of certain differential equation whose solution is expressed as the generalized hyper-spheroidal functions. Are obtained the asymptotic representations of these of function. Are given the results of calculations.

The characteristics of the resonators, formed by the spherical and plane mirrors of finite dimensions with the ideal reflection

coefficient, it is at the present time studied sufficiently in detail. Obtained in the open resonators with such mirrors rarefaction/evacuation of the spectrum for many applications/appendices proves to be insufficient, since the quality of such systems remains still too high. For achievement of necessary selectivity it is necessary to decrease the size/dimension of mirrors (or limiting diaphragms), which leads to worsening/deterioration in the use of space of active material and decrease of power output. One of the solutions of the problem of increasing the power output with the required selectivity is the method of the isolation/liberation of transverse (but not longitudinal) modes in the resonator from two spherical mirrors with the ideal reflection coefficient, proposed by Yu. V. Tyzhnov. The idea of method consists in the location within the resonator across the longitudinal axis of the latticed absorbing selector. If we select the sizes/dimensions of this selector in such a way that its dissipative elements would coincide with zero transverse mode Ψ_{mn} , then its effect on this mode will be insignificant. At the same time the losses of all remaining modes (including longitudinal ones) because of the absorption in the elements/cells of selector will increase. If they increase so, that will exceed the losses of mode Ψ_{mn} , then it will be possible to carry out a generation on one transverse mode. It is here essential to note that if this isolation/liberation of transverse mode is in principle possible, then it is realized on much the higher level of absolute

losses.

Page 122.

Therefore the method proposed can be used in the quantum generators with the highly active media where the selection of longitudinal modes in the resonators, formed by mirrors with the ideal reflection coefficient, is already barely effective. With this method of selection the field at the output proves to be nonuniform on the amplitude and the phase (in the locations of the dissipative elements of selector phase distribution endures jumps on π) that, generally speaking, it is inadmissible for a whole series of applications/appendices and especially in the systems of optical information processing. True, these deficiencies/lacks partially can be reduced by arrangement/position at the output of the quantum generator of the phase-shifting plate, which converts output distribution into the cophasal. Heterogeneous in the amplitude cophasal distribution has single-lobe radiation pattern with the higher with respect to the even distribution side-lobe level.

It is of interest therefore to consider another path of the selection of oscillations/vibrations under the assumption of the increased ohmic losses in the system, by using the resonators, formed by mirrors with the variable/alternating transparency. With this

method we will approach the isolation/liberation of longitudinal modes, so that here simultaneously we get rid both of the number of deficiencies/lacks in the preceding/previous method and of the need in the supplementary elements/cells for the resonator itself.

Let there be the two-dimensional resonator, which consists of the cylindrical mirrors with the variable coefficient of reflection and with radii of curvature of R_a and R_b , distant behind each other up to distance of L . Sizes/dimensions of mirrors respectively $2a$ and $2b$, and the coefficients of reflection $f(x/a)$ on one mirror and $h(y/b)$ - on the second. Here f and h , generally speaking, complex-valued functions and such, that $|f|, |h| \leq 1$.

In this case for field distribution on the mirrors we will have a system of the integral equations:

$$\begin{cases} \sigma^2 X(x) = \int_{-1}^{+1} \sqrt{\frac{ic}{2\pi}} e^{-i\frac{c}{2}(g_a x^2 + g_b y^2 - 2xy)} h(y) Y(y) dy \\ Y(y) = \int_{-1}^{+1} \sqrt{\frac{ic}{2\pi}} e^{-i\frac{c}{2}(g_a x^2 + g_b y^2 - 2xy)} f(x) X(x) dx \end{cases} \quad (1)$$

where

$$x = z/a, \quad y = r/b, \quad c = 2\pi \frac{ab}{\lambda L}, \quad g_a = \frac{a}{b} \left(1 - \frac{L}{R_a}\right), \quad g_b = \frac{b}{a} \left(1 - \frac{L}{R_b}\right).$$

Modulus/module and phase of the eigenvalues σ^2 of this system determine the transmission factors of energy and the frequency of

steady-state oscillations. For the case of infinite mirrors and gaussian functions f and h the solution of system (1) is examined in [1].

Page 123.

For confocal resonator ($g_a = g_b = 0$) in the case of the dependence of the coefficient of reflection of mirrors from the transverse coordinate in the form $h(y) = (1 - y^2)^l$, $l = 1, 2, \dots$, the solution for the rectangular mirrors is given in [2]. In this article is given the generalization of the given in [2] solutions to the case of arbitrary (including composite) l for the resonators both with the rectangular ones and with the circular mirrors.

Let us consider first mirrors in the form of the infinite bands of the assigned width. Let us show that the solution of the integral equation

$$\nu Z(u, c) = \int_{-1}^{+1} (1 - v^2)^{\alpha} e^{icuv} Z(v, c) dv \quad (2)$$

satisfies the general/common/total spheroidal equation

$$(1 - u^2)Z''(u) - 2(1 + \alpha)uZ'(u) + (d - c^2u^2)Z(u) = 0. \quad (3)$$

In fact, it is not difficult to ascertain that occurs the identity

$$\frac{1}{\nu} \int_{-1}^{+1} (1-x^2)^{\alpha} e^{icxy} \hat{L}X(x) dx = \hat{L}X(y) + (1-x^2)^{1+\alpha} e^{icxy} \{X'(x) - i cy X(x)\} \Big|_{x=-1}^{x=+1}, \quad (4)$$

where

$$\hat{L}X(x) = (1-x^2)X''(x) - 2(1+x)xX'(x) - c^2x^2X(x).$$

Since latter/last component/term/addend in right side (4) is equal to zero, we see that $Z(u)$ and $\hat{L}Z(u)$ satisfy one and the same integral equ. (2). Consequently,

$$\hat{L}Z(u) = -dZ(u),$$

where the constant d does not depend on u . Thus, finally for function $Z(u)$ we have differential equation (3). By replacement $Z(u) = (1-u^2)^{-\frac{\alpha}{2}} S(u)$ equ. (3) is reduced to the form

$$(1-u^2)S''(u) - 2uS'(u) + \left(d + \alpha + \alpha^2 - c^2u^2 - \frac{\alpha^2}{1-u^2}\right)S(u) = 0.$$

hence we conclude that formally $S(u)$ is spheroidal function with the index α . Since at the present time there are tables of spheroidal functions only for the whole values α [3], in the case of arbitrary α the solution of equ. (3) can be sought in the form

$$Z(u) = \sum_{k=0}^{\infty} A_k u^{2k}, \quad Z(u) = \sum_{k=0}^{\infty} C_k u^{2k+1}$$

For the even and odd solutions respectively.

Page 124.

In this case for coefficients A_k and C_k we have recurrence formulae:

$$\left. \begin{aligned} (k+0,5)(k+1)A_{k+1} &= \left[k(k+\alpha+0,5) - \frac{d}{4} \right] A_k + \frac{c^2}{4} A_{k-1} \\ (k+1)(k+1,5)C_{k+1} &= \left[(k+0,5)(k+\alpha+1) - \frac{d}{4} \right] C_k + \frac{c^2}{4} C_{k-1} \end{aligned} \right\} \quad (5)$$

eigenvalues d can be found from the transcendental equation in the form of continued fraction as usually for the trinomial formulas. Therefore finding the eigenfunctions of equ. (3) in the case of arbitrary α is not a bit more difficult than for $\alpha=1, 2, \dots$

Let us note that in the case $\alpha=0.5$ the solution is expressed as Mathieu functions. In fact, on the basis of the integral equation for the odd Mathieu functions

$$Se_n(q, \varphi) = p_n \int_0^\pi \sin \varphi \sin \theta e^{i/2 \sqrt{q} \cos \varphi \cos \theta} Se_n(q, \theta) d\theta$$

and assuming/setting $\cos \varphi = x$, $\cos \theta = y$, we will obtain

$$\frac{Se_n(q, \arccos x)}{(1-x^2)^{1/2}} = p_n \int_{-1}^{+1} (1-y^2)^{1/2} e^{i/2 \sqrt{q} xy} \frac{Se_n(q, \arccos y)}{(1-y^2)^{1/2}} dy,$$

i.e. $\frac{Se_n(q, \arccos x)}{(1-x^2)^{1/2}}$ is spheroidal function on the order of 0.5.

Eigenvalues in the case of arbitrary α after the determination of coefficients A_k and C_k can be calculated according to the formulas

$$\nu = 1 - \frac{\sqrt{ic}}{2\pi} \Gamma(1+\alpha) \sum_0^\infty A_k \frac{\Gamma(k+0.5)}{\Gamma(k+\alpha+1.5)} \quad (5a)$$

for the even functions and

$$v = ic \sqrt{\frac{ic}{2\pi}} \frac{\Gamma(1+\alpha)}{C_0} \sum C_k \frac{\Gamma(k+1.5)}{\Gamma(k+\alpha+2.5)} \quad (56)$$

for the odd ones. Equation (3) is encountered also in other regions, such, as the propagation of acoustic or electromagnetic waves in the presence of ellipsoidal structures, the motion of particle in the presence of two attracting/tightening centers, stochastic processes, etc.

H. L. Schmid [4, 5] completely studied the class of trinomial recurrence formulae, which include relationship/ratio (5). Its results establish/install existence and uniqueness with an accuracy to constant factor for coefficients A_k and C_k , and also the resolution of eigenvalue in the converging series.

Let us note here that although is formal solution $Z_n(u)$ (even with wholes α) it coincides with spheroidal function $S_{\alpha n}(u)$, in reality it has distinct nature.

Page 125.

Actually/really, in the existing literature usually with the wholes α

are examined (and they are tabulated) the functions, in which $n-\alpha \geq 0$ and number of zeros in the fundamental interval is equal $n-\alpha$. In this case with fixed/recorded n the value α can be arbitrary. Therefore we will designate the solution of equ. (3) through $S_{0n}^{(\alpha)}(u)$. Virtually the representation of solution of $Z(u)$ in the form of power series proves to be advisable for the values of value c , which do not exceed 5-6, since at the high values it is necessary to consider already many components/terms/addends (their number is approximately/exemplarily equal to c), and, furthermore, for computing coefficients themselves A_k and C_k in this case is required the knowledge of eigenvalue d with the high accuracy. Otherwise the series/row becomes diverging. It is expedient therefore to obtain more convenient representation for solving of $Z(u)$ with large c . Since ideas the constructions of the asymptotic representation of solutions are identical in the cases of rectangular and circular mirrors in order not to be repeated, let us consider them based on the example of the latter, indicating difference as results in the appropriate places. Most suitable for these purposes method (precise, the greater c) is presented in work [6] in connection with confocal resonator with the ideally reflecting mirrors. Here are generalized the obtained there results for the case of arbitrary ones α and the arbitrary relationships/ratios between n and α . Let us show that the analogous generalization allows/assumes confocal resonator with spherical mirrors of circular section. Actually/really, let there be resonator with the circular mirrors

whose transparency is changed according to the law $(1-y^2)^\alpha$. Then for field distribution on the mirrors we have the integral equation

$$\sigma \tilde{X}(x) = i^{m+1} c \int_0^1 (1-y^2)^\alpha y J_m(cxy) \tilde{X}(y) dy, \quad (6)$$

$$c = 2\pi \frac{r_2}{\lambda L}; \quad x = \xi/r_1; \quad y = \eta/r_2; \quad r_1$$

where Λ and r_2 - radii of the outline of mirrors.

In this case it is assumed that the dependence of field on the azimuthal coordinate is expressed in the form $e^{im\varphi}$, where m - whole number. Equation (6) can be presented in the form

$$\sigma X(x) = i^{m+1} \sqrt{\frac{2c}{\pi}} \int_0^1 (1-y^2)^\alpha j_{m-\frac{1}{2}}(cxy) X(y) dy, \quad (7)$$

where $X(x) = \sqrt{x} \tilde{X}(x)$, $j_{m-\frac{1}{2}}(x) = \sqrt{\frac{\pi x}{2}} J_m(x)$, $J_m(x)$ - Bessel function.

Generalizing results [6], let us introduce operator \hat{L} by means of the equality

$$\hat{L}X(t) = (1-t^2)X''(t) - 2(1+t)tX'(t) - \left(c^2t^2 + \frac{m^2-0.25}{t^2}\right)X(t).$$

Page 126.

Then, using equ. (7) and by the relationship/ratio

$$j_{m-\frac{1}{2}}'(t) + \left(1 - \frac{m^2-0.25}{t^2}\right)j_{m-\frac{1}{2}}(t) = 0,$$

we will obtain the identity

$$\begin{aligned} \frac{i^{m+1}}{\sigma} \sqrt{\frac{2c}{\pi}} \int_0^1 (1-y^2)^\alpha j_{m-\frac{1}{2}}(cxy) \hat{L}X(y) dy &= \hat{L}X(x) + \\ &- (1-y^2)^{\alpha+1} \left\{ j_{m-\frac{1}{2}}(cxy) X'(y) - X(y) \frac{dj_{m-\frac{1}{2}}}{dy} \right\} \Big|_{y=0}^{y=1}. \end{aligned}$$

whence during the usually superimposed requirements for the regularity of function $X(t)$, when expression in the curly braces is equal to zero, we see that the solution of integral equ. (7) satisfies the differential equation (let us name its generalized hyper-spheroidal)

$$(1-t^2)X''(t) - 2(1+t)tX'(t) + \left(d - c^2t^2 - \frac{m^2 - 0.25}{t^2}\right)X(t) = 0. \quad (8)$$

We will seek solution (8) in the form

$$X(t) = \sum_0^{\infty} A_k t^{2k+m+0.5}$$

then for coefficients A_k are obtained following recurrence formulae:

$$\left[\left(k+1+\frac{m}{2}\right)^2 - \left(\frac{m}{2}\right)^2\right]A_{k+1} = \left[\left(k+\frac{m}{2}+\frac{1}{4}\right)\left(k+\frac{m}{2}+\alpha+\frac{3}{4}\right) - \frac{d}{4}\right]A_k + \frac{c^2}{4}A_{k-1},$$

i.e. the methodology of solution (8) in no way differs from the solution of equ. (3). In particular, with $\alpha=0.5$ solution can be expressed through the functions of flattened spheroid.

Actually/really, it is not difficult to be convinced directly that the equation

$$(1-t^2)X''(t) - 2tX'(t) + \left(d - c^2t^2 - \frac{m^2}{1-t^2}\right)X(t) = 0$$

by replacement $t = \sqrt{1-x^2}$; $X(t) = x^{-\frac{1}{2}} \sqrt{1-x^2} \varphi(x)$ is converted to the form

$$(1-x^2)\varphi''(x) - 2\left(1 + \frac{1}{2}\right)x\varphi'(x) + \left(d - \frac{3}{4} + c^2 + c^2x^2 - \frac{m^2 - 0.25}{x^2}\right)\varphi = 0.$$

Page 127.

Hence it is apparent that by analogy with spheroidal functions $t^{1/2}(1-t^2)^{-\frac{1}{2}} S_{mn}(-ic, \sqrt{1-t^2})$ it is possible to name hyper-spheroidal function with index 0.5 $t^{\frac{1}{2}}(1-t^2)^{-\frac{1}{2}} S_{mn}(-ic, \sqrt{1-t^2}) = S_{mn}^{(0.5)}(c, t)$.

As in the case of spheroidal equation, the representation of solution (8) in the form of power series proves to be advisable with $c \leq 6$. Let us attempt therefore to find the convenient representation of the solution of hyper-spheroidal equation in the case large c . Let us assume in (8) $t = x/\sqrt{c}$. As a result we will obtain

$$\hat{p}X - \frac{1}{c}\hat{q}X + \frac{d}{c}X = 0,$$

where operators \hat{p} and \hat{q} are determined by the equalities:

$$\hat{p} = \frac{d^2}{dx^2} - \frac{m^2 - 0.25}{x^2} - x^2, \quad \hat{q} = x^2 \frac{d^2}{dx^2} + 2(1-x^2)x \frac{d}{dx}.$$

The solution of equation $\hat{p}\psi + \gamma\psi = 0$, which has n of zeros in interval

$\varphi = \varphi_{m,n}(x) = x^{m-0.5} e^{-\frac{x}{2}} L_n^m(x^2)$,
 $(0, \infty)$, is function Λ where $L_n^m(x)$ — polynomial of Laguerre
of the n degree, if $\gamma = 4n + 2m + 2$. Therefore it is clear that with large
 c the solution of equ. (9) can be represented in the form

$$\left. \begin{aligned} X_{m,n} &= \varphi_{m,n} + \sum_{k=1}^{\infty} \left(\frac{1}{c}\right)^k Y_k(m, n, x; x) \\ \frac{d_{m,n}(c)}{c} &= 4n + 2m + 2 + \sum_{k=1}^{\infty} \left(\frac{1}{c}\right)^k h_k(m, n, x) \end{aligned} \right\} \quad (10)$$

After using the relationships/ratios between Laguerre's polynomials,
it is not difficult to obtain the relationship/ratio

$$\hat{q} \varphi_{m,n} = a_{m,n}^2 \varphi_{m,n+2} + a_{m,n}^1 \varphi_{m,n+1} + a_{m,n}^0 \varphi_{m,n} + a_{m,n}^{-1} \varphi_{m,n-1} + a_{m,n}^{-2} \varphi_{m,n-2},$$

where

$$\begin{aligned} a_{m,n}^2 &= (n+1)(n+2), & a_{m,n}^{-1} &= -2x(n+m), \\ a_{m,n}^1 &= 2x(n+1), & a_{m,n}^{-2} &= (n+m)(n+m-1), \\ a_{m,n}^0 &= -\left[(2n+1)\left(n+m+\frac{1}{2}\right) + \left(x + \frac{3}{4}\right)\right]. \end{aligned}$$

Page 128.

Let us substitute expansion (10) into equ. (9) and will equate zero
expressions with the identical degrees of c . As a result we will
obtain system of equations:

$$\left. \begin{aligned} \hat{p} \varphi_{m,n} + (4n + 2m + 2) \varphi_{m,n} &= 0 \\ \hat{p} Y_k + (4n + 2m + 2) Y_k &= \hat{q} Y_{k-1} - \sum_{j=1}^k h_j Y_{k-j}, Y_0 = \varphi_{m,n} \end{aligned} \right\} \quad (11)$$

After assuming now

$$Y_k(m, n, x; x) = \sum_{i=-2k}^{+2k} A_i^k \varphi_{m, n+i}$$

and after substituting in (11), after the equating of factors with identical numbers $\varphi_{m, n}$ we will obtain recurrence formulae for determining the values A_i^k and h_k :

$$h_k = \sum_{p=-2}^2 a_{m, n-p}^p A_{-p}^{k-1},$$

$$4sA_s^k = \sum_{j=1}^k h_j A_s^{k-j} - \sum_{l=-2}^2 a_{m, n+s-l}^l A_{s-l}^{k-1},$$

$$\left(\begin{matrix} k-1, 2, \dots \\ s = -2k, -2k+1, \dots, 2k \end{matrix} \right).$$

Hence, in particular, we find

$$h_1 = a_{m, n}^0 = - \left[(2n+1) \left(n+m+\frac{1}{2} \right) + \left(x + \frac{3}{4} \right) \right], \quad A_0^1 = 0,$$

$$A_{-2}^1 = \frac{1}{8} (n+m)(n+m-1), \quad A_1^1 = -\frac{1}{2} x (n+1),$$

$$A_{-1}^1 = -\frac{1}{2} x (n+m), \quad A_2^1 = -\frac{1}{8} (n+1)(n+2),$$

$$h_2 = -\frac{1}{4} (m+2n+1) [2n^2 + 2n(m+1) + m+2 - 4x^2].$$

Solution takes the form

$$X_{m, n}^1(t) = \varphi_{m, n}(x) + \sum_{k=1}^{\infty} \left(\frac{1}{c} \right)^k \sum_{p=-2k}^{2k} A_p^k \varphi_{m, n+p}, \quad x = \sqrt{c} t. \quad (12)$$

The right side of expression (12) after return to initial by the

AD-A106 474 FOREIGN TECHNOLOGY DIV WRIGHT-PATTERSON AFB OH
ANTENNA (SELECTED ARTICLES). (U)
OCT 81 L A VENGROVICH, L D BAKHRAKH
UNCLASSIFIED FTD-ID(RS)T-0821-81

F/G 9/1

NL

2 of 2

AC
200-100



END
DATE
FILMED
11-81
DTIC

variable/alternating t already more is not arranged/located according to degrees of c^{-1} , since $\varphi_{m,n+1}(\sqrt{c}t)/\varphi_{m,n}(\sqrt{c}t) \sim O(\sqrt{c})$. Therefore range of values t , for which the asymptotic representation of solution given above correctly reflects the behavior of true integral (8), decreases with an increase in number c .

Page 129.

Nevertheless fairly often this representation they use to entire the fundamental interval, which leads to the inaccuracies at the end/lead of the interval. We will use expression (12) for $t < c^{-\frac{1}{4}}$.

If we will assume in (8) $X_{m,n}(t) = t^{m+n} Z_{m,n}(t)$ and $y = \sqrt{1-t^2}$, then we will obtain the representation of solution in interval $c^{-\frac{1}{4}} \leq t \leq 1 - c^{-1}$. As a result of this replacement equ. (8) will pass in

$$(1-y^2)Z'' + \left[\frac{1+2a}{y} - y(2m+3+2a) \right] Z' + \left[d - c^2 + c^2 y^2 - \left(m + \frac{1}{2} \right) \left(m + \frac{3}{2} + 2a \right) \right] Z = 0. \quad (13)$$

Let us substitute the here obtained above expression for eigenvalue of d and will introduce function Y by the relationship/ratio

$$Z = (1-y)^a (1+y)^{-(m+n+1)} y^{-(a+\frac{1}{2})} e^{cy} V.$$

Making again all linings/calculations which in view of their unwieldiness we omit, we will obtain for function Y the equation

$$\frac{d^2}{dy} + O\left(\frac{1}{c}\right) = 0,$$

whence approximately we can assume

$$X_{m,n}^2(t) \approx \frac{t^{m+0.5} (1-y)^n e^{cy}}{y^{\frac{a+1}{2}} (1+y)^{m+n+1}}, \quad y = \sqrt{1-t^2}, \quad c^{-\frac{1}{4}} \leq t \leq 1 - c^{-1}.$$

Let us determine now coupling coefficient between functions $X_{m,n}^1(t)$ and $X_{m,n}^2(t)$. For this let us assume $t = \frac{z}{\sqrt{c}}$ and with fixed/recorded z we will increase c . As a result we will obtain the representations:

$$X_{m,n}^1\left(t = \frac{z}{\sqrt{c}}\right) \sim (-1)^n c^{\left(2n+m+\frac{1}{2}\right)/4} z^{2n+m+\frac{1}{2}} \frac{e^{-\sqrt{c} z^2/2}}{n!},$$

$$X_{m,n}^2\left(t = \frac{z}{\sqrt{c}}\right) \sim c^{-\left(2n+m+\frac{1}{2}\right)/4} z^{2n+m+\frac{1}{2}} e^c \frac{e^{-\sqrt{c} z^2/2}}{2^{2n+m+1}}.$$

Thus, functions $X_{m,n}^1$ and $k_2 X_{m,n}^2$ at the high values of c will continuously pass into each other, if we assume

$$k_2 = \frac{(-1)^n \sqrt{2} e^{-c}}{n!} (4c)^{\left(2n+m+\frac{1}{2}\right)/2}.$$

It is evident that near the center of mirror with large c the presence of variable/alternating transmission in the zero approximation does not affect field distribution.

For obtaining the asymptotic form of solution near $t=1$ let us assume in equ. (13) $y = \frac{u}{c}$, as before utilizing the obtained above

expression for the eigenvalue. In this case equ. (13) can be presented in the form

$$\frac{d^2 Z}{du^2} + \frac{1+2u}{u} \frac{dZ}{du} - Z + O\left(\frac{1}{u}\right) = 0,$$

so that

$$X_{m,n}^3(t) \sim t^{m+0.5} (cy)^{-\alpha} I_{\alpha}(cy), \quad y = \sqrt{1-t^2}.$$

where $I_{\alpha}(x)$ — modified Bessel function of pure imaginary argument.

Joining $k_2 X_{mn}^2$ and $k_3 X_{mn}^3$ when $y = v/\sqrt{c}$, we will obtain coupling coefficient between them. We have (considering that with fixed/recorded v value c is great):

$$X_{m,n}^2(y = v/\sqrt{c}) \sim c^{(\alpha+0.5)/2} e^{\sqrt{c}v} v^{-(\alpha+0.5)},$$

$$X_{m,n}^3(y = v/\sqrt{c}) \sim (2\pi)^{-\frac{1}{2}} c^{-(\alpha+0.5)/2} e^{\sqrt{c}v} v^{-(\alpha+0.5)},$$

so that asymptotic equality $k_2 X_{m,n}^2 = k_3 X_{m,n}^3$ will occur when $k_3 = \sqrt{2\pi} c^{(\alpha+0.5)} k_2$

since

$$\lim_{y \rightarrow 0} (cy)^{-\alpha} I_{\alpha}(cy) = \frac{1}{2^{\alpha} \Gamma(1+\alpha)}.$$

then for the value of function $k_3 X_{m,n}^3$ on the edge of mirror ($t=1$) we obtain

$$k_3 X_{m,n}^3(c, 1) = \frac{(-1)^n \sqrt{\pi}}{n! \Gamma(1+\alpha)} 2^{2n+m-\alpha+\frac{3}{2}} c^{\frac{1}{2}(2n-2\alpha+m+\frac{3}{2})} e^{-c}.$$

Thus, the value of field on the edge of the mirror inside the resonator when the variable coefficient of reflection of form is present, $(1-x^2)^{\alpha}$ grows/rises $\frac{c}{2}^{\alpha} |\Gamma(1+\alpha)|$ once in comparison with the value of field in the resonator, formed by mirrors with the ideal reflection coefficient.

Let us note that during here writing of integral equation accepted function $X(x)$ describes the behavior of the wave front of field directly before the absorbing surface within the resonator on the way to mirror. After being reflected from the mirror and, thus, having twice passed the absorbing surface, this wave front forms/shapes field directly before the absorbing surface in another mirror.

Page 131.

Introduced further function $\tilde{X}(x) = (1-x^2)^{\alpha/2} X(x)$ describes the field between the mirror and the absorbing surface. Let us rewrite equ. (7) in the form

$$\rho X(x) (1-x^2)^{\alpha/2} = \int_0^1 (1-x^2)^{\alpha/2} (1-y^2)^{\alpha/2} K(cxy) X(y) (1-y^2)^{\alpha/2} dy.$$

(14)

where $\rho = \frac{\sigma}{i^m+1} \sqrt{\frac{\pi}{2c}}$, $K(t) = j_{m-\frac{1}{2}}(t)$, and let us attempt to determine the asymptotic behavior $p(c)$ with large c . For this let us differentiate both sides of equ. (14) first on c , and then on x . As a result we will obtain:

$$\begin{aligned} \frac{\partial p}{\partial c} \tilde{X} + p \frac{\partial \tilde{X}}{\partial c} &= \int_0^1 (1-x^2)^{\alpha/2} (1-y^2)^{\alpha/2} xy K'(cxy) X(y) dy + \\ &+ \int_0^1 (1-x^2)^{\alpha/2} (1-y^2)^{\alpha/2} K(cxy) \frac{\partial \tilde{X}(y)}{\partial c} dy, \\ p \frac{\partial \tilde{X}}{\partial x} &= \int_0^1 cy (1-x^2)^{\alpha/2} (1-y^2)^{\alpha/2} K'(cxy) \tilde{X}(y) dy - \\ &- \frac{\alpha X}{1-x^2} \int_0^1 (1-x^2)^{\alpha/2} (1-y^2)^{\alpha/2} K(cxy) \tilde{X}(y) dy, \\ \tilde{X}(t) &= (1-t^2)^{\alpha/2} X(t), \end{aligned}$$

or

$$\begin{aligned} \frac{\partial p}{\partial c} \tilde{X} + p \frac{\partial \tilde{X}}{\partial c} &= \frac{x}{c} p \frac{\partial \tilde{X}}{\partial x} + \frac{\alpha}{c} \frac{x^2}{1-x^2} p \tilde{X} + \int_0^1 (1-x^2)^{\alpha/2} \\ &\times (1-y^2)^{\alpha/2} K(cxy) \frac{\partial \tilde{X}}{\partial c} dy. \end{aligned}$$

After multiplying both parts of this equality to $\tilde{X}(x, c)$ and after integrating from 0 to 1, we will obtain

$$\begin{aligned} \frac{\partial p}{\partial c} \|\tilde{X}\|^2 &= \frac{p}{c} \left\{ \frac{1}{2} \left[x \tilde{X}^2(x, c) \right]_{x=0}^{x=1} - \|\tilde{X}\|^2 \right\} + \\ &+ \alpha \int_0^1 \frac{\tilde{X}^2(x)}{1-x^2} dx - x \|\tilde{X}\|^2, \quad \|\tilde{X}\|^2 = \int_0^1 \tilde{X}^2(x) dx. \end{aligned}$$

Hence already it is possible to do a conclusion about different character of dependence of losses in cases $\alpha=0$ and $\alpha \neq 0$. Actually, when $\alpha=0$ we have

$$\frac{\partial p}{\partial c} = \frac{p}{2c} \left[\frac{X^2(c, 1)}{\|X\|^2} - 1 \right].$$

In the approximation/approach in question the norm of function $\|X(t)\|^2$ is determined in essence by contribution from $X_{m,n}^1(c, t)$, so that

$$\|X\|^2 \cong \frac{1}{1/c} \int_0^c e^{-t^2} t^{2m+1} [L_n^m(t^2)]^2 dt \cong \frac{\Gamma(n+m+1)}{2\sqrt{c}\Gamma(n+1)}.$$

Thus, for eigenvalue of $p(c)$ finally we have

$$\sqrt{\frac{2}{\pi}} p \cong \text{const} \frac{1}{1/c} e^{-\frac{\pi \cdot 2^{4n+2m+2}}{\Gamma(n+1)\Gamma(n+m+1)}} e^{-2c} c^{2n+m+1}$$

Since the losses in the system with $c=\infty$ are absent, the present here constant is equal to unity. Using the fact that with large c the index of exponential curve - small number, we obtain

$$\sqrt{\frac{2}{\pi}} p_n(c) \cong \frac{1}{1/c} - \frac{\pi \cdot 2^{4n+2m+2}}{\Gamma(n+1)\Gamma(n+m+1)} c^{2n+m+1} e^{-2c}.$$

It is evident, thus, that the losses in systems are determined by the intensity of field on the edge of mirror, through which occurs leakage of energy. Let us consider now the case $\alpha \neq 0$. For the mirrors with the variable/alternating transparency we have

$$\frac{\partial p}{\partial c} = -\frac{p}{2c} \left\{ (1+2x) - 2x \frac{1}{\|x\|^2} \int_0^1 \frac{\tilde{X}^2(x)}{1-x^2} dx \right\}. \quad (15)$$

Since function $X(x)$ is final with $x=1$, for any $\alpha > 0$ integral in right side (15) converges and losses, thus, are determined by the values of the intensity of field $X^2(x)$ on the entire surface of mirror, but not only on the edges. This undoubtedly it answers the physical essence of problem, since in the presence of variable/alternating transparency in the mirrors of resonator energy passes through the mirrors (or it is absorbed) on the entire surface.

Let us rate/estimate integral in the curly braces of equality (15). Since fundamental contribution introduces function $X_{m,n}^1(c, x)$, then approximately we have

$$\begin{aligned} \frac{1}{\|X\|^2} \int_0^1 \frac{\tilde{X}^2(x) dx}{1-x^2} &\approx \frac{1}{\|X\|^2} \int_0^{\frac{1}{c}} \frac{\tilde{X}^2(x) dx}{1-x^2} \approx \\ &\approx 1 + \frac{1}{\|X\|^2} \int_0^{\frac{1}{c}} x^2 \tilde{X}^2(x) dx = 1 + \frac{1}{2c} \frac{1}{\|X\|^2} \int_0^{\frac{1}{c}} e^{-x} x^{(m+1)} [L_n^m(x)]^2 dx. \end{aligned}$$

Page 133.

Since c is great, it is possible to use the equality

$$\begin{aligned} \int_0^\infty e^{-x} x^{m+1} [L_n^m(x)]^2 dx &= \frac{(m+1) \Gamma(n+m+1)}{\Gamma^2(n+1)} \\ &\times \left[\frac{d^n}{dy^n} \left[\frac{F\left(\frac{2+m}{2}, \frac{m+3}{2}, m+1; \frac{4y}{(1+y)^2}\right)}{(1+y)^{m+2}} \right] \right]_{y=0} \end{aligned}$$

where $F(a; b; c; z)$ - hypergeometric function. Thus,

$$\ln p \cong \ln \frac{1}{1-c} - \frac{\alpha(m+1)}{c\Gamma(1-n)} a_n^m - \ln \sqrt{\frac{2}{\pi}}$$

where

$$a_n^m = \frac{d^n}{dy^n} \left[\frac{F\left(1 + \frac{m}{2}, \frac{m}{2} + \frac{3}{2}; m+1; \frac{4y}{(1-y)^2}\right)}{(1+y)^{2+m}} (1-y) \right]_{y=0}$$

or

$$\sqrt{\frac{2}{\pi}} p = \text{const} \frac{1}{1-c} \left(1 - \frac{(1+m)}{\Gamma(1-n)} a_n^m \frac{\alpha}{c} \right).$$

Are here left two terms of the expansion of exponent into series/row, since with fixed/recorded m , n , α and large c second term is small. The being present here constant, as in the case $\alpha=0$, it is equal to unity. This can be comprehended from the following considerations: in spite of the absence of ideal reflection from the mirrors of resonator modes of vibration with increase c brace themselves to the center of mirror, so that in the limit they are degenerated into the infinitesimally narrow peak, which occupies position $t=0$, where the reflection coefficient is equal to one. Therefore with $c=\infty$ losses in such a system as before will not be. This fact will occur not only for the confocal geometry, but also for any resonator, formed by spherical mirrors of an arbitrary radius

(but not by the flat/plane or to them equivalent) and locating in the stability region.

Thus, finally we obtain

$$\sigma_{mn} \approx i^{2n+m+1} \left(1 - \frac{1+m}{n!} a_n^m \frac{a}{c} \right). \quad (16)$$

Page 134.

The corresponding relationship/ratio for the resonator in the form of infinite bands will be

$$\sigma_n \approx i^n \left(1 - (2n+1) \frac{a}{2c} \right). \quad (17)$$

Hence, in particular, for the fundamental oscillation we obtain, which in this approximation/approach of loss in the resonator with the circular mirrors is two times more.

The account of variable reflection coefficient for the eigenvalue of equ. (3) leads to the representation

$$d \approx (2n+1)c - \left[\frac{n(n+1)}{2} + a + \frac{3}{4} \right] + \frac{1}{2c} (2n+1) \times \\ \times \left[a^2 - \frac{n^2+n+3}{8} \right].$$

In Fig. 1 and 2 are constructed according to formulas (5a) and (5b) the square modulus of the eigenvalues σ with $\alpha=0.5$; 1.5; 2.0; 2.5. Are there for the comparison given the values for $\alpha=0$ and $\alpha=1$,

undertaken from work [2].

Fig. 3 gives the eigenfunctions of resonator with the mirrors in the form of infinite bands for $\alpha=0; 0.5; 1.0; 1.5; 2.0; 2.5$ with $c=4$. Is evident the increase of effective radius of field distribution with the post α .

Fig. 4 depicts the results of calculating the square moduluses $|\sigma_0|^2$ for the same values α .

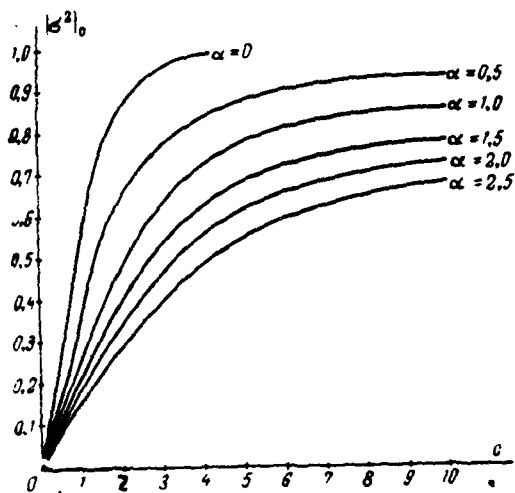


Fig. 1.

Page 135.

Let us note also that the diagram of the solution of equ. (3) and (8) remains previous and when α -composite number. A change in the coefficient of reflection of mirror according to the law $(1-l^2)^{\alpha+1/2}$ will be equivalent in this case to a usual change in the coefficient of reflection of mirrors according to the law $(1-l^2)^{\alpha}$ and certain of their curve.

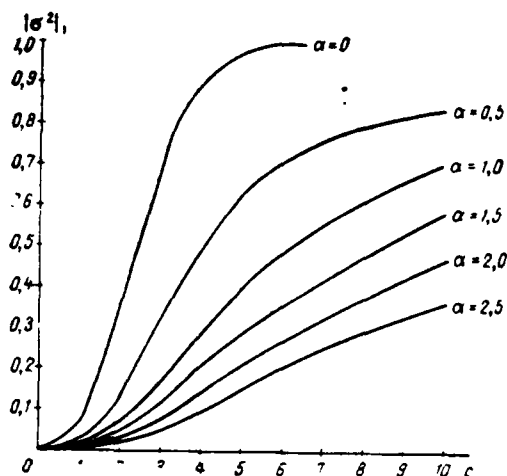


Fig. 2.

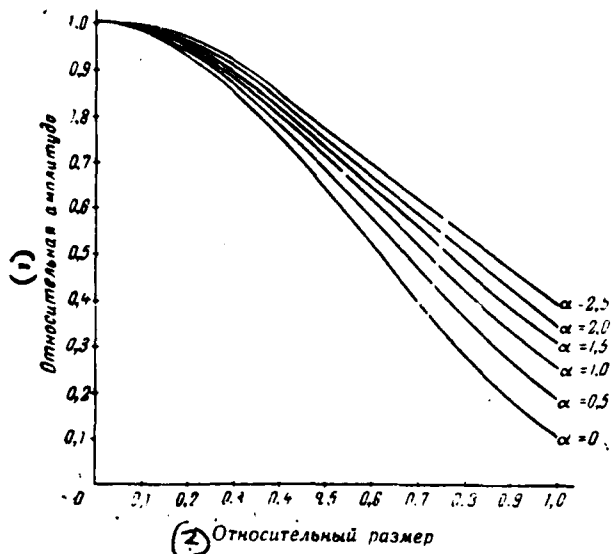


Fig. 3.

Key: (1). Relative amplitude. (2). Relative size/dimension.

Page 136.

If we present the form of the mirrors of symmetrical resonator in the form $z_1(x) = \frac{a^2}{2L} f(x)$, $z_2(y) = L - \frac{a^2}{2L} f(y)$, then it is easy to ascertain that factor $(1-l^2)^{1/2}$ leads to the curve of the form of the mirrors of confocal resonator, determined by the relationship/ratio

$$f(x) = x^2 + \frac{B}{c} \ln(1 - x^2).$$

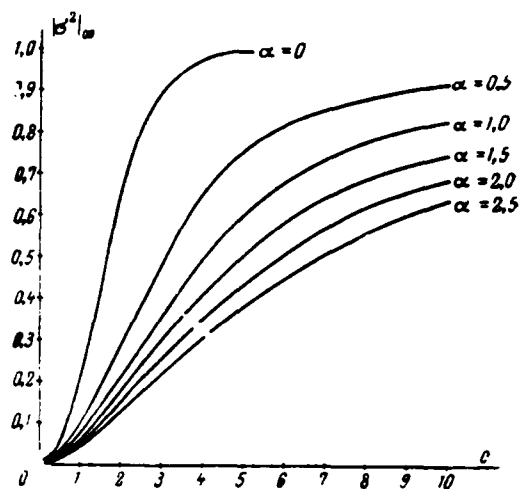


Fig. 4.

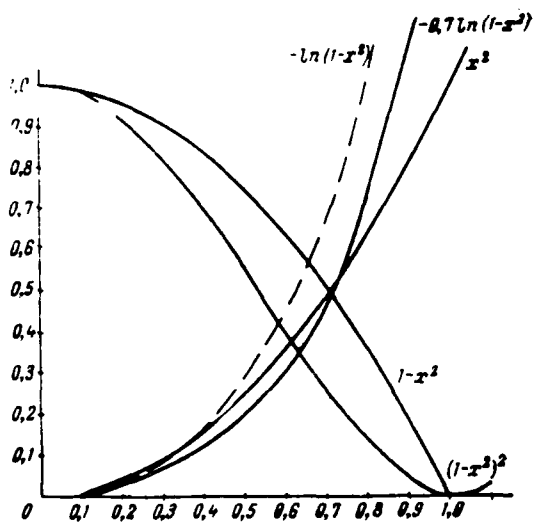


Fig. 5.

Hence it is apparent that this change in the reflection coefficient does not answer physically correct problem, since with $x \rightarrow 1$ the divergence of the form of mirror from the plane approaches infinity. However, as show to Fig. 5, on the larger part of the surface of mirror (up to 0.8-0.85) the value $-0.7 \ln(1-x^2)$ comparatively little differs from x^2 ; therefore it is possible to expect that the solutions, obtained from (3) and (8) with the composite α , will satisfactorily describe the resonators, formed by spherical mirrors of arbitrary radius of curvature.

Fig. 6 and 7 depict the results of calculation for $c=3$, $A=0$, $B=2.1$, which approximately corresponds to the resonator, formed by flat/plane mirrors. There for the comparison (broken lines) are presented the results for the exact solution of flat/plane resonator. It is evident that the coincidence is satisfactory, with exception of the behavior of phase on the edges of mirrors.

From a theoretical point of view the resonators examined are interesting in that the integral equation for them is reduced to the differential whose solution simpler and with the small numbers c ($c \leq 6$) is obtained rapidly by the method of continued fractions. For large c it is possible to use asymptotic representation.

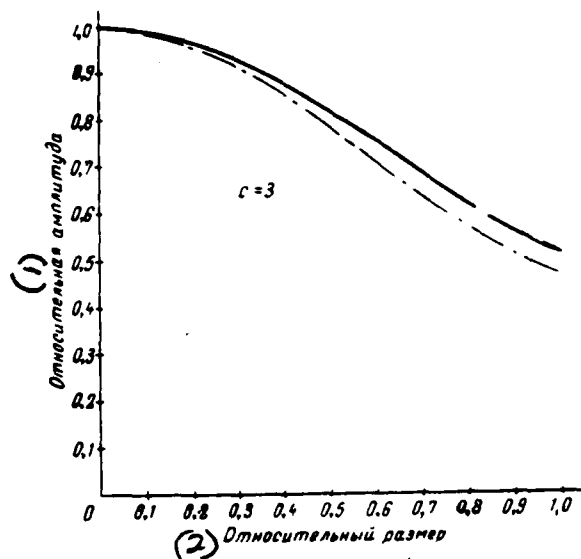


Fig. 6.

Key: (1). Relative amplitude. (2). Relative size/dimension.

Page 138.

However, from the practical side the resonators with the variable reflection coefficient from the mirrors make it possible to obtain the supplementary rarefaction/evacuation of the spectrum. Let us compare the given results with the results, obtained in work [1], where the coefficient of reflection of mirrors is accepted by that changing according to the law $e^{-2\left(\frac{x}{a}\right)^2}$. In the approximation/approach in

question for the confocal resonator accordingly [1] we have

$$|\sigma| = 1 - (2n + 1) \frac{1}{c}.$$

Comparing this expression with (17), we see that with $\alpha > 2$ it is possible to ensure large selectivity. In work [1] the parameter α defines simultaneously both the character of a change in the reflection coefficient and effective size/dimension of mirrors (i.e. parameter c). In this case there is one additional parameter, namely α . Since the value α is inexpedient to select too large, then it is clear that the law of a change in the selectivity little is sensitive to the law of a change in the coefficient of reflection of mirrors.

For the comparison of selectivity with the nonconfocal geometries (in this case with the composite ones α) it is necessary in formula (15) to take into account the members of order $1/c^2$.

The authors are grateful to L. A. Weinstein for the attention to the work.

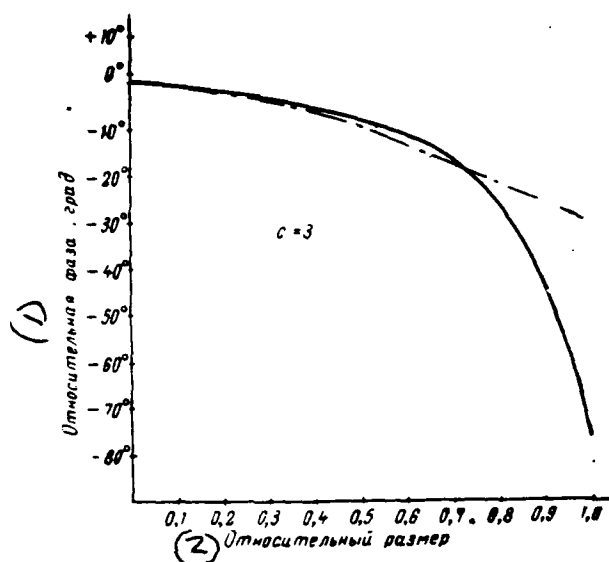


Fig. 7.

Key: (1). Relative phase deg. (2). Relative size/dimension.

Page 139.

REFERENCES.

1. Вахитов Н. Г. Открытые резонаторы с зеркалами, обладающими переменным коэффициентом отражения. «Радиотехника и электроника», 1965, т. X, № 9, стр. 1676—1683.
2. Власов С. Н. Резонаторы с зеркалами с переменным коэффициентом отражения. «Радиотехника и электроника», 1965, т. X, № 9, стр. 1715—1718.
3. Фламммер К. Таблицы сферических функций. ВЛ АН СССР, 1962.
4. Schmid H. L. «Mathematische Nachrichten», 1948, № 1, S. 377—398.
5. Schmid H. L. «Mathematische Nachrichten», 1949, № 2, S. 35—44.
6. Slepian D. Prolate Spheroidal Wave Functions, Fourier Analysis and Uncertainty-IV: Extensions to Many Dimensions: Generalized Prolate Spheroidal Functions. «The Bell System Technical Journal», Nov. 1946, v. 43, № 6, p. 3009—3057.

Page 140.

Method of the study of complex waveguide junctions with one or several regions of communication.

S. V. Butakova.

Is obtained the formula of the scattering matrix of the connections of regular waveguides with the heterogeneities, which makes it possible to perform the calculation of different plumbing on the computer(s) with any preset accuracy. are brought out the particular formulas of the scattering matrices of several devices/equipment SVCh in rectangular waveguide with waves H_{me} .

Introduction.

In different waveguide diagrams extensively is used slotted bridge [1, 2] and waveguide development on 180° [2]. The simplest slotted bridge consists of the pair of rectangular waveguides of identical height, which have the general/common/total narrow wall, theoretically infinitely thin, from which is distant the cut by

length l . Formed thus wide waveguide by length l call region connections/communications. During the specific selection of the relationships/ratios between the sizes/dimensions of waveguides, the length of the region of connection/communication and the wavelength two of adjacent arm prove to be untied, and in other two arms high-frequency energy is divided in the preset sense.

Waveguide development can be obtained from the slotted bridge by installing a short-circuiting plate in the transverse jointing plane of wide waveguide with the narrow ones. In the waveguide development geometric dimensions are selected from the condition that entire/all energy from one arm passes into another at the preset wavelength. Are known the methods of calculation of these devices/equipment of simplest form [1, 2].

Real bridge and development differ from ideal ones in terms of the final wall thickness between the narrow waveguides. Furthermore, for an improvement in the range properties in the bridge and the development usually provide for elements/cells agreements. As the latter sometimes are utilized the steps in the region of connection/communication (an abrupt change in the cross section of wide waveguide). The calculation of bridge and development of complex form is absent.

For the study of bridge and development let us use the detailed apparatus of linear-network theory. From the point of view of this theory the devices/equipment being investigated are the multiples a number of terminals/grippers of which is equal to a total quantity of taken into consideration its own waves in four bridge arms or in two arms of development. In the theory of circuits the devices/equipment dismember to the separate sufficiently simple elements/cells and by at first any method are determined the scattering matrices of these elements/cells. Then, utilizing connection conditions, find scattering matrix devices/equipment as a whole [1-6].

Page 141.

Let us divide bridge and development by transverse planes so as to separate/liberate the regular cuts of waveguides from the heterogeneities. For example, it is possible to isolate two waveguide joints and regular regions of the wide waveguide of connection/communication. Let us assume that it was possible to find the scattering matrices of heterogeneities, in reference to the limiting planes. For the determination of full/total/complete scattering matrix as conveniently it is accurately necessary to consider the following special features/peculiarities of the connecting waveguides.

With the incidence/drop on the heterogeneity of any own type of waves in the adjacent waveguides is excited denumerable set of natural waves. Each its own wave is characterized by different from by another phase velocity (with exception of the degenerate modes). Therefore, after covering a distance from one heterogeneity to another, each of modes acquires different phase displacement, proportional to their longitudinal wave number.

In the existing works where is used the analogous method of the separation of plumbing in the regular and irregular regions, waveguides were examined in the form of long lines, since was considered the single propagated transmission mode [7, 8]. This simplification is useful only when the heterogeneities are arranged/located sufficiently far from each other. The simplification indicated cannot be used in the case when in the regular waveguides can be propagated two and more than waves.

The purpose of this work was the development of the method of computing the scattering matrix complicated waveguide junction taking into account special features/peculiarities indicated above and the use/application of a method for obtaining the scattering matrix of slotted bridge and waveguide development with two H-plane jumps of cross section in the region of connection/communication upon consideration of the general/common/total wall thickness of two

waveguides. In the latter case was utilized the exact solution of the electrodynamic task about the wave diffraction on the edge of the infinitely thin ideally conducting semi-infinite plate, placed into infinite rectangular waveguide in parallel to narrow wall. Scattering matrix of the joint of wide waveguide with two narrow ones in the transverse plane, passing through the edge of plate. It was obtained in work [2] by Wiener-Hopf-Foch's method.

General method of the solution of problem.

Let us examine the waveguide junction, shown in Fig. 1. In the region of connection/communication S_1 converge the semi-infinite regular waveguides A, ..., B, ..., C and the cuts of the regular waveguides T, V, W ..., which connect S_1 with the regions of connection/communication S_2, S_3, S_4 ... and having lengths l_1, l_2, l_3 Waveguides D, ..., F, ..., G; K, ..., M, ..., N; P, ..., Q, ..., R, ..., which converge in S_2, S_3, S_4 , regular, semi-infinite. Small letters in Fig. 1 designated transverse boundary planes, relative to which are determined the scattering matrices of the regions of connection/communication $\bar{S}_1, \bar{S}_2, \bar{S}_3, \bar{S}_4$...

Page 142.

Let us find the scattering matrix \bar{S} of complicated waveguide

junction (Fig. 1) from the known scattering matrices of the regions of connection/communication, the longitudinal wave numbers of its own waves of the waveguides of connection/communication T, V, W ... and the preset lengths l_1, l_2, l_3, \dots

By analogy with works [3, 6] let us compose of the coefficients of girders $\bar{S}_1, \bar{S}_2, \bar{S}_3, \dots$ compound matrix/die \bar{S}_c . It are conveniently composed so that it would be possible to break into the cages by the horizontal and vertical solid lines, which separate/liberate the submatrices, which relate to the boundary planes of semi-infinite waveguides, from the submatrices, which relate to the boundary planes of the waveguides of connection/communication. In accordance with that presented compound matrix/die \bar{S}_c can be presented in the form of the cell matrix/die:

$$\begin{array}{c}
 I \text{ II} \dots \dots \dots Z, 1, 2, \dots p, p+1, \dots, 2p \\
 a, b, c, d, f, g, k, m, n, p, q, r, t, v, w, \tau, \varphi, \psi \\
 \begin{array}{c}
 I \\
 a \\
 b \\
 c \\
 d \\
 f \\
 g \\
 k \\
 m \\
 n \\
 p \\
 q \\
 r \\
 t \\
 v \\
 w \\
 \tau \\
 \varphi \\
 2p \\
 \psi
 \end{array}
 \begin{array}{c}
 \bar{\gamma}_{11} \quad 0 \quad 0 \quad 0 \quad \bar{\gamma}_{12} \quad 0 \quad 0 \quad 0 \\
 0 \quad \bar{\gamma}_{11} \quad 0 \quad 0 \quad 0 \quad \bar{\gamma}_{12} \quad 0 \quad 0 \\
 0 \quad 0 \quad \bar{\epsilon}_{11} \quad 0 \quad 0 \quad 0 \quad \bar{\epsilon}_{12} \quad 0 \\
 0 \quad 0 \quad 0 \quad \bar{\epsilon}_{11} \quad 0 \quad 0 \quad 0 \quad \bar{\epsilon}_{12} \\
 \bar{\gamma}_{21} \quad 0 \quad 0 \quad 0 \quad \bar{\gamma}_{22} \quad 0 \quad 0 \quad 0 \\
 0 \quad \bar{\gamma}_{21} \quad 0 \quad 0 \quad 0 \quad \bar{\gamma}_{22} \quad 0 \quad 0 \\
 0 \quad 0 \quad \bar{\epsilon}_{21} \quad 0 \quad 0 \quad 0 \quad \bar{\epsilon}_{22} \quad 0 \\
 0 \quad 0 \quad 0 \quad \bar{\epsilon}_{21} \quad 0 \quad 0 \quad 0 \quad \bar{\epsilon}_{22}
 \end{array}
 \end{array}
 = \left[\begin{array}{cc} \bar{S}^{\alpha\alpha} & \bar{S}^{\alpha\beta} \\ \bar{S}^{\beta\alpha} & \bar{S}^{\beta\beta} \end{array} \right] \quad (1)$$

Here $\bar{\gamma}_{11}, \bar{\gamma}_{12}, \bar{\epsilon}_{11}, \bar{\epsilon}_{12}, \dots$ — the cages of matrices/dies $\bar{S}_1, \bar{S}_2, \bar{S}_3, \bar{S}_4, \dots$; indices α relate to the boundary planes of semi-infinite waveguides; indices β — to the boundary planes of the waveguides of connection/communication.

Page 143.

In the designation of matrix/die \bar{S}_c is introduced dual numbering for the rows and the columns. The series/row of numbers I, II, ..., Z ($Z \rightarrow -$) belongs to the amplitudes of its own waves from the lowest to the high ones in the boundary planes semi-infinite

waveguides. Series/rows 1, 2, ..., p and p+1, ..., 2p ($p \rightarrow \infty$) relate to the amplitudes of their own waves in the limiting planes of the waveguides of connection/communication (t, v, w, \dots and $r, \phi, \psi \dots$ respectively). If the values of values Z and p are final, then this means that in the semi-infinite waveguides it is taken into consideration in sum of Z of its own waves, and in the waveguides of connection/communication - p of their own waves.

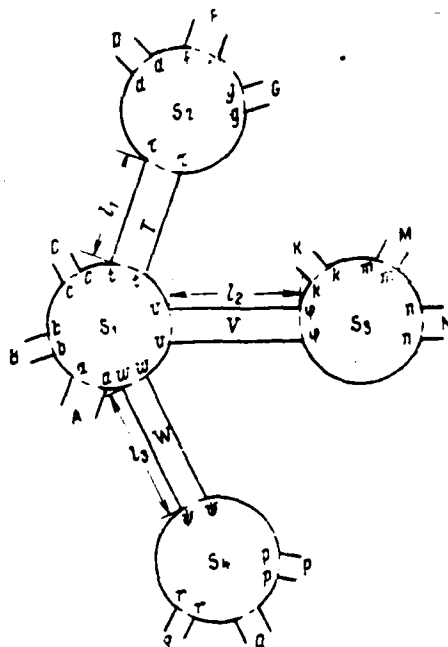


Fig. 1.

Page 144.

Equations for the amplitudes of the incident (+) and reflected (-) their own waves in the boundary planes of regular waveguides take the form:

$$\begin{aligned}\bar{U}_\alpha^- &= \bar{S}^{\alpha\alpha} \bar{U}_\alpha^+ + \bar{S}^{\alpha\beta} \bar{U}_\beta^+; \\ \bar{U}_\beta^- &= \bar{S}^{\beta\alpha} \bar{U}_\alpha^+ + \bar{S}^{\beta\beta} \bar{U}_\beta^+.\end{aligned}\quad (2)$$

Here $\bar{U}_\alpha^+, \bar{U}_\beta^+, \bar{U}_\alpha^-, \bar{U}_\beta^-$ — cell matrix columns:

$$\bar{U}_a^+ = \begin{bmatrix} \bar{u}_a^+ \\ \bar{u}_b^+ \\ \vdots \\ \bar{u}_r^+ \end{bmatrix}, \bar{U}_a^- = \begin{bmatrix} \bar{u}_a^- \\ \bar{u}_b^- \\ \vdots \\ \bar{u}_r^- \end{bmatrix}, \bar{U}_\phi^+ = \begin{bmatrix} \bar{u}_\phi^+ \\ \bar{u}_\psi^+ \\ \vdots \\ \bar{u}_\psi^+ \end{bmatrix}, \bar{U}_\phi^- = \begin{bmatrix} \bar{u}_\phi^- \\ \bar{u}_\psi^- \\ \vdots \\ \bar{u}_\psi^- \end{bmatrix}, \quad (3)$$

where \bar{u}_i^\pm ($i = a, b, \dots, \phi, \psi$) - the matrix columns, elements/cells of which are the amplitudes of their own waves in the appropriate boundary planes.

To matrix equ. (2) must be superimposed connection conditions, in order to exclude voltages $\bar{U}_\phi^+, \bar{U}_\phi^-$. These conditions must consider the special features/peculiarities of the connecting waveguides, indicated in the introduction. In contrast to [3, 6], connection conditions for the regular waveguides T, V, W ... let us record in the form:

$$\begin{aligned} \bar{u}_t^+ &= \bar{T} \bar{u}_t^-, & \bar{u}_t^- &= \bar{T} \bar{u}_t^+, \\ \bar{u}_\phi^+ &= \bar{V} \bar{u}_\phi^-, & \bar{u}_\phi^- &= \bar{V} \bar{u}_\phi^+, \\ \bar{u}_\psi^+ &= \bar{W} \bar{u}_\psi^-, & \bar{u}_\psi^- &= \bar{W} \bar{u}_\psi^+. \end{aligned} \quad (4)$$

where

$$\begin{aligned}
 \bar{T} &= \begin{bmatrix} e^{i\gamma_1 l_1} & 0 & \dots & \dots \\ 0 & e^{i\gamma_2 l_2} & 0 & \dots \\ \vdots & 0 & e^{i\gamma_3 l_3} & \dots \\ \vdots & \vdots & 0 & \ddots \end{bmatrix} \\
 \bar{V} &= \begin{bmatrix} e^{i\gamma_1 l_1} & 0 & 0 & \dots \\ 0 & e^{i\gamma_2 l_2} & 0 & \dots \\ \vdots & 0 & e^{i\gamma_3 l_3} & 0 \\ \vdots & \vdots & 0 & \ddots \end{bmatrix} \\
 \bar{W} &= \begin{bmatrix} e^{i\gamma_1 l_1} & 0 & 0 & \dots \\ 0 & e^{i\gamma_2 l_2} & 0 & \dots \\ 0 & 0 & e^{i\gamma_3 l_3} & 0 \\ \vdots & \vdots & \vdots & \ddots \\ \vdots & \vdots & 0 & \ddots \end{bmatrix} \quad (5)
 \end{aligned}$$

T_i, V_i, W_i ($i=1, 2, \dots$) - longitudinal numbers of modes in waveguides T, V, W . Let us designate

$$\bar{\bar{g}} = \begin{bmatrix} 0 & \bar{\eta} \\ \frac{0}{\bar{\eta}} & 0 \end{bmatrix}, \text{ где } \bar{g} = \begin{bmatrix} \bar{T} & 0 & 0 & \dots \\ 0 & \bar{V} & 0 & \dots \\ 0 & 0 & \bar{W} & \dots \\ \vdots & \vdots & 0 & \ddots \end{bmatrix} \quad (6)$$

Page 145.

If there is a single waveguide of the connection/communication by length l , in which is considered only one transmission mode with the longitudinal wave number T , cell matrix/die (6) is converted into the known scattering matrix of long line with the electrical length

$\theta = T_1$ [time function $\exp(-i\omega t)$]:

$$\bar{\theta}_{a1} = \begin{bmatrix} 0 & e^{i\theta} \\ e^{i\theta} & 0 \end{bmatrix}. \quad (6a)$$

By analogy it is possible to name/call the infinite square cell quasi-diagonal matrix/die $\bar{\theta}$, preset by expression (6) taking into account (5), the scattering matrix of the waveguides of connection/communication.

Taking into account designations (5), (6) the conditions of connection/communication (4) let us record in the form:

$$\bar{U}_\beta^+ = \bar{\theta} \bar{U}_\beta^-. \quad (7)$$

After substituting equalities (7) into the system of equ. (2), we eliminate fields in the waveguides of connection/communication. As a result we obtain the unknown matrix/die \bar{S} of complicated waveguide circuit (Fig. 1):

$$\begin{aligned} \bar{U}_\alpha^- &= \bar{S} \bar{U}_\alpha^+, \\ \bar{S} &= \bar{S}^{aa} + \bar{S}^{ab} (\bar{\theta}^{-1} - \bar{S}^{bb})^{-1} \bar{S}^{ba}. \end{aligned} \quad (8)$$

After excluding voltages \bar{U}_α^- from system (2) with the aid of conditions (4), we obtain voltages on the boundary planes of the waveguides of the connection/communication:

$$\bar{U}_\beta = \bar{U}_\beta^+ + \bar{U}_\beta^- = [(\bar{I} + \bar{\theta}^{-1})(\bar{\theta}^{-1} - \bar{S}^{bb})^{-1} \bar{S}^{ba}] \bar{U}_\alpha^+. \quad (9)$$

where \bar{I} - unit matrix, order of matrix/dia $\bar{\theta}^{-1}$.

Use/application of the obtained results to special cases.

A. System, depicted in Fig. 1, when single waveguide of connection/communication is present, is converted into device/equipment of type of directional coupler (Fig. 2a), which is extensively used in different waveguide diagrams.

Page 146.

For this case

$$\bar{S} \rightarrow \bar{T} = \begin{bmatrix} 0 & \bar{T} \\ \bar{T} & 0 \end{bmatrix}. \quad (10)$$

Matrix/die \bar{T} let us name/call scatterings of regular waveguide. The matrix elements of scattering the connection with one waveguide of connection/communication, depicted in Fig. 2a, can be found from the formulas:

$$\bar{S}^{AB} = \bar{S}^{ab} + \bar{S}^{ad} (\bar{T} \bar{S}^{cc}) [\bar{I} - (\bar{T} \bar{S}^{cc}) (\bar{T} \bar{S}^{dd})]^{-1} (\bar{T} \bar{S}^{db}), \quad (11)$$

$$\bar{S}^{AG} = \bar{S}^{ad} [\bar{I} - (\bar{T} \bar{S}^{dd}) (\bar{T} \bar{S}^{cc})]^{-1} (\bar{T} \bar{S}^{cb}), \quad (12)$$

$$\bar{S}^{DB} = \bar{S}^{db} [\bar{I} - (\bar{T} \bar{S}^{cc}) (\bar{T} \bar{S}^{dd})]^{-1} (\bar{T} \bar{S}^{cb}), \quad (13)$$

$$\bar{S}^{DG} = \bar{S}^{dg} + \bar{S}^{dc} (\bar{T} \bar{S}^{dd}) [\bar{I} - (\bar{T} \bar{S}^{dd}) (\bar{T} \bar{S}^{cc})]^{-1} (\bar{T} \bar{S}^{cb}). \quad (14)$$

It is not difficult to see that equalities (11)-(14) are

DOC = 81082105

PAGE

125

suitable for the determination of the cages of matrix/die \bar{S} of the junction of two regions of connection/communication independent of a quantity of semi-infinite waveguides, which converge in regions S_1 , S_2 .

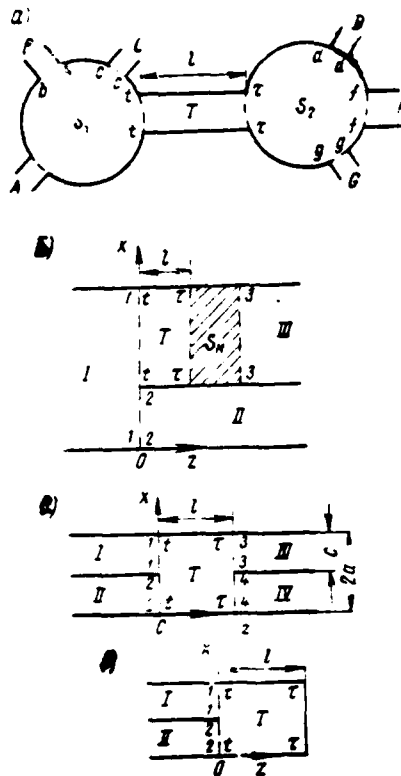


Fig. 2.

Page 147.

B. Some concrete/specific/actual embodiment of system with one waveguide of connection/communication are represented in Fig. 2b, c, d. Are given H -plane sections of three devices/equipment on rectangular waveguides. The transverse plane $z=0$ in these devices/equipment is the jointing plane of two narrow waveguides with the wide; this joint we will consider the first region (here - by

plane) of connection/communication.

The scattering matrix of joint $z=0$ in the designations of figure 2b is written/recorded in the form

$$\bar{S}_{z=0} = \begin{bmatrix} \bar{S}^{11} & \bar{S}^{12} & \bar{S}^{1l} \\ \bar{S}^{21} & \bar{S}^{22} & \bar{S}^{2l} \\ \bar{S}^{l1} & \bar{S}^{l2} & \bar{S}^{ll} \end{bmatrix} = \begin{bmatrix} \{Mm\} & \{Nm\} & \{Rm\} \\ \{Mn\} & \{Nn\} & \{Rn\} \\ \{Mr\} & \{Nr\} & \{Rr\} \end{bmatrix}. \quad (15)$$

In the right matrix/die stand the designations of cages from work [2], in which were obtained the formulas for from the computation.

The second region of connection/communication Fig. 2b depicts by certain heterogeneity in one of the narrow waveguides with the scattering matrix \bar{S}_n :

$$\bar{S}_n = \begin{bmatrix} \bar{S}^{33} & \bar{S}^{3r} \\ \bar{S}^{r3} & \bar{S}^{rr} \end{bmatrix}. \quad (16)$$

The calculation of this device/equipment is conducted according to formulas (11)-(14), where they are done:

$$A \rightarrow I; B \rightarrow II; D, G \rightarrow III, \\ a \rightarrow 1; b \rightarrow 2; d, g \rightarrow 3.$$

Under condition $l=0$ $\bar{T}=\bar{I}$. In this case the formulas of

matrices/dies S^{11} , S^{111} , S^{1111} become analogous to expressions (2) - (4) work [4], by the obtained method of the generalized scattering matrix. If load is the ideally reflecting wall, then matrix elements \bar{S}_i are represented in the form

$$\bar{S}^{11} = -\bar{I}, \bar{S}^{12} = 0.$$

Then with $l=0$ from formulas (11)-(14) are obtained the cages of the scattering matrix of step in the waveguide (joint of the wide waveguide I with narrow II):

$$\bar{S}_{\text{cavity}}^{AB} = \bar{S}^{ab} - \bar{S}^{a1} (\bar{I} + \bar{S}^{11})^{-1} \bar{S}^{1b}, \quad (17)$$

where with $A=I$, $II a=1.2$; with $B=I$, $II b=1.2$.

The formulas of matrices/dies \bar{S}^{11} , \bar{S}^{111} steps, obtained from (17), are analogous to equalities (32), (33) work [4]. However, the full/total/complete matrix/die of step in work [4] was not determined.

Page 148.

C. In simplest slotted bridge, depicted in Fig. 2c, second region of connection/communication is mirror reflection of joint $z=0$. In accordance with the designations, accepted by Fig. 2c, the scattering matrices of joints take the form

$$\begin{bmatrix} \bar{S}^{11} & \bar{S}^{12} & \bar{S}^{13} \\ \bar{S}^{21} & \bar{S}^{22} & \bar{S}^{23} \\ \bar{S}^{31} & \bar{S}^{32} & \bar{S}^{33} \end{bmatrix} = \begin{bmatrix} \{Mm\} & \{Nm\} & \{Rm\} \\ \{Mn\} & \{Nn\} & \{Rn\} \\ \{Mr\} & \{Nr\} & \{Rr\} \end{bmatrix} = \begin{bmatrix} \bar{S}^{11} & \bar{S}^{12} & \bar{S}^{13} \\ \bar{S}^{21} & \bar{S}^{22} & \bar{S}^{23} \\ \bar{S}^{31} & \bar{S}^{32} & \bar{S}^{33} \end{bmatrix}. \quad (18)$$

The cages of the scattering matrix of the simplest slotted bridge are determined by formulas (18), (11)-(14), in which it is necessary to replace in accordance with the designations in Fig. 2c:

$$\left. \begin{array}{ll} \text{при } A = I, II & a = 1, 2; \\ \text{при } D = III, IV & d = 3, 4; \end{array} \right\} \begin{array}{ll} \text{при } B = I, II & b = 1, 2 \\ \text{при } G = III, IV & g = 3, 4 \end{array} \quad (19)$$

Key: (1). with.

The waveguide development by 180° in Fig. 2d differs from the slotted bridge only in terms of presence of the short-circuiting cross connection instead of joint $z=1$. In this case (11) - (14) is obtained the expression for the determination of the cages of the scattering matrix of the simplest development:

$$\bar{S}_{\text{разворот}}^{AB} = \bar{S}^{ab} - \bar{S}^{ad} (\bar{I} + \bar{T} \bar{T} \bar{S}^{dd})^{-1} \bar{T} \bar{T} \bar{S}^{db}, \quad (20)$$

where with $A=I, II$ $a=1,2$, with $B=I, II$ $b=1,2$.

In work [2] by the experiment of repeated re-reflection and mutual transformations of its own waves in the region of the connection/communication of bridge and development with the identical narrow waveguides obtained elements/cells with indices of the II

following cases of scattering matrices:

$$\left. \begin{array}{l} (1) \text{ для моста } S_{11}'' = S_{11}''' = E', S_{11}''' = E_N'', S_{11}^{IV} = E_R'' \\ (2) \text{ для разворота } S_{11}'' = E_N', S_{11}''' = E_R' \end{array} \right\}. \quad (21)$$

Key: (1). for the bridge. (2). for development.

In equalities (21) to the right stand designations of work [2]. Let us note that the mentioned method of the generalized scattering matrix [4] so, the account of the re-reflection of single the mode between two waveguide joints [7, 8], is a special case of the method of the study of repeated re-reflection and mutual transformations of waves on heterogeneities [2]. In the first two methods are not considered the mutual transformations of modes that it does not give the possibility to conduct the calculation of the devices/equipment, which consist of the heterogeneities, connected by the cuts of the regular waveguides of finite small length. At the same time the investigation, made in work [2], can be considered the illustration of the general physical laws, described by formulas (8), (9) this work.

Page 149.

D. From formulas (8), (9) as special case escape/ensue expressions for scattering matrix of junction of linear multipoles - (7.111), (7.113) in monograph [3]. Let in the semi-infinite

waveguides of the system Fig. 1 it calculate on the basis of one own type of waves, and in the waveguides of connection/communication T, V, W-f, (g-f), (p-g) waves respectively. If the length of the waveguides of connection/communication is made equal to zero, then for this system equivalent diagram will take the form, shown in Fig. 3a. For the case

$$(\bar{\theta}_{l=0})^{-1} = \left[\begin{array}{c|c} 0 & \bar{\Gamma}^* \\ \hline \bar{\Gamma}^* & 0 \end{array} \right] = \bar{\Gamma}. \quad (6a)$$

in question.

It is obvious that in this formula the order of matrices/dies $\bar{\theta}^{-1}$ and $\bar{\Gamma}$ is identical, and the order of matrix/die $\bar{\Gamma}^*$ half the order of matrix/die $\bar{\theta}^{-1}$.

Taking into account (6b) formulas (8), (9) take the form:

$$\bar{S} = \bar{S}^{\alpha\alpha} + \bar{S}^{\alpha\beta} (\bar{\Gamma} - \bar{S}^{\beta\beta})^{-1} \bar{S}^{\beta\alpha}, \quad (22)$$

$$\bar{U}_\beta = [(\bar{\Gamma} + \bar{\Gamma}^* (\bar{\Gamma} - \bar{S}^{\beta\beta})^{-1} \bar{S}^{\beta\alpha})] \bar{U}_\alpha. \quad (23)$$

Formulas (22), (23) differ from (7.111), (7.113) only in terms of the presence of the square matrix/die $\bar{\Gamma}$ instead of introduced in this work matrix/die $\bar{\Gamma}$.

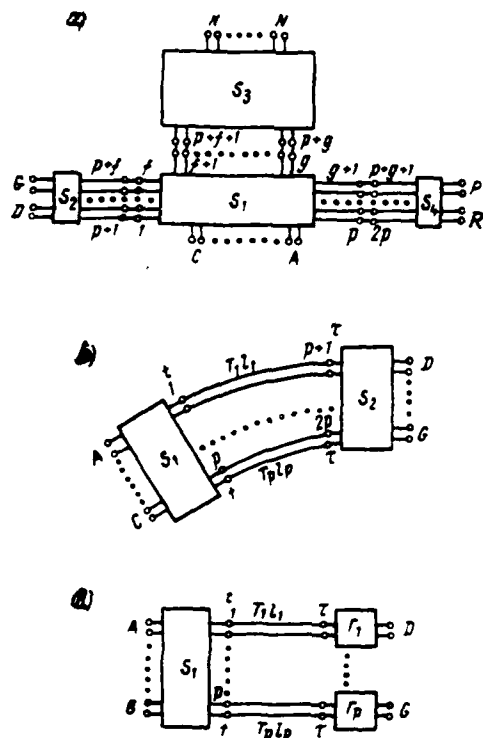


Fig. 3.

Page 150.

Matrix elements \bar{P} are unity and zero, moreover unity relate to the terminals/grippers, which are subject to the connection/communication between themselves; remaining coefficients are equal to zero. Taking into account that in Fig. 3a are connected terminals/grippers 1 and $p+1$, 2 and $p+2$, ..., p and $2p$, we note that for this numbering matrix/die \bar{P} is equal to $\bar{1}$. The formula, which

considers repeated wave diffractions around the bodies of complex form, obtained in [5] by the method of scattering matrices, differs from (22) only in terms of the designations of the matrices/dies of partial heterogeneities and in terms of matrix/die ϵ (instead of 1), which makes sense of value $\bar{\epsilon}$.

E. Expressions (11)-(14) it is not difficult to use for calculating scattering matrix system of two multipoles, connected with cuts of long lines with an electrical length of $\theta_i = T_{i1}$, where $i=1, 2, \dots, p$ (Fig. 3b). For this in (11)-(14) it is necessary to introduce the replacement:

$$\bar{T} - \bar{S}_n = \begin{bmatrix} e^{i\theta_1} & 0 & 0 & \dots & \dots \\ 0 & e^{i\theta_2} & 0 & \dots & \dots \\ 0 & 0 & e^{i\theta_3} & 0 & \dots \\ \vdots & \vdots & 0 & \vdots & \ddots \\ \vdots & \vdots & \vdots & \vdots & \ddots \end{bmatrix} \quad (24)$$

A finally special case of the reference system, depicted in Fig. 1, is the multipole to which are connected the quadrupoles by the cuts of long lines (Fig. 3c). The scattering matrix of the i quadrupole let us designate \bar{T}_i , the electrical length of the corresponding long line of communications θ_i ($i=1, 2, \dots, p$).

The formula of the scattering matrix of the system, depicted in Fig. 3c, we will obtain from expressions (6), (8) by replacement

$\bar{S} \rightarrow \bar{S}_n$, where \bar{S}_n is preset by equality (24). If in the case of connection/communication of two multipoles (Fig. 3b) in compound matrix/die (1) at places \bar{S}_{ik} , \bar{S}_{ik} , \bar{S}_{ik} stand corresponding indexes i, k of the cage of the matrices/dies of multipoles $\bar{S}_2, \bar{S}_3, \dots$, then for the case of Fig. 3c at the places of compound matrix/die indicated stand number-elements/cells of the square matrices/dies of second order \bar{S}_i .

The system, depicted Fig. 3b, and also a special case of the zero length of all lines ($l_i = 0$) in Fig. 3c examines in [1]. However, there the analysis conducted is very complex.

Taking into account that outlined above, it is possible to make the conclusion that formulas (8), (9) generalize the results of the theory of linear multipoles [3, 6] and long lines with loads [1], and also the method of the generalized scattering matrix [14] and account of repeated diffractions with the aid of the scattering matrices [5] to the calculation of complicated regular circuits with the heterogeneities.

7. Let us use described method to determination of scattering matrix of slotted bridge and waveguide development with thick internal wall and steps in region of connection/communication. In Fig. 4a, is shown the section of bridge in plane H. Waveguide

development we will obtain from this bridge, after supplying shorting device in the plane rr .

Page 151.

During the derivation of the formulas of the scattering matrices of such devices/equipment let us take as the base the scattering matrix of the waveguide joint, shown in Fig. 4a in plane $z=0$. Scattering matrix of this joint was determined by formula (15). The scattering matrix of joint $z=1$ in Fig. 4a let us determine in accordance with the designations, accepted by this figure, in the form

$$\bar{S}_{z=1} = \begin{bmatrix} \bar{S}^{11} & \bar{S}^{12} & \bar{S}^{14} \\ \bar{S}^{21} & \bar{S}^{22} & \bar{S}^{24} \\ \bar{S}^{41} & \bar{S}^{42} & \bar{S}^{44} \end{bmatrix}_l = \begin{bmatrix} \{Mm\} & \{Nm\} & \{Rm\} \\ \{Mn\} & \{Nn\} & \{Rn\} \\ \{Mr\} & \{Nr\} & \{Rr\} \end{bmatrix}_l \quad (25)$$

In equality (25) index l is set in order to emphasize a difference in the geometric dimensions of joints $z=0$, $z=l$ in Fig. 4a.

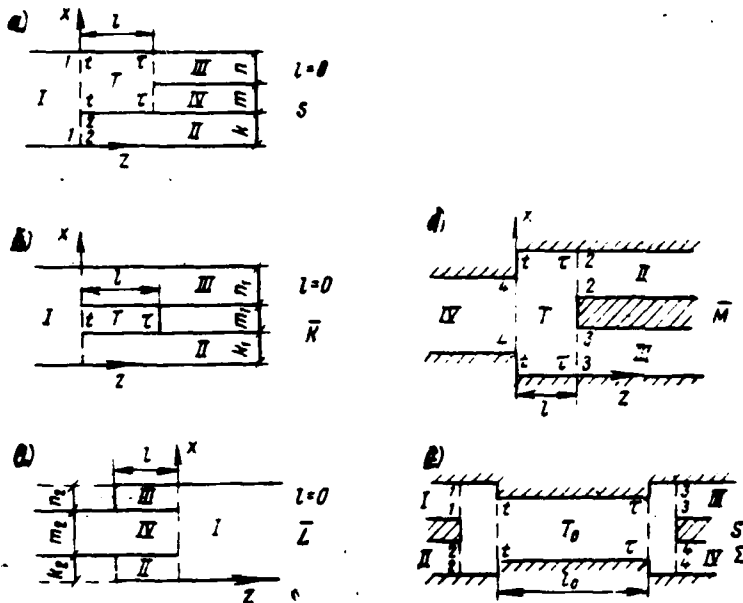


Fig. 4.

Page 152.

Let us use formulas (11)-(14) to the device/equipment, depicted in Fig. 4a. Taking into account designations (15), (25) with $l=0$ we will obtain the formulas of the cages of the scattering matrix of the transition/junction of wide waveguide to three narrow ones:

$$\bar{S}^{AB} = \bar{S}^{ab} + \bar{S}^{aI} \bar{S}^{II} (\bar{I} - \bar{S}^{II} \bar{S}^{II})^{-1} \bar{S}^{Ib},$$

(1) где при $A = I, II$ $a = 1, 2$, а также при $A = III, IV$ $a = 3, 4$,
 (2) при $B = I, II$ $b = 1, 2$, (3) при $B = III, IV$ $b = 3, 4$;
 $\bar{S}^{AG} = \bar{S}^{aI} (\bar{I} - \bar{S}^{II} \bar{S}^{II})^{-1} \bar{S}^{Ig},$
 (4) где при $A = I, II$ $a = 1, 2$, а также при $A = III, IV$ $a = 3, 4$
 (5) при $G = III, IV$ $g = 3, 4$ (6) при $G = I, II$ $g = 1, 2$

(26)

Key: (1). where with. (2). and also with. (3). with.

Let us place shorting device into the average/mean narrow waveguide of the joint of three waveguides with one wide, as shown in Fig. 4b. With $l=0$ this device/equipment is converted into the joint of wide waveguide with two by narrow ones, that have thick general/common/total wall. The scattering matrix of joint with the thick wall (Fig. 4b, $l=0$) let us designate \bar{K} . After using formulas (11)-(14), taking into account (26) we obtain the cages of matrix/die \bar{K} :

$$\bar{K}^{AB} = \bar{S}_I^{AB} - \bar{S}_I^{AIV} (\bar{I} + \bar{S}_I^{IVIV})^{-1} \bar{S}_I^{IVB}, \quad (27)$$

where $A, B = I, II, III$.

Supplementary indices 1 are set in (27) in order to note that matrix/die \bar{K} is determined for the joint with a width of the narrow waveguides of k_1 and n_1 and with a thickness of wall of m_1 .

Let us now place shorting devices into two extreme narrow

waveguides, as shown in Fig. 4c. With $l=0$ we obtain steps in the waveguide in plane H (coupling the waveguides of identical height and different width). Let us designate the scattering matrix of this coupling by symbol \bar{L} . After using formula (22), we obtain expressions for matrix/die \bar{L} :

$$\bar{L} = \left[\frac{\bar{S}_2^{IV}}{\bar{S}_2^{IV I}} \left| \frac{\bar{S}_2^{IV}}{\bar{S}_2^{IV IV}} \right| \right] - \left[\frac{\bar{S}_2^{III}}{\bar{S}_2^{IV III}} \left| \frac{\bar{S}_2^{III}}{\bar{S}_2^{IV III}} \right| \right] \cdot \left[\bar{I} + \left| \frac{\bar{S}_2^{III}}{\bar{S}_2^{III III}} \right| \frac{\bar{S}_2^{III III}}{\bar{S}_2^{III III}} \right]^{-1} \times \\ \times \left[\frac{\bar{S}_2^{III}}{\bar{S}_2^{III I}} \left| \frac{\bar{S}_2^{III}}{\bar{S}_2^{III IV}} \right| \right]. \quad (28)$$

Indices 2 V (28) correspond to the width of the narrow waveguide m_2 and to the heights of steps k_2, n_2 (Fig. 4c), moreover $k_1 + m_1 + n_1 = k_2 + m_2 + n_2$.

After substituting the cages of matrix/die \bar{K} into formulas (11)-(14), we obtain expressions for the cages of the scattering matrix \bar{M} of the waveguide branching off, shown in Fig. 4d:

$$\left. \begin{aligned} \bar{M}^{IV IV} &= \bar{L}^{IV IV} + \bar{L}^{IV I} (\bar{T} \bar{K}^{II}) [\bar{I} - (\bar{T} \bar{K}^{II}) (\bar{T} \bar{L}^{II})]^{-1} (\bar{T} \bar{L}^{I IV}) \\ \bar{M}^{IV B} &= \bar{L}^{IV I} [\bar{I} - (\bar{T} \bar{L}^{II}) (\bar{T} \bar{K}^{II})]^{-1} (\bar{T} \bar{K}^{I B}) \\ \bar{M}^{A IV} &= \bar{K}^{A I} [\bar{I} - (\bar{T} \bar{K}^{II}) (\bar{T} \bar{L}^{II})]^{-1} (\bar{T} \bar{L}^{I IV}) \\ \bar{M}^{AB} &= \bar{K}^{AB} + \bar{K}^{A I} (\bar{T} \bar{L}^{II}) [\bar{I} - (\bar{T} \bar{L}^{II}) (\bar{T} \bar{K}^{II})]^{-1} (\bar{T} \bar{K}^{I B}) \end{aligned} \right\} \quad (29)$$

where A, B=II, III.

Utilizing again formulas (11)-(14) for series connection of

identical joints with matrix/die M, shown in Fig. ^{42.} ~~poisson~~, we obtain the unknown scattering matrix of H-plane slotted bridge with the thick internal wall and the steps in the region of the connection/communication:

$$\begin{aligned} \bar{S}_{1 \text{ MOCTA}}^{AB} &= \bar{M}^{AB} - \bar{M}^{AT} (\bar{T}_0 \bar{M}^{TT}) [\bar{I} - (\bar{T}_0 \bar{M}^{TT}) (\bar{T}_0 \bar{M}^{TT})]^{-1} (\bar{T}_0 \bar{M}^{TB}) \\ \bar{S}_{1 \text{ MOCTA}}^{AG} &= \bar{M}^{AT} [\bar{I} - (\bar{T}_0 \bar{M}^{TT}) (\bar{T}_0 \bar{M}^{TT})]^{-1} (\bar{T}_0 \bar{M}^{TG}) \end{aligned} \quad (30)$$

where T=IV; A, B=I, II or III, IV; with A=I, II G=III, IV; with A=III, IV G=I, II.

The scattering matrix of waveguide development with the thick internal wall and the stepped contraction of the region of connection/communication in plane H is determined from the expression

$$\bar{S}_{1 \text{ pasopora}}^{AB} = \bar{M}^{AB} - \bar{M}^{AT} [\bar{I} + (\bar{T}_0 \bar{T}_0 \bar{M}^{TT})^{-1} \bar{T}_0 \bar{T}_0 \bar{M}^{TB}] \quad (31)$$

where T=IV; A, B=I, II.

At conclusion of present section it is necessary to emphasize that method examined here of computing the scattering matrices complicated plumbing is based on repeated use of one and the same algorithm, determined by formula (8).

This order of computation is very convenient for the realization on the computer(s), since it requires the use of one routine for calculating the most varied plumbing.

Page 154.

Conclusion

1. In the present work is obtained scattering matrix of complicated waveguide junction of regular waveguides with several regions of connection/communication. In the method in question the calculation of the scattering matrices of different complicated waveguide junctions is conducted by repeated use of one and the same algorithm, convenient for the calculation on the computer(s).

2. It is shown that known results of theories of connected linear multipoles and long lines with loads, and also method of generalized scattering matrix and account of repeated diffractions with the aid of scattering matrices can be obtained from scattering matrix of complicated waveguide junction as special cases.

3. Are brought out formulas of scattering matrices:

- joint of wide waveguide with three narrow, that have infinitely thin common walls;

- regular waveguide with jump of cross section;

- thick metallic semi-infinite plate, situated in rectangular waveguide in parallel to narrow wall;

- slotted bridge and waveguide development with thick wall between narrow waveguides and two irregularly cross section in region of connection/communication.

In conclusion the author expresses gratitude to G. A. Yevstropov for the discussion of the manuscript of article.

REFERENCES

1. Котан Н. Л., Машковцев Б. М., Цибисов К. Н. Сложные волноводные системы. Судпромгиз, 1963.
2. Евостропов Г. А., Бугакова С. В. К расчету щелевого моста и развоя на 180° в прямоугольном волноводе. Сборник «Вычислительные методы и программирование». Вып. 13, изд. МГУ (в печати).
3. Машковцев Б. М., Цибисов К. Н., Емелин Б. Ф. Теория волноводов. Изд-во «Наука», 1966.
4. Rase J. R., Mittra R. Метод обобщенной матрицы рассеяния. Proc. Symp. Quasi-Optics, New York, 1964. Brooklyn, Polytech. Press. Polytech. Inst. 177—197.
5. Кинбер Б. Е. Об учете многократных дифракций методом матриц рассеяния. «Радиотехника и электроника», 1964, т. 9, № 9.
6. Машковцев Б. М. Метод анализа многоконтурных направленных фильтров с вращающейся поляризацией поля. «Радиотехника», 1962, т. 17, № 6, стр. 3—10.
7. Kaden H. Электромагнитные волны в разветвлениях прямоугольных волноводов. «Archiv der Elektrischen Übertragung», Bd. 15, 1961, № 2, стр. 61—70.
8. Attiya F. S. Щелевой направленный ответвитель со связью по широкой стенке между двумя одинаковыми прямоугольными волноводами. «Archiv der Elektrischen Übertragung» Bd 18, 1964, № 8, стр. 487—496.

Three-stage commutation field of the system of the repeated use of short-wave receiving antennas.

V. D. Chelyshev.

Three-stage commutation systems are examined taking into account the special features/peculiarities, which escape/ensue from the admissibility of simultaneous connection to one antenna of the group of receivers. The fundamental characteristics of three-stage commutation fields are given in the comparison with the single-stage field of the same capacity/capacitance.

Introduction.

The numerous specific special features/peculiarities of short-wave radio communication lead to the need for having radio centers with a maximally possible number of simultaneously serviced correspondents (frequencies and routings) with the minimally necessary number of antennas. The important composite/compound component part of this radio center is the system of the repeated use of antennas with the developed commutation field, which ensure the

mutual commutation of the inputs of receivers and antenna introductions/inputs [1].

In the general case of substances the process of operation any of the receivers can be required any of the antennas independent of a number of already established/installed junctions, i.e. switching system must be sufficiently flexible, fully accessible. On the other hand, under difficult conditions of shortwave communication, in the connection/communication with the highly mobile objects and in other cases is required the sufficiently frequent cross-communication of antennas up to the automatic selection, i.e. switching system must be sufficiently high speed, operational. Best in this respect would be the fully accessible system of operational commutation. However, this system always cannot be realized, especially at the radio centers of great capacity. Furthermore, this diagram is characterized by the large redundancy of commutation points, it requires complicated feeder separation and it is deprived of the universality of the use/application at the radio centers of a different capacity/capacitance. To virtually each receiver for the elongation/extent relative to the prolonged intervals of time is necessary operational commutation from the limited, small number of antennas with the nonoperational, but fully accessible replacement of this set/dialing of antennas. In other words, acceptable should be counted system with the operational not entirely accusable

commutation and the nonoperational fully accessible commutation of antennas.

Page 156.

Let us designate through M a maximum number of simultaneously serviced frequencies and routings (receivers), and through N - maximum number of antennas of radio center (antenna introductions/inputs). We will be oriented toward value of M , which reaches hundred and more, and at value of N , which reaches several ten.

General/common/total characteristic of three-stage fully accessible commutation field.

In the simplest case for guaranteeing total accessibility and effectiveness of commutation it suffices to have common single-stage commutator with a capacity/capacitance of field of $M \times N$, as shown in Fig. 1. However, it is not always possible to use in the practice this solution. First, the fulfillment of commutator with values of M , $N \gg 30 \div 40$ is connected with the serious ones [1]. In the second place, this commutator is deprived of the universality of its use/application at the radio centers of different capacity/capacitance. Thirdly, although a similar single-stage

diagram has the smallest number of coupling feeders, the lengths of most numerous group M of the coupling feeders of a commutator-receiver are large. Fourthly, diagram is characterized by the large redundancy of commutation points. Therefore at the radio centers more frequently is applied the single-stage diagram, which includes not one, but several (k) commutators of small amount of capacitance $M' \times N'$ with $M' < M$ and $N' < N$, as shown in Fig. 2.

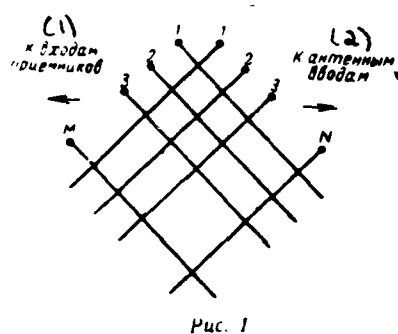


Fig. 1.

Fig. 1.

Key: (1). To the inputs of receivers. (2). To antenna introductions/inputs.

Page 157.

Antenna introductions/inputs for the separate commutators are

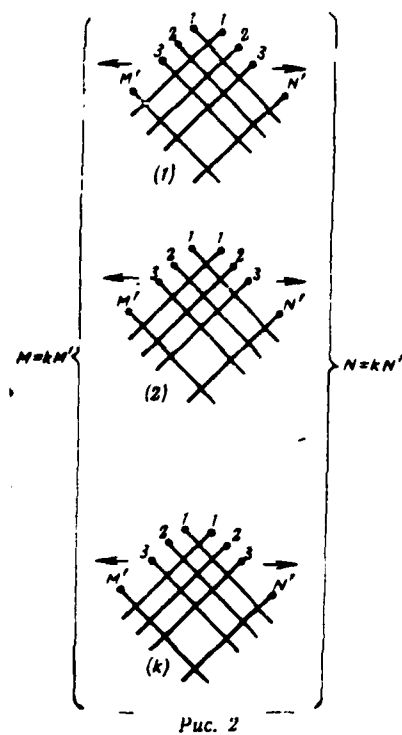


Fig. 2.

obtained from the outputs of the splitters of the power of antenna amplifiers, and a number of these introductions/inputs considerably increases. With $N' < N$ the diagram is deprived of total accessibility. In order to expand the possibilities of diagram and to draw it nearer the fully accessible, increase the capacity/capacitance of commutators in input ($N' \rightarrow N$), run supplementary feeders from the splitters power to the commutators and between the separate commutators. As the final result taking into account the possibility of the manual cross-communication of antennas with the aid of the supplementary feeders the diagram approaches in its commutation characteristics single-stage fully accessible, being inferior to it in a number of coupling feeders and in the possibilities of the automation of the processes of commutation.

From the theory of fully accessible commutation systems it is known that more effective in comparison with the single-stage is three-stage system [2]. Its block diagram is given in Fig. 3 and is commutation field with a capacity/capacitance of $M \times N$ with $M \leq N$, consisting of the totality of the separate commutators of small amount of capacitance, grouped into three cascades/stages. For guaranteeing of total accessibility and effectiveness of commutation it is necessary to satisfy the following conditions:

- a) in the first cascade/stage to begin to operate M/n

commutators by capacity/capacitance $[n \times (2n-1)]$ each;

b) in the second cascade/stage to begin to operate $(2n-1)$ commutators by capacity/capacitance $[(M/n) \times (N/n)]$ each;

c) in the third cascade/stage to begin to operate N/n commutators by capacity/capacitance $[(2n-1) \times n]$ each;

d) interstage junctions to satisfy in such a way that each commutator of the previous cascade/stage on the output would have at least one junction with each commutator of the subsequent cascade/stage on the input.

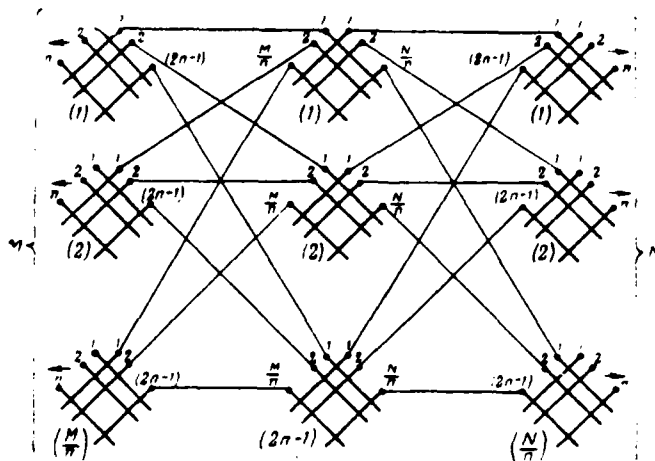


Fig. 3.

Page 158.

Here n - certain commutation number whose sense will be clarified below.

The distinctive special feature/peculiarity of the commutation field of the system of the repeated use of antennas consists in the fact that in it, as a rule, always $M > N$, a number of receivers exceeds a number of antennas, but the connection of receiver with the antenna remains available independent of a number of already connected to this antenna receivers.

Because of these special features/peculiarities structural

diagram in Fig. 3 retains its form, also, with $M > N$, but by the force of inequality $M > N$ a capacity/capacitance of the commutators of the second cascade/stage and a number of commutators of the third cascade/stage decrease [3].

Let us examine the most difficult case. assume it is necessary to carry out a connection between an i - receiver, connected to one of the commutators of the first cascade/stage, and a j - antenna, connected to one of the commutators of the third cascade/stage. Moreover to $(n-1)$ receiver of the commutator of the first cascade/stage in question is already connected $(n-1)$ antenna, none of which is required for an i -receiver, and $(n-1)$ antenna of the commutator of the third cascade/stage in question is distributed on the receivers, which form part of other commutators of the first cascade/stage. All connections from that examined/considered of the commutators of the first cascade/stage and to that examined/considered the commutators of the third cascade/stage pass through the different commutators of the second cascade/stage. Then a number of occupied commutators of the second cascade/stage, through which it is possible to carry out ij connection in question, composes $2(n-1) = 2n-2$. Since in the second cascade/stage will begin to operate $(2n-1)$ commutator, then remains one additional commutator, through which it is possible to carry out the requiring ij connection.

We analyze function of total number of commutation points of the system T_3 (M , N , n) in question depending on the commutation parameter n at the given ones by M and N . From the diagram in Fig. 3.

$$T_3 = \frac{M}{n} [n(2n-1)] + (2n-1) \left(\frac{M}{n} \frac{N}{n} \right) + \frac{N}{n} [(2n-1)n] =$$

$$= (2n-1) \left(M + N + \frac{MN}{n^2} \right). \quad (1)$$

Let us introduce designation $n_0^2 = MN/(M+N)$ and will consider that in the single-stage diagram $T_1 = MN$, then equ. (1) will take the form

$$T_3 = \frac{T_1}{n_0^2} (2n-1) \left(1 + \frac{n_0^2}{n^2} \right). \quad (1a)$$

Page 159.

Of greatest interest is three-stage diagram with a minimum number of commutation points $T_{3\text{ min}}$. Investigating equality (1a) to the extremum, we will obtain the equation of form.

$$n^3 - n_0^2 n + n_0^2 = 0. \quad (2)$$

This equation has the unique solution, which satisfies the physical realizability of diagram (root of equation has real positive value moreover $n > 1$) at the value of discriminant $\frac{n_0^4}{108} (27 - 4n_0^2) \leq 0$, i.e. with $n_0 \geq 2.6$. The approximately optimum value of commutation parameter $n = n_{\text{opt}}$ at which occurs a minimum number of commutation points, can be defined as [4]:

$$n_{\text{opt}} \simeq \frac{2n_0}{\sqrt{3}} \cos \left[\frac{1}{3} \left(\pi - \arccos \frac{3\sqrt{3}}{2n_0} \right) \right]. \quad (3)$$

In the concrete/specific/actual diagram of commutation field value n must be not only whole, but also common multiple for M and N . In this case values M and N are rounded off to the appropriate nearest values toward the increase (by this is considered a promising increase in the capacitance of radio center), and value n_{opt} and $T_{3 \text{ min}}$ it is possible to determine from the approximate equalities, valid already with $n_0 \gg 4.5$:

$$\left. \begin{aligned} n_{\text{opt}} &\approx n_0 = \sqrt{\frac{MN}{M+N}} \\ T_{3 \text{ min}} &\approx 4 \sqrt{\frac{MN(M+N)}{}} \end{aligned} \right\} \quad (3a)$$

Since values n it is necessary to round off during the development of one or the other diagram, then is of interest dependence $\frac{T_3}{T_{3 \text{ min}}}$ on n which it is easy to obtain from the equ. (1, 1a; 3 and 3a) in the precise and approximate form:

$$\frac{T_3}{T_{3 \text{ min}}} = \frac{(2n-1) \left(1 + \frac{n_0^2}{n^2} \right)}{(2n_{\text{opt}}-1) \left(1 + \frac{n_0^2}{n_{\text{opt}}^2} \right)} \quad (4)$$

$$\frac{T_3}{T_{3 \text{ min}}} \approx \frac{1}{2} \frac{2n-1}{2n_0-1} \left(1 + \frac{n_0^2}{n^2} \right) \quad (4a)$$

Functional dependences (4) and (4a) show that change n with respect to n_0 within relatively wide limits from $n=1.7 n_0$ to $n=0.5 n_0$ and less leads to an increase in the number of commutation points not more than by 250/o.

Furthermore, for values of $n_0 = 4 \div 8$ more advantageous is rounding n toward decrease, since in this case a number of commutation points increases more slowly than with the rounding to the large side.

Let us examine conditions, with which three-stage commutation field has the total number of commutation points T_3 , is less than the single-stage field, which has $T_1 = MN$, i.e. when $T_1/T_3 > 1$. For the optimum three-stage diagram taking into account (1a) and (3a) we will obtain

$$\frac{T_1}{T_{3 \text{ min}}} = \frac{n_0}{(2n_{\text{opt}} - 1) \left(1 + \frac{n_0^2}{n_{\text{opt}}^2} \right)} \geq 1. \quad (5)$$

In the most important for the practice cases when $n_0 \approx n_{\text{opt}} \geq$

$4 \div 5$, we find

$$\frac{T_1}{T_{3 \text{ min}}} \approx \frac{n_0^2}{2(2n_0 - 1)} \approx \frac{n_0}{4} > 1. \quad (5a)$$

Condition (5a) shows that the three-stage commutation field becomes equivalent to single-stage or more profitable according to a number of commutation points at values of $n_0 > 4$, where $n_0 = \sqrt{\frac{MN}{M+N}}$. Since in the system of the repeated use of antennas $M > N$, i.e. $M = kN$, $k > 1$, then it is possible to record:

$$\begin{aligned} N &= n_0^2 \left(1 + \frac{1}{k} \right), \quad M = n_0^2 \left(1 + \frac{1}{k} \right) k, \\ T_1 &= MN = n_0^4 \left(1 + \frac{1}{k} \right)^2 k. \end{aligned} \quad (6)$$

Analyzing equ. (6), it is possible to note that three-stage commutation field profitably according to a number of commutation points, beginning from the initial capacitance of radio center $T_1 = MN = 10^3$ (for example, $M \times N = 64 \times 16$), but at values of $T_1 = 6 \cdot 10^3$ (for example, $M \times N = 192 \times 32$) three-stage diagram provides gain in a number of commutation points not less than 1.5-2.0 times. The noted advantages do not exhaust the possibilities of three-stage diagrams. Taking into account the specific character of the work of the system of the repeated use of antennas, it is possible to an even greater degree to realize gain in a total number of commutation points. Let us pause at one of the possible versions of this perfection of three-stage diagram.

Three-stage commutation field from the limited by accessibility operational commutation.

The three-stage diagram examined provides total accessibility and effectiveness of commutation at any moment of time and independent of a number of established/installed connections.

156

This operational total accessibility of commutation for the systems of the repeated use of short-wave antennas is not necessary. To each receiver and to their even group with the similar conditions according to the connection/communication during those relatively extended segments of time it is necessary to have only a limited set of antennas for operative commutation and automatic selection. In a single-stage circuit as a result of the impossibility of providing complete accessibility of commutation with a large initial capacity of the radio center an attempt is made to use separate commutators with the maximum possible capacity. In a completely accessible three-stage circuit it is not necessary to select individual high-capacity commutators. Thus each commutator of the first stage, which endures direct commutation of the receiver inputs, can be selected with the number of inputs $n \approx \sqrt{\frac{MN}{M+V}}$. In this case at any moment of time to each receiver is available any of

the available by N antennas. Taking into account the possibility of selecting the receivers in such small groups according to the principle of the similarity of conditions according to the connection/communication, it is possible the same n of antennas to select not on n , but to the large group of receivers qn with $q > 1$. In this case there is no possibility to ensure total accessibility of commutation for each receiver at any moment of time without any mechanical reconnection/recombination to completely renew set/dialing from the n antennas on any of the commutators of the first cascade/stage. Let us examine the simplest case when coefficient q is selected identical for all commutators of the 1st cascade/stage $q = q_0$. The structure of the construction of diagram remains the same as in Fig. 3. Will change only a number and the capacitance of the commutators of the first and the second of cascades/stages. Thus, in the first cascade/stage must be begun to operate M/qn commutators by capacitance $[qn \times (2n-1)]$, the secondly - the same $(2n-1)$ of commutator, but by capacitance $(M/qn \times N/n)$. Total number of

commutation points for the changed diagram

$$T_s = (2n - 1) \left(M + N + \frac{MN}{qn^2} \right). \quad (7)$$

Taking into account that during the composition of the concrete/specific/actual diagram it is necessary to round off, we will be restricted to the examination only of the approximate solutions. Minimum number of commutation points with

$$n'_{\text{opt}} \simeq n'_0 = \sqrt{\frac{MN}{q(M+N)}} = \frac{n_0}{\sqrt{q}} \quad (8)$$

it is possible approximately to find from the relationship/ratio

$$T'_{s_{\text{min}}} \simeq 4n'_0(M+N) = \frac{T_{s_{\text{min}}}}{\sqrt{q}}. \quad (9)$$

Page 162.

The analysis conducted shows that the diagram with limited accessibility of operational commutation with $q > 1$ provides supplementary gain in a number of commutation points \sqrt{q} once in comparison with the three-stage fully accessible diagram and $\frac{4\sqrt{q}}{n_0}$ once in comparison with the single-stage diagram. Thus, with $q \gg 2.54$ diagram from the limited total accessibility operational commutation becomes profitable than the single-stage, beginning from the initial capacitance of radio center $N \times M = 10^2$.

The analysis of the three-stage commutation field of the system

of the repeated use of antennas conducted makes it possible to make following conclusions.

1. Three-stage commutation diagrams include totality of commutators of small amount of capacitance and differ in terms of large universality uses/applications at radio centers of most varied capacitance.

2. Considerable changes in structure of three-stage diagram do not lead to sharp increase in number of commutation points in comparison with optimum diagram.

3. Optimum fully accessible three-stage diagram becomes profitable according to number of commutation points in comparison with single-stage, beginning from relatively small initial capacitance of radio center $M \times N \approx 10^3$.

4. Further possible considerable increase in profitability of three-stage track layouts of corresponding limitation of total accessibility of operational commutation.

The given numerical characteristics of three-stage diagrams can serve as base for the selection of the versions of commutation diagrams during their comparative evaluation according to the

operational possibilities, the electrical and operating parameters.

Literature.

1. Барановский Б. К. Аппаратура многократного использования коротких волновых приемных антенн. Изд-во «Связь», 1966.
2. Closs C. A study of non-blocking switching networks. «The Bell System Technical Journal», v. XXXII, 1953, № 2.
3. Челышев В. Д. Повышение эффективности высокочастотных коммутационных систем приемных радиоцентров. Тезисы докладов XXII областной научно-технической конференции, посвященной 50-летию Великого Октября и Дню радио. Л., НТОРиЭ им. А. С. Попова, 1967.
4. Бронштейн И. Н. и Семендяев К. А. Справочник по математике. ГИТТЛ, 1957.

END

DATE
FILMED

11-81

DTIC